

Republic of Iraq
Ministry of Higher Education
and Scientific Research



**POST-BUCKLING AND POST-YIELDING
ANALYSIS OF IMPERFECT THIN PLATE BY
FINITE DIFFERENCE METHOD**

A Thesis

**Submitted to the College of Engineering
of the University of Babylon in Partial
Requirements of the Fulfillment
for the Degree of Master
of Science in Civil
Engineering**

By

HAIDER KADEM AMASH

Supervised by

ASST. PROF. DR. HAITHAM AL-DAAMI

Thu-Alhejjah ١٤٢٣

February ٢٠٠٣

جمهورية العراق
وزارة التعليم العالي والبحث العلمي



تحليل ما بعد الانعاج وما بعد الخضوع
للصفات الحقيقية غير المضطربة
بترقته الفروقات المحددة

رسالة

مقدمة إلى كلية الهندسة في جامعة بابل
كجزء من متطلبات نيل درجة الماجستير
في علوم الهندسة المدنية

من قبل

حيدر كاظم عمّاش

أشرف

أ.م.د. هيثم الداعي

ذو الحجة ١٤٢٣

شباط ٢٠٠٣

ز

وَأَنْ لَّيْسَ لِلْإِنْسَانِ إِلَّا مَا سَعَى * وَأَنْ سَعْيُهُ سَوْفَ يُرَى * ثُمَّ
يُجْزَاهُ الْجِزَاءَ الْأَوْفَى *

صدق الله العلي العظيم

سورة النجم، الآية (٣٨-٤٠)

الخلاصة

تُقدم هذه الدراسة طريقة حسابية مُبسطة لتحليل مسائل ما بعد الانبعاج وما بعد الخضوع لصفائح رقيقة مستطيلة ذات سُمك ثابت أو مُتغير المقطع. تم تبسيط المسألة بطريقة الفروقات المحددة. لقد اشتمت معادلة تفاضلية لأفعال الأغشية (membrane actions) لصفائح ذات سُمك مُتغير. أُخذ بنظر الاعتبار اللاخطية الهندسية ولاخطية تصرف المادة لدراسة تحليل ما بعد الانبعاج وما بعد الخضوع.

هذه الدراسة قُسمت إلى جزئين, الجزء الأول يتضمن تحليل ما بعد الانبعاج لصفائح رقيقة مستطيلة تحت تأثير أحمال ضغط في المستوي. في هذا الجزء, أُهملت لاخطية تصرف المادة. لقد أُخذ بنظر الاعتبار تأثير التقوسات الابتدائية, ظروف الإسناد, نوع التحميل, نسب التغير في السمك, واتجاه تأثير الحمل. تم تحليل الصفيحة لمختلف نسب التقوسات الابتدائية ($w_o/t = 0.0, 0.1, 0.5$) من سمك الصفيحة و مختلف نسب التغير في السمك ($1.0, 1.25, 1.5, 1.75, 2.0$). ($t_a/t_o =$

أُستنتج من ذلك إن الانبعاج اللاحق حساس جدا إلى قيمة التقوس الابتدائي وإلى قيمة نسبة التغير في السمك.

يتضمن الجزء الثاني تحليل المرونة-اللدونة لصفائح رقيقة مستطيلة تحت تأثير حمل ضغط في المستوي. في هذا الجزء اللاخطية الهندسية ولاخطية تصرف المادة أُخذت بنظر الاعتبار. كذلك تم الأخذ بنظر الاعتبار: تأثير التقوسات الابتدائية, ظروف الإسناد, نسب النحافة, نسب الأبعاد, ونسب التغير في السمك على المقاومة القصوى.

أُستنتج من ذلك إن المقاومة القصوى تقل مع زيادة نسب التقوسات الابتدائية وتصل مقدار النقصان حوالي (15 %) عند نسبة التقوسات الابتدائية ($w_o/t = 0.5$). لنفس نسب التقوسات الابتدائية ($w_o/t = 0.5$) فإن المقاومة القصوى تقل مع زيادة نسبة التغير في السمك وتصل نسبة النقصان إلى حوالي (20 %) عندما تكون نسبة التغير في السمك ($t_a/t_o = 2.0$).

ABSTRACT

A simplified computational procedure for post-buckling and post-yielding problems of rectangular thin plates with constant or variable thickness is presented. The discretization of the problem is carried out by means of finite differences. The basic (governing) differential equation for membrane actions of plate with variable thickness is derived. Geometric and material non-linearity are considered to study the post-buckling and post-yielding behavior.

This study is divided into two parts, the first includes the post-buckling analysis of rectangular thin plate under the action of in-plane compression loading. In this part, the material non-linearity is neglected. The effects of initial imperfections, boundary conditions, type of loading, tapering ratios, and the direction of load actions on the post-buckling behavior are considered. The plate is analyzed with different initial imperfections ($w_0/t = 0.1, 0.2, 0.3, \text{ and } 0.5$) times the thickness of the plate and different tapering ratios ($t_a/t_0 = 1.1, 1.2, 1.3, 1.4, \text{ and } 1.5$).

It is concluded that the post-buckling behavior of thin plate is very sensitive to the magnitude of initial imperfection and magnitude of tapering ratio.

The second part includes the elasto-plastic analysis of rectangular plate under the action of in-plane compression loading. In this part, geometric and material non-linearity are included. The effect of initial imperfections, boundary conditions, slenderness ratios, aspect ratios, and tapering ratios on the ultimate strength are considered.

It is concluded that the ultimate strength decreases with the increasing of the initial imperfection and tapering ratio (for the same volume of plate).

LIST OF NOTATIONS

<i>Symbol</i>	<i>Description</i>
A	$6h_x^4 + 6h_y^4 + 8h_x^2h_y^2$
$[A]$	In-plane stiffness matrix.
a, b	Plate dimensions in x and y -directions, respectively.
B_x	$-4h_y^2(h_x^2 + h_y^2)$
B_y	$-4h_x^2(h_x^2 + h_y^2)$
C	$2h_x^2h_y^2$
c	Clamped edge.
$[C]$	Bending stiffness matrix.
c_t	$(t_a - t_o)/at_o$: Slope coefficient for thickness of plate.
D	$(Et_o^3)/12(1 - \nu^2)$ Flexural rigidity.
D_x	h_y^4
D_y	h_x^4
E	Modulus of elasticity.
$[E]^*$	Tangential elasto-plastic modular matrix.
f	Yield function.
G	Shear modulus.
h_x, h_y	Mesh size in x and y -direction, respectively.
m	Number of half-waves developed in the buckled shape.
M_x, M_y, M_{xy}	Bending and twisting moments (per unit width).
N_x, N_y, N_{xy}	In-plane stress resultants (per unit width).
P_x	Applied load in x -direction.
q	Uniformly distributed load (per unit area).
Q_x, Q_y	Shear forces (per unit width).
s	Simply supported edge.
S_{ij}	Deviatoric stress tensor.
t	Plate thickness.

t_a	Thickness at the side $x=a$.
t_o	Thickness at the side $x=0$.
t_{av}	Average thickness $((t_a+t_o)/2)$.
u_x	Displacement in x -direction.
ν	Poisson's ratio.
v_y	Displacement in y -direction.
w	Out-of-plane displacement.
w_o	Amplitude of initial imperfection.
$\{w\}$	Generalized nodal out-of-plane displacements.
x,y,z	Co-ordinates.
σ_o	Uniaxial yield stress.
$\bar{\sigma}$	Equivalent stress.
σ	Average applied uniaxial stress.
σ_{ij}	Total stress.
σ_b	Bending stress.
σ_m	Membrane stress.
ε	Average uniaxial strain.
ε_o	(σ_o/E) Uniaxial yield strain.
ε_{ij}	Strain tensor.
ε_{ij}^p	Plastics strain tensor.
τ	Shear stress.
τ_b	Bending shear stress.
τ_m	Membrane shear stress.
γ_{xy}	Shear strain.
$\Delta\lambda$	Plastic strain rate multiplier.
Φ	Stress function.
$\{\Phi\}$	Generalized nodal stress functions.

ACKNOWLEDGMENTS

I wish to express my continual thanks to my supervisor **Dr. Haitham Al-daami** for suggesting the problem and for his assistance and continuous guidance.

I am grateful to the Dean of the College of Engineering and the Head of the Civil Engineering Department in the University of Babylon for their co-operation and assistance.

Special thanks are presented to **Prof. Dr. Husain Mohammed Husain** for his help during the research.

Always, great thanks for my family, especially for my parents for their support to finish this work, for my brothers, for my sisters, and for my wife.

Finally, all my words cannot express about my thanks for all my friends, especially for **Muthana, Mushtaq, Mohammed S., Mohammed N., Sayed Ayad, my uncle Sayed Hamed** and **Ali A.** for their interests and support during this study.



*Haider Kadem
Amash*

٢٠٠٣

CERTIFICATION

We certify that we have read this thesis, titled (**Post-buckling and Post-yielding Analysis of Imperfect Thin Plate by Finite Difference Method**), and as examining committee examined the student **Haider Kadem Amash** in its contents and in what is connected with it, and that in our opinion it meets the standard of thesis for the Degree of Master of Science in Civil Engineering (**Structure**).

Signature: Asst. Prof. Dr. Amar Y. Ali **Signature:**

Name: (Member) **Name: Asst. Prof. Dr. Nameer A. Alwash**
(Member)

Date: ٥ / ٧ / ٢٠٠٣

(Member)

Date: ٥ / ٧ / ٢٠٠٣

Signature:

Name: Prof. Dr. Husain M. Husain
(Chairman)

Date: ٣٠ / ٦ / ٢٠٠٣

Signature:

Name: Asst. Prof. Dr. Haitham Al-Daami
(Supervisor)

Date: ١ / ٧ / ٢٠٠٣

Approval of the Civil Engineering Department
Head of the Civil Engineering Department

Signature

Name: Asst. Prof. Dr. Nameer A. Alwash

Date: ٥ / ٧ / ٢٠٠٣

Approval of the Deanery of the College of Engineering
Dean of the College of Engineering

Signature

Name: Asst. Prof. Dr. Haroun A. K. Shahad
Dean of the College of Engineering

University of Babylon

Date: ٨ / ٧ / ٢٠٠٣

Contents		Pages
Acknowledgment		
Abstract		<i>i</i>
Contents		<i>ii</i>
	Notations	<i>v</i>
Chapter One Introduction		
۱.۱ General		۱
۱.۲ Buckling Behavior of Plates.		۳
۱.۳ Modeling of Fabrication-induced Imperfections		۴
۱.۴ Scope of This Study		۵
Chapter Two Review of Literature		
۲.۱ General		۶
۲.۲ Buckling Analysis of Thin Plate		۶
۲.۳ Large Deflection Analysis of an Isolated Thin Plate		۹
۲.۴ Elasto-Plastic Analysis of an Isolated Thin Plate		۱۷
۲.۵ Large Deflection Elasto-Plastic Analysis of Thin Plate		۱۹
Chapter Three Post-buckling Analysis of Rectangular Thin Plate with Initial Imperfection		
۳.۱ General		۲۹
۳.۲ Geometric Non-linearity		۳۰
۳.۳ Basic Assumptions		۳۱
۳.۴ Theory of Plate Analysis		۳۱

۳.۴.۱ Marguerre's Theory	۳۱
۳.۴.۲ Background to Marguerre's Theory	۳۲
۳.۵ Derivation of Marguerre's Equations for an Initially Imperfect Elastic Plate	۳۳
۳.۵.۱ Plate with Constant Thickness	۳۳
۳.۵.۲ Plate with Variable Thickness	۳۸
۳.۶ Boundary Conditions	۴۱
۳.۷ Membrane Stress Distribution Inside The Plate	۴۴

Chapter Four

Elasto-Plastic Analysis of Rectangular Thin Plate with Initial Imperfection

۴.۱ General	۴۵
۴.۲ Material Non-linearity	۴۷
۴.۲.۱ Yield Criterion	۴۷
۴.۲.۲ Elasto-Plastic Stress-Strain Relationships	۴۸
۴.۳ Yield Criterion Formulation	۵۰
۴.۴ Incremental Forms of The Governing Differential Equations	۵۳
۴.۵ Ultimate Strength of Plate Panel under The Action of Complex Stress Distribution	۵۵
۴.۵.۱ Unbuckled Behavior	۵۶
۴.۵.۲ Post-buckling Behavior	۵۷
۴.۵.۳ Ultimate Load Behavior	۵۸
۴.۶ Solution of Non-linear Equations by Numerical Methods	۵۸

Chapter Five Applications and Discussions of Results

٥.١ General	٦١
٥.٢ Computer Program	٦٢
٥.٣ Post-buckling Analysis	٦٤
٥.٣.١ Mesh Effect	٦٤
٥.٣.٢ Comparison with Experimental Investigation	٦٥
٥.٣.٣ Comparison with Available Theoretical Investigation	٦٧
٥.٣.٤ Parametric Study	٧٢
٥.٣.٤.١ Effect of Boundary Conditions	٧٢
٥.٣.٤.٢ Effect of Tapering Ratio	٧٥
٥.٤ Elasto-Plastic Analysis	٧٨
٥.٤.١ Plate Dimensions and Properties	٧٨
٥.٤.٢ Effect of Plate Aspect Ratio (a/b)	٧٨
٥.٤.٣ Comparison with Other Investigations	٨٠
٥.٤.٤ Parametric Study	٨٧

Chapter Six Conclusions and Recommendations

٦.١ General	٩٣
٦.٢ Conclusions	٩٣
٦.٣ Recommendations	٩٤
References	٩٦

CERTIFICATION

I certify that this thesis titled “**Post-buckling and Post-yielding Analysis of Imperfect Thin Plate by Finite Difference Method**”, was prepared by “**Haider Kadem Amash**” under my supervision at Babylon University in partial requirements of the fulfillment for the degree of Master of Science in Civil Engineering.

Signature:

Name: Haitham hassan Al-daami

Date: / / ٢٠٠٣

INTRODUCTION

1.1 General

Thin-walled structures are widely used as load carrying members of structures such as bridges, ships, aircraft and buildings with steel framing. The cross section of a thin-walled structure is made up of thin plates with constant or variable thickness joined along their edges. The plate thickness is small compared with other cross-sectional dimensions, which are in turn often small compared with the overall length of the member or substructure.

There are several reasons why thin-walled structures must be given special consideration in their analysis and design. That is because of their inherent properties of thickness, which is small when compared with other dimensions. This will make these structures susceptible to failure by instability. Accurate determination of the buckling load incorporating all the possible failure modes including local, local-torsional, distortional, and flexural-torsional buckling, as shown in Figure (1.1), is therefore very important⁽¹³⁾.

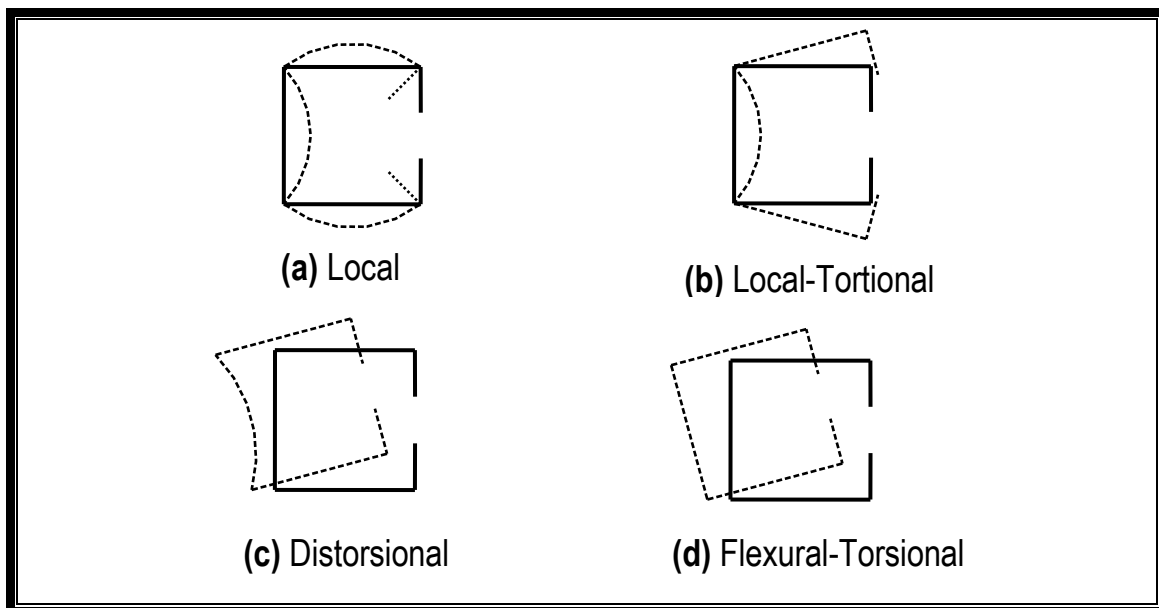


Figure (1.1): Possible buckling modes⁽¹³⁾.



To maximize the saving in self-weight, the component plates of the structural member are designed to be of slender properties. They will then have a low elastic critical load and will normally operate in the post-buckling range so that advantage must be taken of their post-buckling reserve of strength.

Traditionally, such structures have been designed according to the allowable stress principles so that a linear elastic analysis of the stress distribution was sufficient. To produce design rules of reasonable simplicity, plastic collapse mechanism has been proposed for the prediction of the ultimate load capacity^(r_a). These are normally derived from an assumed collapse mode based on the observation of experimental behavior.

A collapse mechanism, by definition is based on an assumed state of stress in a girder at failure. It makes no attempt to consider the behavior during the approach to failure in the non-linear post-buckling range. A proper analysis of this phase of behavior can provide a better understanding of the development of non-linearity and the spread of yielding leading to collapse. Any assumed collapse mechanism can be then placed on a firmer footing and its range of application extended without the need for extensive and expensive experimentation.

This study describes the development of such analysis, employing the finite difference method for rectangular thin plates. The analysis is applicable to different plates with various boundary conditions and various initial imperfections, which continue to operate in the post-buckling range. It must be; therefore, taken into account the effects of geometric non-linearity arising from the plate buckling and also the effects of material non-linearity due to the spread of yielding during the approach to collapse.



1.2 Buckling Behavior of Thin Plates

Plate elements are used in naval and aerospace applications, and in construction of civil structures and industrial buildings. These elements are subjected to normal and shearing forces acting in the plane of the plate, as shown in Figure (1.2). The most important phenomenon in such structures is the local buckling of the plate element. The load producing this phenomenon is called the critical load. This critical load state characterizes the natural equilibrium of an axially loaded plate. At this state, it is observed that the plate would keep the small out-of-plane perturbations and still remains stable. The importance of the critical load is the initiation of a deflection pattern, which, if the load is further increased rapidly leads to very large lateral deflections and eventually to a complete failure of the plate. It is a dangerous condition, which must be avoided^(1,2).

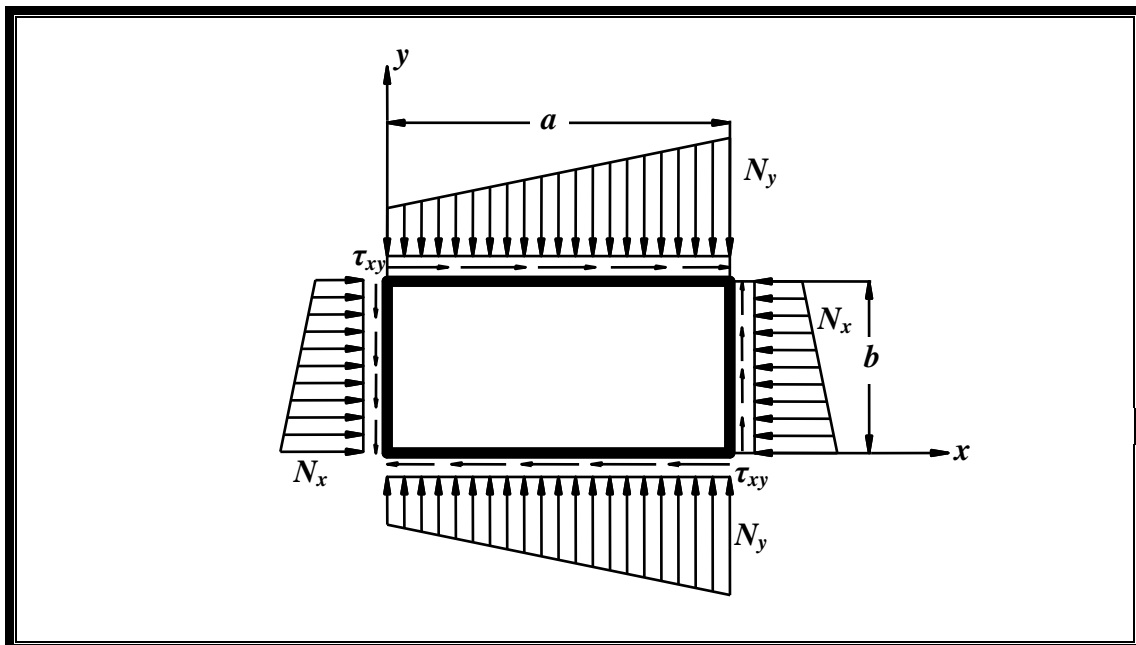


Figure (1.2): Plate under a general pattern of combined external loads.

1.3 Modeling of Fabrication-induced Imperfections

When the plates are fabricated the factory will not be able to produce perfectly flat surface for plates but thus they will have very small initial imperfection. Also to fabricate stiffened plate structures, welding is normally used and thus the post-welding initial imperfections (initial deflections and residual stresses) are developed in the structure. In an advanced structure design capacity calculations should accommodate post-weld initial imperfections as parameters of influence.

Figure (1.3) shows schematic of the post-weld initial deflections in ship stiffened plate structures. The measurements of welding-induced initial deflection for plating in merchant ship structures reveal a complex multi-wave shape in two directions^(6,7).

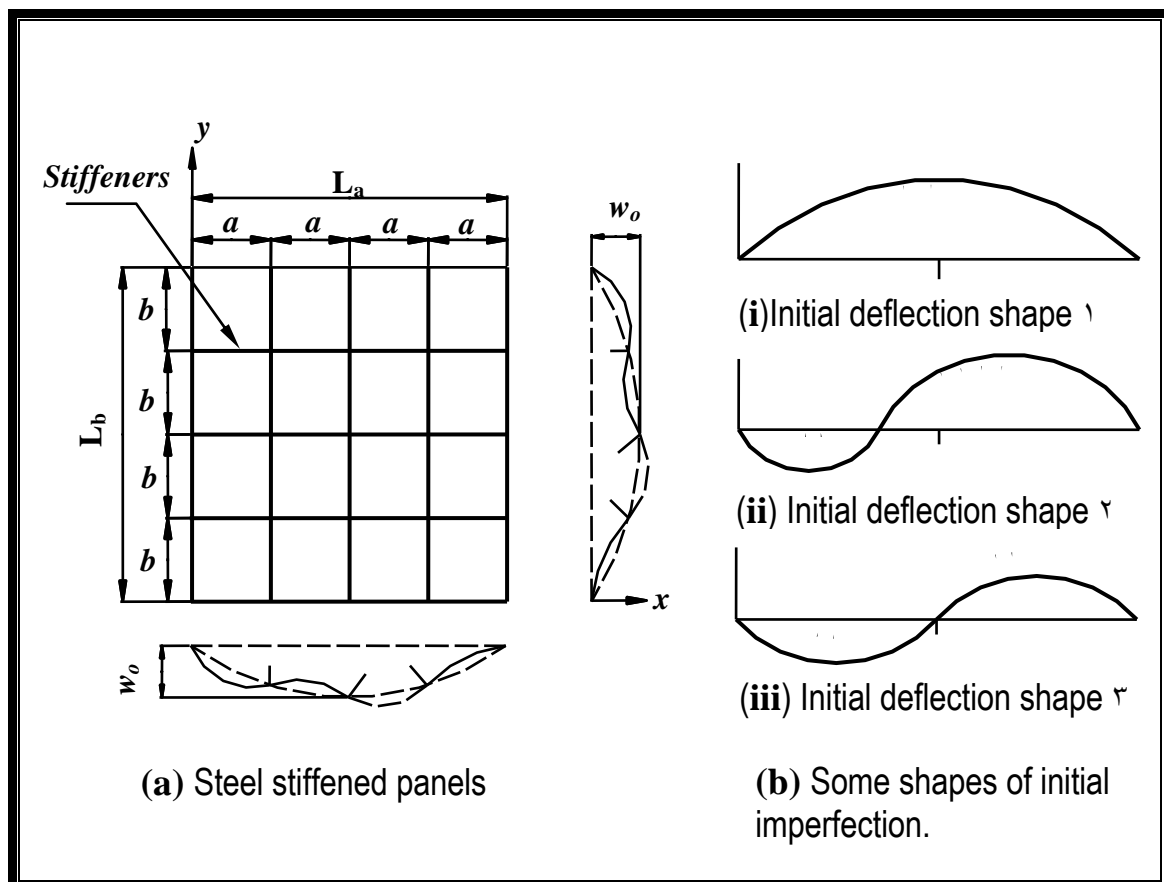


Figure (1.3): Fabricated related initial deflection in steel stiffened panels.

1.4 Scope of This Study

This study is divided into two parts; in the first, there is an attempt for formulating a simplified finite difference method to analyze the elastic large deflection behavior of rectangular thin plates. The effect of initial imperfection, boundary conditions, type of loading, tapering ratios, and direction of loading are considered.

The second part deals with a large deflection elasto-plastic analysis of rectangular thin plates. The effect of initial imperfection, boundary conditions, aspect ratios, slenderness ratios, tapering ratios, and direction of loading are considered.

The present study is given through six chapters. This introduction represents chapter one. In chapter two, a brief of review of early studies and the more advanced studies on the subject are given with an interpretation of the results as possible. A post-buckling behavior of rectangular thin plate with initial imperfection is presented in chapter three. An elasto-plastic behavior of rectangular thin plate with initial imperfection is presented in chapter four. The application and the presentation of the results with discussion are given in chapter five. Finally chapter six introduces the conclusions and recommendations for further studies.



REVIEW OF LITERATURE

2.1 General

The review presented here aims at showing the most important developments and steps that have been taken on the path leading to the knowledge of today in this subject. As mentioned in the introduction, the problems concerning compressive loads applied to a thin plate have interested a large amount of researchers all over the world.

In this chapter the literature survey is divided into four major scopes: -

1. Buckling Analysis of Thin Plate.
2. Large Deflection Analysis of an Isolated Thin Plate.
3. Elasto-Plastic Analysis of an Isolated Thin Plate.
4. Large Deflection Elasto-Plastic Analysis of Thin Plate.

2.2 Buckling Analysis of Thin Plate

As cited in Ref. (10), **Bryan**⁽⁹⁾ [1891] solved the problem of a simply supported rectangular thin plate with two opposite sides carrying uniform compressive loads. His study was the first attempt to derive the solution of plate buckling problem by the using energy principle method.

Salvadori⁽¹⁰⁾ [1949] introduced a numerical and graphical computation of buckling loads by successive approximation. The finite difference method was used to solve the buckling problem. This solution is obtained purely by numerical computations, which is greatly enhanced by a simple method of extrapolation. This procedure was applied to various cases of buckling of beams, plates, and shells.



Chehil and Dua⁽¹¹⁾ [1993] employed a perturbation technique to determine the critical buckling stress of a simply supported rectangular plate with variable thickness cross section. The differential equation was derived for a general thickness variation in one direction. Their analysis included a stiffened plate, this stiffener is fabricated from the factory. The major advantage of this analysis lies in the fact that the fabrication of these stiffened plates is very simple as compared to the manufacturing of plate, which has a linear or exponential taper.

Kobayashi and Sonoda⁽¹²⁾ [1990] used a power series method with the use of a co-ordinate transformation to solve analytically the buckling problem of uniaxially compressed rectangular plates with linearly tapered thickness. This solution was limited where the compressed edges were simply supported and the unloaded edges are (simply supported, clamped, or free). Their conclusion was that the buckling load is highly dependent on the thickness variation.

Recently, **Chin, et al.**⁽¹³⁾ [1993] used the finite element method to predict the buckling capacity of arbitrary shaped thin-walled members under any general load and boundary conditions. The thin plate elements used in this method contained 30 degree of freedom (d.o.f): [14 d.o.f for the in-plane (membrane) action and 16 d.o.f for the out-of-plane (bending) action]. The linear and geometry stiffness matrices for the thin plate element was derived explicitly based on the principle of minimum total potential energy. This method was used for thin-walled structures involving distortional and flexural-torsional buckling failure mode.

Ohga, et al.⁽¹⁴⁾ [1995] used an analytical procedure for the elastic buckling problems of thin-walled members with variable thickness cross section by using the transfer matrix method. The transfer matrix was derived from the non-linear differential equations for the plate panels with variable thickness by using the Fourier series expansion in the



longitudinal direction and then applied a numerical integration in the lateral direction.

Husain, et al. ^(v) [2002] used the finite difference method to estimate the buckling factor of a rectangular thin plate with variable thickness cross section. Their results were presented graphically for the buckling coefficients for uniaxially compressed plates and the loaded edges were (simply and clamped supported) and for different plate aspect ratios, different tapering ratios, and different boundary conditions. This study has showed that the value of the buckling load is very sensitive for tapering ratio.

2.3 Large Deflection Analysis of an Isolated Thin Plate

The large deflection theory of isolated plates is more complicated than the small deflection theory because of the geometric non-linearity. The non-linearity arises because the deflection increases the membrane stresses and these stresses are redistributed and begin to dominate over flexural action. This problem was treated by Von-Karman's equations and Marguerre's equations^(vi).

Coan ^(vii) [1951] solved Marguerre's equations to study the post-buckling behavior of plates by assuming the deflected shape of a rectangular simply supported plate as a double Fourier series and overcame the restriction on Levy's solution. Edge pull-in of three kinds was allowed for by adding further complementary functions to the expressions for the stress function (Φ). The theory was applied to a square plate with the central initial deflection ($w_0 = \cdot \cdot t$) and the results were compared with the experimental values.

Yamaki ^(viii) [1959] gave an extension of Levy and Coan's works by solving the problem with different boundary conditions, combining two kinds of loading conditions [**case (1)**], the edges are kept straight by the distribution of the normal stresses, while in **case (2)**, the edges are free



from stresses]. The solution of Marguerre's fundamental equations for large deflections of thin plates with slight initial curvature was presented in his study for the case of a rectangular plate subjected to edge compression load by using a double trigonometric series with coefficients to solve these equations. The conclusions from this study are: -

١. The deflection in **case (١)** is always smaller than the corresponding value in **case (٢)**.
٢. Under loads much greater than the critical, the net deflection for the initially deflected plate is smaller than that for the initially flat plate.

Stein^(٦١) [١٩٦٠] proposed a purely mathematical approach to explain the possibility of a change of buckling wave form. He investigated the post-buckling behavior of simply supported rectangular plates in end compression load by solving the first few equations and presented non-dimensional load-shortening curves for plates with various length-width ratio (a/b) (١ to ٥). These curves were obtained by using the values of (m), which intersect with these basic curves for the range plotted. The intersections of the load-shortening curves indicate possible changes in buckle pattern, as shown in Figure (٢.١).

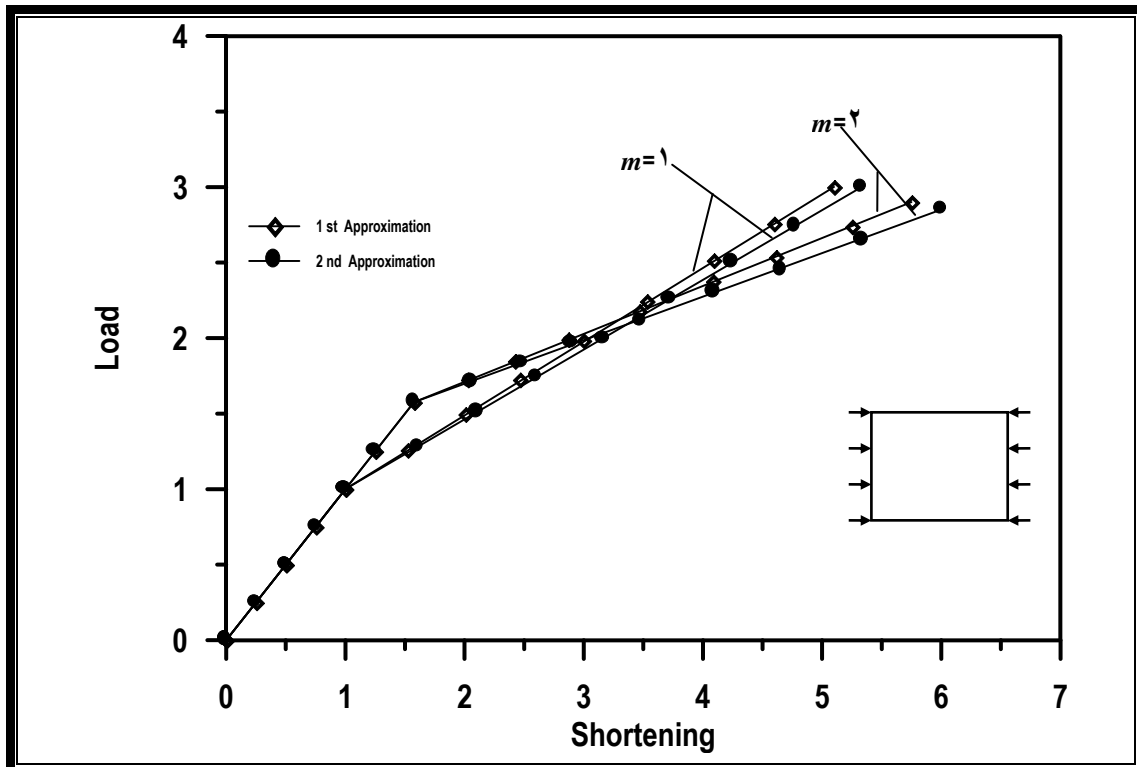


Figure (٢.١): Non-dimensional load-shortening curves of rectangular simply supported plates in compression, $a/b=١$.

Basu and Chapman⁽⁴⁾ [1966] used the finite difference method to investigate the large deflection behavior of transversely loaded rectangular orthotropic plates, having elastic flexural, and extensional and shearing edge restraint and derived the differential equations and boundary conditions and showed the effect of membrane action at a large displacement stage.

Aalami and Chapman⁽¹⁾ [1969] used the finite difference method for the large deflection behavior of rectangular orthotropic (including isotropic) plates under symmetrical or anti-symmetrical transverse loading and in-plane loading. The essential difference between **Basu and Chapman** [1966] and **Aalami and Chapman** [1969] is that the last studied the behavior of plates under transverse and in-plane loading and with initial imperfection and rotational nodes and tangential boundary restraints.

Rushton⁽²⁾ [1969] demonstrated the dynamic relaxation method to analyze the post-buckling behavior of plates with variable thickness and with edge restrained against lateral expansion. In this approach the nodes had been considered to have a constant thickness different from the thickness of the previous node. A variable thickness plate was considered in which the thickness is defined by:

$$t_x = t_0 e^{\lambda x} \quad (2-1)$$

with λ chosen so that at the thicker end $t = \nu t_0$.

He observed that the finite difference tends to underestimate the initial buckling load by about 3% when compared with the exact solution.

Sherbourne and Korol⁽³⁾ [1972] used experimental and theoretical investigations for the post-buckling behavior of axially compressed plates. They observed that the load predictions were overestimation to



the real capacity of the plates and they also observed that when the imperfections were incorporated into the theoretical solution the scale-down values of the theoretical prediction accord more nearly with the experimental results.

Colville, et al. ⁽¹⁵⁾ [1973] used a general method for the solution of the Von-Karman plate equations by using a direct iterative finite element procedure. Their study included all applicable non-linearity in the strain displacement equations and the use of fully compatible finite element for both the in-plane and bending action and resulted in monotonic convergence to the theoretical solution as the structure idealization. This procedure gave minimum computational time.

Williams and Walker ⁽¹⁶⁾ [1975] derived an explicit expression for the load-deflection relationship for simply supported uniformly loaded square plate based on the perturbation approach. The results were presented for the plates with variety of geometries, boundary constraints and in-plane loading conditions. The accuracy of these results was sufficient for engineering design purposes.

Colville and Shye ⁽¹⁷⁾ [1979] used the finite element method to investigate the post-buckling behavior of plates. In this study, the finite element solution procedure was employed for the large deflection problems based on the theory developed by Collvile, who had shown that for post-buckling applications the uncoupled equilibrium equations may be written as: -

$$[\mathbf{K}_w + \mathbf{K}_N]\{\mathbf{w}\} = \mathbf{q} - [\mathbf{K}_g]\{\mathbf{w}\} \quad (2-2)$$

$$[\mathbf{K}_u]\{\mathbf{u}\} = \mathbf{f} - \mathbf{G}_N \quad (2-3)$$

in which \mathbf{K}_w = bending stiffness of the undeformed plate; \mathbf{K}_g = the geometric stiffness of the plate; \mathbf{K}_N = the non-linear stiffness matrix; \mathbf{w} =



nodal bending displacements; q = applied bending loads; K_u = in-plane stiffness of the undeformed plate; G_N = a non-linear membrane correction force vector; u = nodal in-plane displacements; f = applied in-plane loads.

As cited in Ref. (εο), **Fok**⁽¹⁰⁾ [1980] used the finite difference method to study the influence of imperfections in non-linear behavior of rectangular plates. He analyzed the elastic post-buckling behavior of seventy-three isolated plates and confirmed his study by experimental work. The conclusion was that the post-buckling is very sensitive to the imperfections and the finite difference method gives results close to the experimental results.

Sridhran and **Graves-Smith**⁽¹¹⁾ [1981] used two versions of the finite strip method for the post-buckling behavior of prismatic plate structures under compression load. Version I based on the classical approximation is found to be a powerful method for dealing with a variety of plate structures of practical interest. Version II which is complementary to version I, is shown to be necessary when investigating the effect of corner displacements on the stiffness of the structures.

Usami⁽¹²⁾ [1982] used the finite element method to investigate the elastic post-buckling behavior of rectangular plates in combined compression and bending. The analysis started with Marguerre compatibility and used the energy method to obtain the solution. An effective width formula was proposed to analyze the post-buckling behavior of thin-walled steel members in bending or in combined compression and bending.

Fok⁽¹³⁾ [1984] presented two numerical methods for correlating the experimental critical load and the initial imperfection of rectangular plates loaded in edge compression from recordings of load and deflection. The three points technique makes use of three sets of such readings to

form a system of non-linear simultaneous equations, the solution of which yields the critical load, initial imperfection, and the constant governing the curvature of the load-deflection curve. The least square technique employs an applicable solution to the neutral bifurcation. Both of the two techniques were applied to various experimental results and it was found that the calculated values were very close to the experimental values.

Galerkin method has been widely applied to both static and dynamic problems in the area of solid mechanics. The idea of the method is minimization of error by orthogonalizing the error with respect to a set of given (or basis) functions⁽¹²⁾.

Ueda, et al. ⁽¹³⁾ [1988] studied the large deflection behavior of a rectangular plate by an efficient semi-analytical method. An incremental form of the governing differential equations of plates and stiffened plate with initial deflection had been derived. For each load increment, these equations were solved by the Galerkin method with especial consideration of simply supported boundaries. These equations take the following form: -

$$D\nabla^4(\Delta w) = \left(\begin{array}{l} \frac{\partial^2 \Phi_{i-1}}{\partial y^2} \frac{\partial^2(\Delta w)}{\partial x^2} + \frac{\partial^2(\Delta \Phi)}{\partial y^2} \frac{\partial^2 w_{i-1}^t}{\partial x^2} \\ + \frac{\partial^2 \Phi_{i-1}}{\partial x^2} \frac{\partial^2(\Delta w)}{\partial y^2} + \frac{\partial^2(\Delta \Phi)}{\partial x^2} \frac{\partial^2 w_{i-1}^t}{\partial y^2} \\ - 2 \frac{\partial^2 \Phi_{i-1}}{\partial x \partial y} \frac{\partial^2(\Delta w)}{\partial x \partial y} - 2 \frac{\partial^2(\Delta \Phi)}{\partial x \partial y} \frac{\partial^2 w_{i-1}^t}{\partial x \partial y} \\ + \frac{\Delta q}{t} \end{array} \right) \quad (2-8)$$

$$\nabla^4(\Delta \Phi) = Et \left(2 \frac{\partial^2 w_{i-1}^t}{\partial x \partial y} \frac{\partial^2(\Delta w)}{\partial x \partial y} - \frac{\partial^2 w_{i-1}^t}{\partial x^2} \frac{\partial^2(\Delta w)}{\partial y^2} - \frac{\partial^2 w_{i-1}^t}{\partial y^2} \frac{\partial^2(\Delta w)}{\partial x^2} \right) \quad (2-9)$$

where w_i = total deflection at the end of the load increment ($i-1$), Φ_{i-1} = stress function at the end load increment ($i-1$), Δw_i = increment of deflection through current load increment, $\Delta \Phi_i$ = increment of stress function through current load increment. A procedure of equilibrium correction at intermediate load steps must maintain that good accuracy of the solution may be maintained with larger load steps because the small quantities of higher order of (Δw , and $\Delta \Phi$) are neglected.

Recently, **Sun and Williams**⁽¹⁷⁾ [1997] employed Koiter's theory to analyze the initial post-buckling behavior of prismatic plate assemblies which are composed of isotropic materials and subjected only to longitudinal compressive load. The post-buckling equations were solved exactly and the post-buckling coefficients were obtained by exact integration for all component plates. Their conclusion was that the post-buckling characteristics of the stiffened plate are influenced significantly by the height of the stiffener.

Lam⁽¹⁸⁾ [1998] used computational procedure for the post-buckling behavior of a strut with initial imperfection under progressive end shortening. A polynomial expression was used to simulate the actual initial imperfection, while the deformations were expressed by a suitable trigonometric series. The non-linear equilibrium equations were solved by a Newton-Raphson procedure. His results were compared with other solutions and with experimental results.

Bjelajac⁽¹⁹⁾ [2000] used the finite difference method for the post-buckling behavior of thin elastic plates subjected to in-plane loading. This method was used to analyze plates with initial curvature and with variable boundary conditions. He derived equations from the minimum potential energy in a potential force field in a manner, which does not

involve additional nodal displacements. This study considered that the unloaded edges are kept straight and fixed ($u_x=0$). His results were compared with other methods.

Mirambell and Zarate^(xi) [2007] used the finite element method to investigate the post-buckling behavior of plates with variable depth under in-plane shear loading. Their conclusion was that the post-buckling and the strength reserves tend to diminish by increasing the slope of the bottom flange, this is due to the decrease in the vertical component of the tension field.

In 2007, **Sun, et al.**^(xv) proposed a procedure to analyze the post-buckling behavior of isotropic prismatic plate assemblies. The perturbation method combined with the variable separation method was used to obtain the perturbation equations of first and second order. The first order problem is a transcendental eigen-values problem and it is solved analytically by using Wittrick-William's algorithm. The second order problem solved analytically to obtain displacement functions corresponding to axially constant and axially harmonic problems.

Jayachandran, et al.^(xv) [2007] derived incremental matrices for thin initially imperfect plates with small out-of-flatness by using the minimum potential energy principles. Explicit coefficients of the displacement gradient tensor had been evaluated. These matrices were used in combination with any thin plate element. The formulations were incorporated in a software plot-cold.

Mohammed^(xv) [2007] studied the buckling and post-buckling behavior by finite element method of rectangular isolated steel plates under in-plane shear load. This study considered the effect of initial imperfection and boundary condition on the total behavior of the plate.

His study was divided into two parts, the first included analysis of isolated plates under in-plane shear load with different values of initial shapes. The second part included analysis of isolated plates under in-plane shear load with different cases of condition support. His conclusion was that the behavior of a thin-walled structure is usually sensitive to the nature and magnitude of initial imperfection.

More recently, **Zou** and **Qiao**^(vii) [2002] presented a higher order finite strip method for the post-buckling behavior of imperfect composite plates subjected to progressive end shortening. The arbitrary nature of the initial geometric imperfection induced during manufacturing was accounted for in the analysis. The non-linear equilibrium equations were solved by a Newton-Raphson method. This study showed that the post-buckling behavior of an imperfect composite plate depends not only on the material lay up, snap-to-thickness and anisotropy of the laminate, but also on the direction of induced out-of-plane imperfection.

2.3 Elasto-Plastic Analysis of Isolated Plates

Most engineering structural materials such as steel and aluminum are ductile where their strains grow much more than at elastic limit, as the structure is loaded beyond the elastic limit. Plastic strain occurs and causes a redistribution of stress. The computation of this distribution of stress has been considered to be complicated; and a simplified method to compute the ultimate strength of the structure under a monotonic proportional load has been given by many investigators. This method, known as limit analysis, is to calculate the upper bound and lower bound of the system of loads, which the structure can take without collapse. In the limit analysis, the material is generally assumed to be ideally plastic and the strain hardening effect is neglected.

In the upper bound theorem: if a collapse configuration is assumed, the external loads computed by the principle of “virtual velocities w_i ” will be equal to or greater than the true collapse load.

In the lower bound theorem: if a stress configuration can be found which exceeds yields nowhere in the structure and which is in equilibrium with the external loads, these external loads will be equal to or less than the true collapse limit^(r4).

Hodge^(r4) [1959] gave a summary of the limit analysis theory pertaining to rectangular slabs. Using trial distribution of moments and deflections, he utilized the equilibrium and energy approach respectively, and arrived at lower and upper bounds on the collapse load with the Von-Mises failure condition. Combination of the best upper and lower bounds yields a difference of about 2.0%.

As cited in Ref. (5), **Koopman** and **Lance**^(r4) [1965] introduced the idea of linear programming combined with finite difference approximations to arrive at lower bounds of the collapse load of continuous structural components made of perfectly plastic material. The lower bounds obtained for a square plate with simply supported and clamped edges agree very favorably with the existing upper bounds. The method is applicable to arbitrary structural components with arbitrary loading. A relatively coarse grid size gives a satisfactory solution. It is perhaps possible, using the linear programming approach and energy considerations to obtain upper bounds of the collapse load.

Bhaumik and **Hanley**⁽⁵⁾ [1967] introduced an analysis of square plates in elastic and elasto-plastic states by finite difference method by using three different criteria (Johanson, Von-Mises, and Tresca). The finite difference technique has the added advantage of assuring a convergence criterion as the grid size is reduced. To illustrate the

potential of the method, two plates with simply and clamped supported had been analyzed. The results of the collapse load are shown in Table (۲.۱).

Table (۲.۱) Collapse load (q_a^*/M_p) by finite difference analysis of square plates.

Boundary Conditions	Von-Mises	Tresca	Johanson
Simply Supported plate	۲۴.۰	۲۲.۱	۲۰.۰
Clamped Plate	۴۱.۷۷	۳۷.۴۳	۴۱.۸۴

The limit analysis works well for ideally plastic structures but it is not applicable to structures with strain hardening. Many structures are of materials with strain hardening; therefore, a method to calculate the redistribution of the stress caused by plastic strain is needed. Rectangular plates under bending have commonly occurred in structures. A detailed procedure for calculating the stresses and deflections of rectangular plates subjected to an arbitrary sequence of loads in the plastic range was described by **Lin** and **Ho**^(۳۶) [۱۹۶۸].

Lin and **Ho**^(۳۶) [۱۹۶۸] used the analogy between the body force and the plastic strain gradient as a method of analysis in their work. This concept has been successfully applied to compute the creep and plastic bending of circular plates and creep bending of rectangular plates. It was shown that the elastic strain in plates has the same effect on causing stress and strain field as the set of lateral loads, edge forces and moments. Strain beyond the elastic limit in crystalline materials consists of two parts: the elastic part caused by the elastic deformation of the lattice structure, and the plastic part caused by slip of one layer of atoms over another.

2.4 Large Deflection Elasto-Plastic Analysis of Plates

The recent years have seen an increasing tendency to design large structural members as in welded steel stiffened plate systems. The geometries used in many heavy structures fail in compressive load by a combination of yielding and buckling. Analysis of strength of plates in such structures is complicated by the non-linearities caused by the large out-of-plane displacements and by yielding of parts of the plate. The obvious significance of initial out-of-flatness was shown in many simplified analyses.

Wah^(r) [1958] introduced a closed form solution for the deflections, residual deflection, residual membrane tensions, and other quantities of engineering interest for infinitely long clamped rectangular plates with large deflections under uniform pressure. The analysis assumed infinite rigidity, in the plane of the plate, of the boundary supports. His formula is based on several idealizations, which cannot be exactly duplicated in practice.

Abdel-Sayed^(r) [1969] introduced a formula for the effective width of wide thin plates, under end compressive load in their planes by solving the Von-Karman governing differential equations. This solution was based on the assumption that the deflection form at the instant of buckling is preserved after loading exceeds the buckling limit. This formula was used for plates with a small initial deflection or for plates with edges parallel to loading was free to move in the plane of the plate. This formula takes the following form: -

$$\frac{\lambda}{t} = \frac{1}{2} \left[1 + \frac{n_{cr} \left(\frac{e}{e + e_o} \right)}{n_x} \right] \frac{b}{t} \quad (2-7)$$

to find the ratio $(e/e + e_o)$, the unknown magnitude of the deflection e , will be calculated by the following equation: -

$$e.n_{cr} = (e + e_o) \left\{ n_a + \frac{Et}{16} \pi^2 \left[\left(\frac{a}{L} \right)^2 + \left(\frac{a}{b} \right)^2 \right] \frac{1}{b^2} (e^2 + 2e.e_o) \right\} \quad (2.1)$$

here λ = effective width; n_{cr} = critical compressive force per unit width; b = width of plate; a = length of one buckled panel of plate; n_x = axial loading per unit length; n_a = average loading per unit width of plate; e = magnitude of deflection.

As cited in Ref. (v), **Moxham**^(xi) [1991] used Ritz procedure to solve the large deflection in elasto-plastic behavior of plates with a small initial imperfection under in-plane compression load. This study included plasticity through a volume integration in which the plate was divided into five layers through its thickness. His results were given for plates with different slender ratios ($b/t=3, 4, 5, 6$) and with a very small initial imperfection ($w_o/t=0.05$ and 0.1) and with the edges of the panel simply supported and free to pull-in.

Lin, et al.^(vii) [1992] introduced an analytical method for predicting the elasto-plastic bending of rectangular plates with large deflection. The effects of the plastic strain and the large deflection on plate deformation were shown to be the same as a set of applied external forces on the plate in the classical elastic small deflection theory. Their observation was that the deflection increased only slightly by plastic strain and the maximum extreme fiber stress relieved by plastic yielding.

Crisfield^(viii) [1995] used a finite element formulation for the large deflection elasto-plastic analysis of thin mild steel plates subjected to in-plane compressive load. This method was used to trace the behavior of



imperfect steel panels over the full load range, including the unloading stage following collapse. A series of simply supported thin plates under uniaxial compression were analyzed to study different in-plane boundary conditions, levels of geometric imperfection and residual stress. The load-shortening curves to predict the behavior of wide eccentricity stiffened plates subjected to uniaxial compression had been derived. He obtained good correlation with experimental and showed that the imposition of straight edge constraint to the unloaded edges had no influence on the behavior of moderately stocky plates whereas increases in the collapse load of (5-10%) were achieved for thinner plates.

Harding, et al. ⁽³⁷⁾ [1977] introduced a finite difference formulation for the large deflection elasto-plastic analysis of initially imperfect thin rectangular plates subjected to in-plane loads. The elasto-plastic rigidities were calculated by using a rigorous multi-layer approach, and the governing equations were solved in an incremental form by using dynamic relaxation. Their program was used to study the effects of both uniaxial and biaxial residual stresses due to welding and out-of-plane imperfection. The loading included tension and compression and their interaction with co-existing shear. Their conclusion was that the effect of initial imperfection on the ultimate collapse behavior of shear is small and a partially restrained panel (without transverse restraint on top and bottom edges) offers a considerable increase in design strength over the four edges of unrestrained condition.

Little ⁽³⁸⁾ [1977] used a simple formulation of a minimum energy principle for the analysis of plate collapse. This method is rigorous and yet economical in its use of the computer. His collapse analysis included a procedure which makes allowance for the effect of a large shortening increment where his results showed, surprisingly, that the predicted load-

shortening response of a typical plate was only marginally dependent on the increment size. He presented results for biaxial in-plane compression and compared his results with previous theoretical work, both elastic and elasto-plastic analysis where gave agreement.

Frieze, et al. ⁽¹⁹⁾ [1978] presented a theoretical treatment for the large deflection elasto-plastic analysis of plates by using a finite difference formulation with dynamic relaxation iteration. Increment form was used to the tangential elasto-plastic rigidities so that it can be used in the constitutive equations. The in-plane loading was applied by means of displacements. Their conclusion was that the dynamic relaxation is suitable to study plastic large deflection behavior of plates and that it probably offers both computer time and storage advantages for such analysis.

Rerkshanandana, et al. ⁽²⁰⁾ [1981] applied a finite element method to study the elastic-plastic post-buckling behavior of initially deflected and eccentrically loaded steel plates and box sections. A computer program based on a finite element (rectangular element) incremental displacement method had been developed. The mathematical formulation was based on an incremental virtual Lagrangian formulation and used a modified Ilyusion yield criterion with the associated flow rule to incorporate in the analysis the plasticity effect of the plate material. Their proposition was that the empirical formula to predict the ultimate strength of eccentrically loaded plates whose unloaded edges are either simply supported-simply supported, clamped-clamped, or simply supported – clamped is to be based on an extensive numerical study.

Ueda and Yao ⁽²¹⁾ [1982] presented a new mechanism of plastic hinge based on the incremental theory of the plasticity and derived the elastic-plastic and plastic stiffness matrices for one-dimensional



members. Using this plastic hinge, a method of elastic-plastic analysis of space-framed structures was well developed including the effect of large deflection. This basic idea of plastic hinge method for plates and solid bodies was developed. The basic theory of the new method was based on using the ordinary finite element method (the stiffness method).

In this theory, the yield condition at the i th node of an element is described as follows: “the i th node becomes plastic when the resultant stresses at this node satisfy the appropriate plasticity condition and the plastic deformation is developed only at the nodes”.

For the element with k plastic nodes, the relation between the increments of the nodal force, df , and the nodal displacement, du , is derived in the following form:

$$df = k^p du \quad (2-1)$$

in this equation k^p is either elastic-plastic or plastic stiffness matrix and was expressed in explicit form. When an element is subjected to constant strain, the element becomes plastic in the entire volume if the yield condition is satisfied at any point. Simultaneously, the plastic node is formed at every node of the element. Completely the same plastic stiffness matrix is obtained by either the ordinary finite element method or by the plastic node method. From these facts the accuracy of the solution by this method is anticipated to be of the same order as that by the ordinary finite element method when the element division increases.

Bradfield and **Stonor**^(A) [1982] presented a simplified elastic-plastic analysis for plates uniaxially compressed in their plane. Their assumption was that the plates are not initially flat and contain residual stresses due to welds at the longitudinal edges and the formulation was based on physical models and tested with other previous numerical

solutions. These solutions based on full section yield criterion. A simple criterion was given for the plate shortening at which the maximum loads were carried by welded and unwelded plates. These lead to single calculations of plate strength.

Paik and Kim^(ϵ^v) [1989] presented a new and simplified rectangular finite element having only four corner nodal points to analyze the elastic-plastic large deformation behavior up to the ultimate limit state of plates with initial imperfections. The finite element is contains the geometric non-linearity caused by both in-plane and out-of-plane large deformation because for very thin plates the influence of the former is not negligible. A simple matrix operation was derived for the elastic-plastic large deflection to treat the expanded plastic zone in the plate thickness direction of the element based upon the concept of plastic node method.

Paik, et al.^(ϵ^v) [1992] introduced a new buckling formula for all edge supported plate panels subjected to combined in-plane and lateral loads. This formula included the effect of welding residual stress and edge condition effects. Their conclusion was that by using this formula, about 10% of the critical plate buckling strength is additionally admitted at the severe case and the plate buckling strength is very much dependent on the edge conditions as well as the plate thickness.

Usami^(ϵ^v) [1993] proposed a formula based on extensive numerical results of elastic-plastic large deflection analysis of simply supported imperfect plates in compression as well as in combined compression and bending. This formula expressed as functions of the magnitudes of compressive residual stress and initial out-of-flatness and used to compute the ultimate strength of welded built up beam-column segments.

Mirambell, et al. ^(٤٠) [١٩٩٤] presented experimental investigations and numerical solutions to the behavior of steel plates under pure compression. The measurements are concentrated on the strains at several characteristic points of the panel displacements. A numerical model was developed for the analysis of the geometrical and material non-linearities of steel plate structures, based on the finite element method. Their study showed that the numerical and experimental stress values were close.

Mathlum ^(٣٩) [١٩٩٧] presented a large deflection elasto-plastic analysis by the finite element method to analyze rectangular thin plates under compressive and shear load as well as the ultimate strength of plate girders with longitudinal and diaphragm stiffeners. His study was divided into three parts, the first, included the analysis of isolated plate under compression load. The second part included analysis of isolated plates under shear load. The last part contained analysis of ultimate load of plate girders with transverse and longitudinal stiffeners. His conclusion was that the plate girder without stiffener gives low strength and the plate girder with transverse stiffener has a larger strength more than the plate with longitudinal stiffener.

Lee and Yoo ^(٣٧) [١٩٩٨] introduced a non-linear analysis based on three dimensional finite element models to transversely stiffened plate girder web panels (without longitudinal stiffeners) subjected to pure shear, including the effects of initial out-of-flatness. This study showed that the design for shear in plate girder web panels in (AASHTO) and (AISC) specifications accounts for both elastic shear buckling strength and post-buckling strength separately and combine these resisting capacities which are based on the aspect ratio of the web panel. Although, equations in these specifications predict the overall shear strength with reasonable

accuracy, they often underestimate the elastic shear buckling strength, due to an underestimation of the rigidity at the flange-web juncture and often overestimate the post-buckling strength of certain web panels, as a result of excluding the effect of out-of-plane bending stresses. The first conclusion based on the assumption that the boundary condition at the flange-web juncture is simply supported gives too much conservative shear strength for many plate girder web panels and the second conclusion based on the flange rigidity appears to have little effect on the post-buckling strength of web panels.

Lee and Yoo^(۳۴) [۱۹۹۹] introduced an experimental study on the ultimate shear strength of web panels. In this study, ۱۰ scaled plate girder models were tested to investigate the shear behavior of web panels up to failure. The following conclusions are obtained with regard to the behavior of the plate girder web panels:

۱. The boundary condition at the flange-web juncture in practical design is much closer to the fixity.
۲. In all existing failure mechanisms, the results that the through-thickness bending stress affects the ultimate shear strength are neglected; however, it has been found that very high bending stresses are developed at failure.
۳. An anchoring system, such as flanges, is not needed for the development of the post-buckling strength.

Paik, et al.^(۳۵) [۲۰۰۰] presented a study on five subjects theoretically, numerically, and experimentally: modeling of post-weld initial imperfections (i.e. initial deflections and residual stresses) and their effects, influence of rotational rigidity of support members on the plate buckling strength, ultimate strength design equations under combined loads including biaxial compression/tension, edge shear and lateral

pressure loads, and dynamic collapse strength characteristics under dynamic axial compressive loads or slamming-induced impact lateral pressure loading. Their proposition was a new design formula for more advanced buckling and ultimate strength of ship plating.

More recently, **Turvy** and **Salehi**⁽¹⁷⁾ [2001] introduced a finite difference formulation with of the dynamic relaxation algorithm to solve the governing equations of an elasto-plastic large deflection analysis of pressure loaded sector plate, based on the Ilyusion full- section yield criterion and the flow theory of plasticity. This study showed that the effect of the in-plane edge restraint is more significant in changing the post-yielding response of slender simply supported plates with substantial stiffness increase accompanying the presence of full in-plane restraint. It showed that for slender sector plates the development of plasticity within the plate is quite complicated. At the maximum pressure applied a plastic membrane state is approached in slender sector plates under simply supported in-plane fixed edge conditions, whereas in the case of clamped in-plane fixed edge plates a residual interior elastic zone remains.

Shnan⁽¹⁸⁾ [2001] used a finite element method to analyze isolated steel plates. This study was divided into two parts: plate under shear load was analyzed in first part. In the second part, he analyzed isolated steel plates under compression loads. He also studied the factors affecting the behavior of the plate such as initial imperfection, slenderness ratio (b/t) equal to 226, 256, 289, and 316, and aspect ratio (a/b) equal to 0.75, 1.0, 1.5, and 2.0.

His conclusion was that the stresses produced increase with an increase of both slenderness and aspect ratios especially on the long edges. Plastic mode mechanism was used in the prediction of the ultimate load capacity of plate structures.

In the present study, the effect of initial imperfection, boundary condition, aspect ratios, and the effect of tapering cross section on post-buckling and elasto-plastic behavior will be investigated based on the finite difference idealization. The effect of geometric and material nonlinearities are considered in this study.

POST-BUCKLING ANALYSIS OF RECTANGULAR THIN PLATE WITH INITIAL IMPERFECTION

3.1 General

The use of thin-walled structures, which are popular in aerospace applications, is an increasing construction in civil and industrial buildings. The technology of cold-formed steel structures is finding wide applications. The major advantage of cold-formed steel sections over hot rolled sections is found in the relative thickness of the sections, which can lead to highly efficient and weight effective members and structures^(xy). The most important phenomenon in such structures is the local buckling of the constituent plate elements. The evaluation of linear critical stress or the stress at which the local buckling of thin plates is initiated, has been well documented in the contemporary literature. This critical stress state characterizes the neutral equilibrium of an axially loaded plate. At this state, it is observed that the plate would keep the small out-of-plane perturbations and still remain stable. In the case of slender columns, increase in the axial load beyond such a critical state would produce a disproportionate lateral deflection resulting in an unstable state. Nevertheless, edge supported plates do not undergo such unstable deformations immediately after attaining the critical buckling stress, i.e., in the vicinity of the neutral equilibrium, the fibers parallel to edge compression shorten because of elastic strain and bowing effect. The latter causes fiber lengthening in the direction perpendicular to axial compression. This membrane effect tends to stabilize equilibrium of the

plate and results in a possible increase in strength, which is termed as the post-buckling strength. In other words, the plate continues to carry an axial load up to a certain level, even beyond the critical stress and presents a stable equilibrium. The unavoidable imperfections present in the plates cause a qualitative change in the load-deformation characteristics and it is also one of the important factors which contributes to the strength of the plate. It is seen from the above that the problem of assessing the strength of thin plates is basically non-linear and that the linear critical stresses alone are not adequate for the design of plates.

۳.۲ Geometric Non-linearity

If the deflection of a plate is of the order of magnitude of its thickness but it is still small relative to the other dimensions, the analysis of the problem should include the strain of the middle plane of the plate.

Classical formulation of this problem leads to a set of non-linear partial differential equations, which are characterized by the behavior of the plate. These equations are difficult to solve.

In many technical fields of aircraft construction, shipbuilding, and instrument manufacturing, plates are finding use with large deflections. During the fabricating process, the plates usually have inherent initial curvatures. The analyses are more complicated than those for ideally flat plates.

An alternative approach to such problem is now available in the form of a finite difference method. This method achieves the numerical solutions with directly solving the differential equations. Formulations are developed on the basis of Marguerre's equations of large deflection of plates.



3.3 Basic Assumptions

Because of the non-linearity, the large deflection analysis of imperfect metal plates is complex. Certain simplified assumptions must be made to provide a solution that is reasonably good and consuming less efforts and computational time.

The main assumptions made in the present study are as follows: -

1. The material of the plate is homogeneous and isotropic.
2. Thin plate theory applies so that plane section remains plane and transverse shear deformations are neglected; again this is acceptable for plate structures.
3. A Lagrangian (fixed) co-ordinate system is used. This formulation is valid provided that the slope $\frac{\partial w}{\partial x}, \frac{\partial w}{\partial y} \ll 1.0$.
4. The residual stresses resulting from the restraining effect of the welded edges after buckling are neglected.

3.4 Theory of Plate Analysis

The finite difference formulation is used to solve Marguerre's theory for thin plates with constant or variable thickness cross section and with initial imperfection for various boundary conditions and various types of loading.

3.4.1 Marguerre's Theory

The following theory is used to analyze the behavior of an isolated rectangular thin plate which is initially deformed out of its plane and which carries in-plane and normal load. The plate is treated like a shell. The accuracy of this theory is studied by a lot of researchers⁽³⁹⁾.

A finite out-of-plane deformation analysis is carried out on isolated plate using the finite difference method based on strain-displacement relationships given by Marguerre's theory. The applied load is an in-plane compressive loading.

3.4.2 Background to Marguerre's Theory

The membrane theory of plates was first studied by **Euler** [1766], and the flexural theory by **Bernoulli** [1789] and **Navier** [1832]. **Kirchhoff** [1877] and **Saint-Venant** [1883] developed the theory for combined membrane and flexural effects^(xi).

At the turn of last century, the equation governing the buckling of flat plates was available and it was known that it formed the basis of an Eigen-value problem. At that time it was not recognized that, as the plate buckled, the values of in-plane stresses at a given point would vary because of the stretching of the plate.

The next development that overcame this deficiency was due to **Fopple**, who introduced the concept of the stress function [1907] and paved the way for **Von-Karman** [1910] to derive the two governing equations for perfectly flat plates. These equations enabled the post-buckling behavior of perfectly flat plates to be studied and the large deflection analysis of a plate, subjected to transverse loads only.

The Von-Karman large deflection equations for perfectly flat isotropic plates with in-plane loading were modified to account for the effects of initial imperfections in the late 1940's.

Marguerre's equations of imperfect plates were derived in 1938 and can be used to study a number of cases of practical interest. Isolated plates with initial imperfections have been solved by approximate analytical methods (e.g. by **Coan**^(xi), **Yamaki**^(vii)).

Also, **Bilstein** (according to Ref. (ε)) obtained a number of solutions for an imperfect stiffened plate by using an iterative Runge-Kutta method. His study showed that a stiffened plate with a small initial imperfection would reach the point of first yielding at a much lower load than one, which is perfect. This has important implications for designers who may be required to carry out checks to ensure that no part of the panel yield at working loads (serviceability checks) and for fabricators who could be asked to build such a panel to be within specified tolerances. A considerable number of particular solutions of Marguerre's equations for imperfect plates have been given by **Rushton**^(ε) [1969], **Aalami** and **Chapman**⁽¹⁾ [1969].

3.5 Derivation of Marguerre's Equations for an Initially Imperfect Elastic Plate.

3.5.1 Plate with Constant Thickness

The following theory is used to analyze the behavior of an isolated rectangular thin plate, which is initially deformed out of its plane, and which carries normal load Y per unit area. The plate is treated like a shallow shell with initial shape given by^(ε):

$$w_0 = w_0(x, y) \quad (3-1)$$

It is assumed that (w) is small enough to make the usual approximations for small slopes. The deflection (w) of a point in the middle surface of the plate is measured from its position to its final position in a direction parallel to that of the (z) -axis. Thus, the distance between a general points (x, y) in the deformed plate and the $(x-y)$ plane after deformation is $(w+w_0)$. In a plate of thickness (t) , the stress resultants (per unit width of plate) are listed below. For consistency with most other authors in this field tensile stresses and tensile loads are taken

as positive throughout this section. Thus the critical stresses and end load will be compressive and therefore have negative values.

$$N_x = \int \sigma_x dh$$

$$N_y = \int \sigma_y dh$$

$$N_{xy} = \int \tau_{xy} dh$$

$$Q_x = \int \tau_{xz} dh$$

$$Q_y = \int \tau_{yz} dh$$

$$M_x = \int \sigma_x \cdot h \cdot dh$$

$$M_y = \int \sigma_y \cdot h \cdot dh$$

$$M_{xy} = \int \tau_{xy} \cdot h \cdot dh$$

(r-2)

where the integration are taken from $(-t/2)$ to $(t/2)$ and t is in z -direction. The equilibrium equations on element in its deformed position, as shown in Figure (r.1), are: -

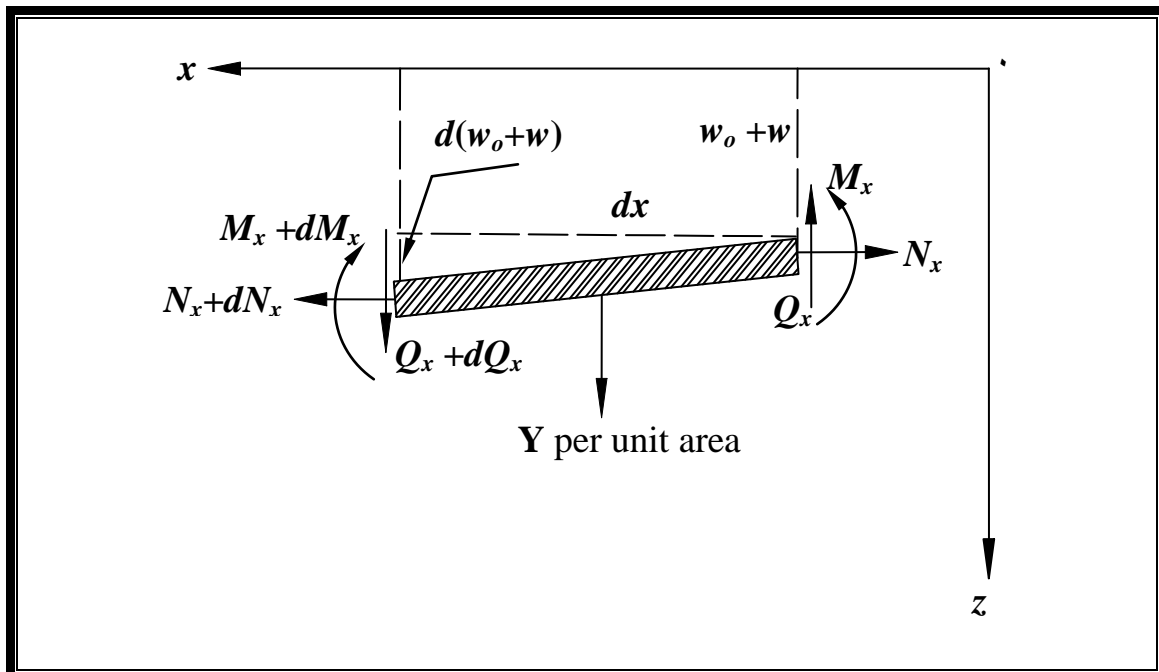


Figure (r.1): Forces acting on an element of a plate in its deformed position^(r.1).

$$\begin{aligned}
\frac{\partial N_x}{\partial x} + \frac{\partial N_{xy}}{\partial y} &= 0 \\
\frac{\partial N_y}{\partial y} + \frac{\partial N_{xy}}{\partial x} &= 0 \\
\frac{\partial Q_x}{\partial x} + \frac{\partial Q_y}{\partial y} + Y &= 0 \quad (r-7) \\
\frac{\partial M_x}{\partial x} + \frac{\partial M_{xy}}{\partial y} + N_x \frac{\partial(w+w_o)}{\partial x} + N_{xy} \frac{\partial(w+w_o)}{\partial y} - Q_x &= 0 \\
\frac{\partial M_y}{\partial y} + \frac{\partial M_{xy}}{\partial x} + N_y \frac{\partial(w+w_o)}{\partial y} + N_{xy} \frac{\partial(w+w_o)}{\partial x} - Q_y &= 0
\end{aligned}$$

The following algebraic manipulations are now carried out. Q_x and Q_y are eliminated from the last three equations (r-7), the first two of equation (r-7) are introduced and finally, the following substitutions, which satisfy the first two of equation (r-7), are made: -

$$\begin{aligned}
N_x &= \frac{\partial^2 \Phi}{\partial y^2} \\
N_y &= \frac{\partial^2 \Phi}{\partial x^2} \quad (r-8) \\
N_{xy} &= -\frac{\partial^2 \Phi}{\partial y \partial x}
\end{aligned}$$

where Φ is a stress function. After ignoring certain terms, which are considered to be small, which this leads to the following equation: -

$$\begin{aligned}
\frac{\partial^2 M_x}{\partial x^2} + 2 \frac{\partial^2 M_{xy}}{\partial x \partial y} + \frac{\partial^2 M_y}{\partial y^2} - N_x \frac{\partial^2(w+w_o)}{\partial x^2} + 2N_{xy} \frac{\partial^2(w+w_o)}{\partial x \partial y} \\
- N_y \frac{\partial^2(w+w_o)}{\partial y^2} &= 0 \quad (r-9)
\end{aligned}$$

These resultant forces can be expressed in terms of usual form (Timoshenko and Woinowdsky-Krieger (1909)),

$$\begin{aligned}
 N_x &= \frac{Et}{(1-\nu^2)}(\epsilon_x + \nu\epsilon_y) ; M_x = \frac{-Et^3}{12(1-\nu^2)}\left(\frac{\partial^2 w}{\partial x^2} + \nu\frac{\partial^2 w}{\partial y^2}\right) \\
 N_y &= \frac{Et}{(1-\nu^2)}(\epsilon_y + \nu\epsilon_x) ; M_y = \frac{-Et^3}{12(1-\nu^2)}\left(\frac{\partial^2 w}{\partial y^2} + \nu\frac{\partial^2 w}{\partial x^2}\right) \quad (r-7) \\
 N_{xy} &= \frac{Et}{2(1+\nu)}\gamma_{xy} ; M_{xy} = \frac{Et^3}{12(1+\nu)}\left(\frac{\partial^2 w}{\partial x\partial y}\right)
 \end{aligned}$$

where ϵ and γ are strains. The compatibility conditions are obtained by considering the geometrical shape as the element is stretched and deformed, as shown in Figure (r.7).

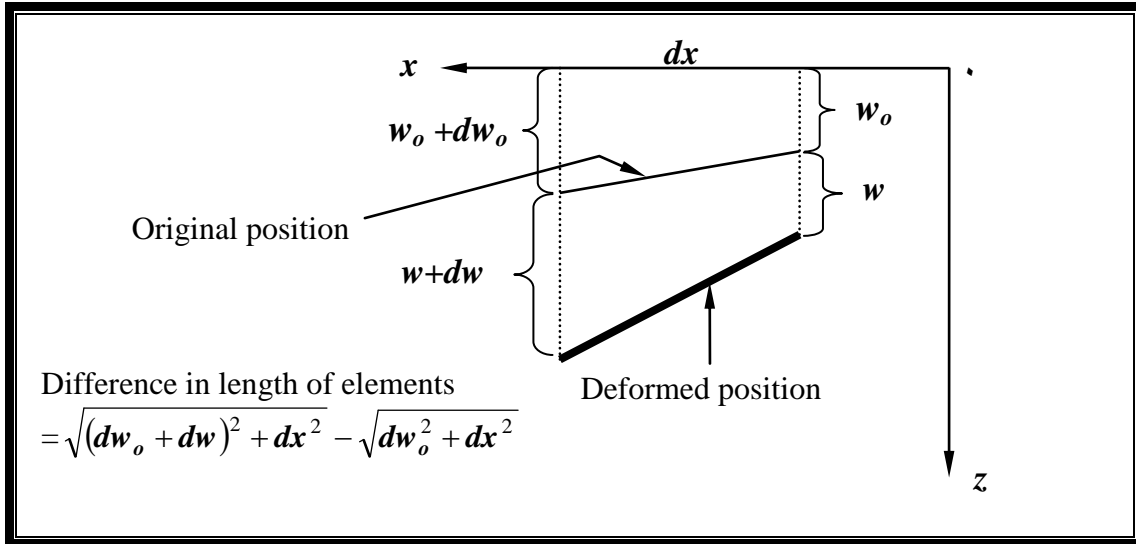


Figure (r.7): Displacement w causes stretching of the element^(ε).

By using Pythagoras' theorem and a truncated binomial expansion it can be shown that the strains and curvatures are^(ε): -

$$\begin{aligned}
 \epsilon_x &= \frac{\partial u_x}{\partial x} + \frac{\partial w}{\partial x} \frac{\partial w_o}{\partial x} + \frac{1}{2} \left(\frac{\partial w}{\partial x} \right)^2 \\
 \epsilon_y &= \frac{\partial v_y}{\partial y} + \frac{\partial w}{\partial y} \frac{\partial w_o}{\partial y} + \frac{1}{2} \left(\frac{\partial w}{\partial y} \right)^2 \quad (r-8) \\
 \gamma_{xy} &= \frac{\partial v_y}{\partial x} + \frac{\partial u_x}{\partial y} + \frac{\partial w}{\partial x} \frac{\partial w_o}{\partial y} + \frac{\partial w}{\partial y} \frac{\partial w_o}{\partial x} + \frac{\partial w}{\partial x} \frac{\partial w}{\partial y}
 \end{aligned}$$

By eliminating u_x and v_y from these equations (3-1), the compatibility equation is obtained: -

$$\begin{aligned} & \frac{\partial^2 \epsilon_x}{\partial y^2} + \frac{\partial^2 \epsilon_y}{\partial x^2} - \frac{\partial^2 \gamma_x}{\partial x \partial y} + \frac{\partial^2 w_o}{\partial x^2} \frac{\partial^2 w}{\partial y^2} - 2 \frac{\partial^2 w_o}{\partial x \partial y} \frac{\partial^2 w}{\partial x \partial y} \\ & + \frac{\partial^2 w_o}{\partial y^2} \frac{\partial^2 w}{\partial x^2} - \left(\frac{\partial^2 w}{\partial x \partial y} \right)^2 + \frac{\partial^2 w}{\partial x^2} \frac{\partial^2 w}{\partial y^2} = 0 \end{aligned} \quad (3-1)$$

After rearranging equation (3-1) so as to express these strains and curvatures as function of the stress resultants and by using equation (3-2), then: -

$$\nabla^4 \Phi - Et \left[\begin{aligned} & - \frac{\partial^2 w_o}{\partial x^2} \frac{\partial^2 w}{\partial y^2} + 2 \frac{\partial^2 w_o}{\partial x \partial y} \frac{\partial^2 w}{\partial x \partial y} - \frac{\partial^2 w_o}{\partial y^2} \frac{\partial^2 w}{\partial x^2} \\ & + \left(\frac{\partial^2 w}{\partial x \partial y} \right)^2 - \frac{\partial^2 w}{\partial x^2} \frac{\partial^2 w}{\partial y^2} \end{aligned} \right] = 0 \quad (3-3)$$

By similar algebraic steps it is possible to write the equilibrium equation in terms of w and Φ thus

$$D \nabla^4 w - \left[\begin{aligned} & q + \frac{\partial^2 \Phi}{\partial y^2} \frac{\partial^2 (w + w_o)}{\partial x^2} - 2 \frac{\partial^2 \Phi}{\partial x \partial y} \frac{\partial^2 (w + w_o)}{\partial x \partial y} \\ & + \frac{\partial^2 \Phi}{\partial x^2} \frac{\partial^2 (w + w_o)}{\partial y^2} \end{aligned} \right] = 0 \quad (3-4)$$

Equations (3-3) and (3-4) are Marguerre's simultaneous non-linear partial differential equations.

3.5.2 Plate with Variable Thickness

The large deflection of an isotropic rectangular plate with linearly tapered thickness in the x -direction is considered, as shown in Figure (3.3). The plate has out-of-plane deformation up to several times of the plate thickness. The basic differential equation for the membrane actions is derived as follows: -

Starting from the equilibrium and compatibility of a thin plate element and expressing the strains and curvatures as functions of the stress resultants, the following equations are presented: -

$$\frac{\partial^2 \epsilon_x}{\partial y^2} + \frac{\partial^2 \epsilon_y}{\partial x^2} - \frac{\partial^2 \gamma_x}{\partial x \partial y} + \frac{\partial^2 w_o}{\partial x^2} \frac{\partial^2 w}{\partial y^2} - 2 \frac{\partial^2 w_o}{\partial x \partial y} \frac{\partial^2 w}{\partial x \partial y} + \frac{\partial^2 w_o}{\partial y^2} \frac{\partial^2 w}{\partial x^2} - \left(\frac{\partial^2 w}{\partial x \partial y} \right)^2 + \frac{\partial^2 w}{\partial x^2} \frac{\partial^2 w}{\partial y^2} = 0 \quad (3.11)$$

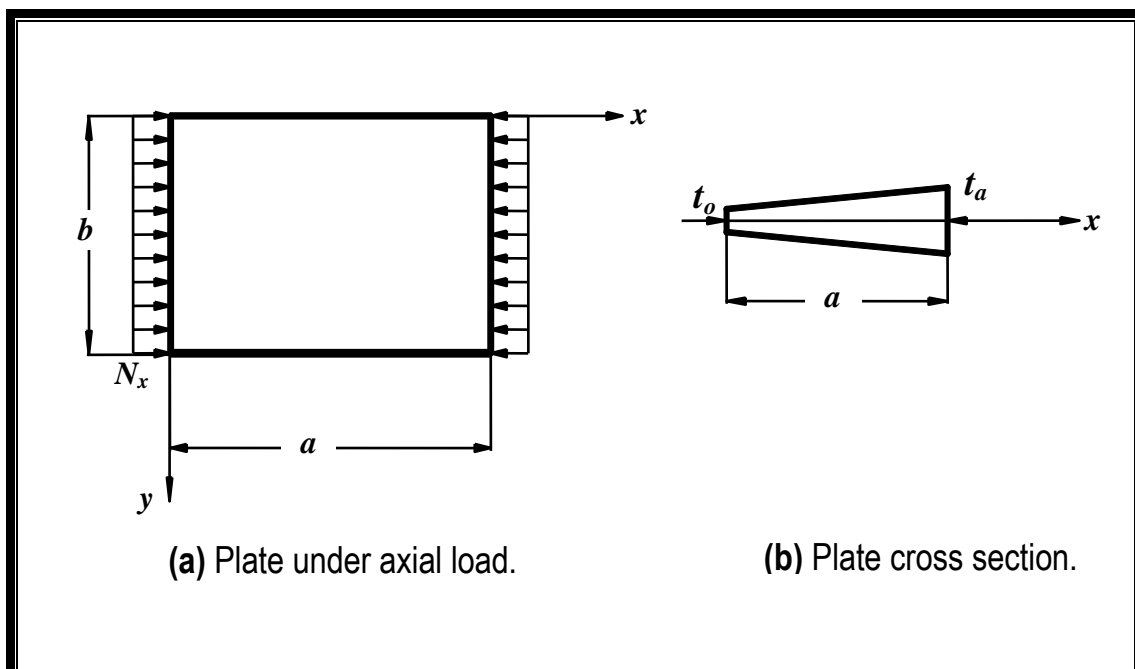


Figure (3.3) Rectangular thin plate with variable thickness under axial load⁽⁷⁰⁾.

The stress-strain relationships become as follows: -

$$\begin{aligned}\varepsilon_x &= \frac{(N_x - \nu N_y)}{Et_x} \\ \varepsilon_y &= \frac{(N_y - \nu N_x)}{Et_x} \\ \gamma_{xy} &= \frac{2(1+\nu)N_{xy}}{Et_x}\end{aligned}\quad (3-12)$$

where $t_x = t_o(1 + c_t x)$; in which $c_t = (t_a - t_o)/at_o$; t_o and t_a denote the thickness at the sides $x = 0$ and $x = a$.

Obtaining the required derivatives for equations (3-12)

$$\begin{aligned}\frac{\partial^2 \varepsilon_x}{\partial y^2} &= \frac{1}{Et_x} \left(\frac{\partial^2 N_x}{\partial y^2} - \nu \frac{\partial^2 N_y}{\partial y^2} \right) \\ \frac{\partial^2 \varepsilon_y}{\partial x^2} &= \frac{1}{Et_x} \left(\frac{2c_t^2}{(1+c_t x)^2} (N_y - \nu N_x) - \frac{2c_t}{(1+c_t x)} \left(\frac{\partial N_y}{\partial x} - \nu \frac{\partial N_x}{\partial x} \right) \right. \\ &\quad \left. + \left(\frac{\partial^2 N_y}{\partial x^2} - \nu \frac{\partial^2 N_x}{\partial x^2} \right) \right) \\ \frac{\partial^2 \gamma_{xy}}{\partial x \partial y} &= \frac{2(1+\nu)}{Et_x} \left(\frac{\partial^2 N_{xy}}{\partial x \partial y} - \frac{c_t}{(1+c_t x)} \frac{\partial N_{xy}}{\partial y} \right)\end{aligned}\quad (3-13)$$

The substitution of these derivatives in equation (3-11) yields: -

$$\begin{aligned}\frac{\partial^2 N_x}{\partial y^2} + \frac{\partial^2 N_y}{\partial x^2} - 2 \frac{\partial^2 N_{xy}}{\partial x \partial y} - \frac{2c_t}{(1+c_t x)} \left(\frac{\partial N_x}{\partial x} + \frac{\partial N_y}{\partial x} \right) + \\ \frac{2c_t^2}{(1+c_t x)^2} (N_y - \nu N_x) - Et_x \left(\frac{\partial^2 w_o}{\partial x^2} \frac{\partial^2 w}{\partial y^2} - 2 \frac{\partial^2 w_o}{\partial x \partial y} \frac{\partial^2 w}{\partial x \partial y} \right. \\ \left. + \frac{\partial^2 w_o}{\partial y^2} \frac{\partial^2 w}{\partial x^2} - \left(\frac{\partial^2 w}{\partial x \partial y} \right)^2 \right. \\ \left. + \frac{\partial^2 w}{\partial x^2} \frac{\partial^2 w}{\partial y^2} \right) = 0\end{aligned}\quad (3-14)$$

By expressing equation (3-15) as a function of stress resultants by using equation (3-16), the compatibility equation (3-15) becomes: -

$$\nabla^4 \Phi - F \left(\frac{\partial^3 \Phi}{\partial x^3} + \frac{\partial^3 \Phi}{\partial x \partial y^2} \right) + Z \left(\frac{\partial^2 \Phi}{\partial x^2} - \nu \frac{\partial^2 \Phi}{\partial y^2} \right) - Et_x \left[\begin{aligned} & \left(\frac{\partial^2 w_o}{\partial x^2} \frac{\partial^2 w}{\partial y^2} + 2 \frac{\partial^2 w_o}{\partial x \partial y} \frac{\partial^2 w}{\partial x \partial y} - \frac{\partial^2 w_o}{\partial y^2} \frac{\partial^2 w}{\partial x^2} \right) \\ & + \left(\frac{\partial^2 w}{\partial x \partial y} \right)^2 - \frac{\partial^2 w}{\partial x^2} \frac{\partial^2 w}{\partial y^2} \end{aligned} \right] = 0 \quad (3-19)$$

where

$$F = \frac{2c_t}{(1 + c_t x)} \quad (3-17)$$

$$Z = \frac{2c_t^2}{(1 + c_t x)^2}$$

By similar algebraic steps it is possible to write the equilibrium equation in terms of w and Φ , thus: -

$$D \nabla^4 w + 2 \frac{\partial D(x)}{\partial x} \left(\frac{\partial^3 w}{\partial x^3} + \frac{\partial^3 w}{\partial x \partial y^2} \right) + 2 \frac{\partial^2 D(x)}{\partial x^2} \left(\frac{\partial^2 w}{\partial x^2} + \nu \frac{\partial^2 w}{\partial y^2} \right) - \left[\begin{aligned} & q + \frac{\partial^2 \Phi}{\partial y^2} \frac{\partial^2 (w + w_o)}{\partial x^2} - 2 \frac{\partial^2 \Phi}{\partial x \partial y} \frac{\partial^2 (w + w_o)}{\partial x \partial y} \\ & + \frac{\partial^2 \Phi}{\partial x^2} \frac{\partial^2 (w + w_o)}{\partial y^2} \end{aligned} \right] = 0 \quad (3-18)$$

These equations (3-19) and (3-18) may be considered as the basic (or governing) differential equations for a plate with constant or variable thickness and subjected to transverse and axial compressive load, as shown in Figure (3.3).



The finite difference method offers an alternative and very powerful way of solving equation (3-10) used by **Fok**⁽¹⁸⁾ [1980]. Also the same method was used to solve the equation (3-11) by **Husain, et al.**⁽¹⁹⁾ [2002], to obtain the critical stresses and the buckling mode for a rectangular thin plate and with variable thickness with various boundary conditions.

To study the behavior of a plate with initial imperfection ($w_0 \neq 0$), it is necessary to solve the simultaneous non-linear Marguerre's equations. There appears to be no exact solution but the equations have been solved for isolated plates by approximate analytical methods (e.g. **Coan**⁽¹²⁾ [1951], **Yamaki**⁽¹⁷⁾ [1959]) and by numerical methods (e.g. an iterative Runge-Kutta method and the finite difference method).

3.1 Boundary Conditions

Yamaki⁽¹⁷⁾ [1959] and **Abdel-Sayed**⁽²⁾ [1969] solved Marguerre's equations for various boundary conditions. Their analyses cover three different cases with pinned end conditions.

I-Case (a): The edges parallel to the x -axis ($y=0, b$) are kept straight and fixed ($v_y=0$). In practice, this represents a plate, which is restrained against lateral movement by massive framing with other members.

II-Case (b): The edges parallel to the x -axis ($y=0, b$) are kept straight ($v_y = \text{constant}$). This case represents a plate panel in a wide stiffened plate with axial loading. The edges of the plate panel are constrained to remain straight by the surrounding plate panels but they can move inwards.

III-Case (c): The edges parallel to the x -axis ($y=0, b$) are free so they can develop in-plane displacement as the plate buckles ($v_y \neq \text{constant}$). An example of this kind is the buckling of a plate panel in a narrow stiffened



plate. In this case the surrounding plate cannot prevent in-plane distortions.

For the present problem, the covering plates are spread widely and hence the boundary condition of the plate elements is of the second kind.

Figure (۳.۴) illustrates the buckling of a stiffened panel. In order to isolate the plate panel for the purpose of analysis, basic assumptions must be made in regard to the flexural and membrane boundary conditions.

If the laterally loaded plate is simply supported and subjected to uniform in-plane compressive load (N_x) in the x -direction, and if the loaded edges are free from shear stress and the unloaded edges are stress-free, the boundary conditions can be written as: -

A-Unloaded Edges

A-۱- Flexural Boundary Conditions: -

At $y = ۰$ and $y = b$

The deflection at edges is equal to zero ($w=۰$) and bending moment in y -direction is equal to zero ($M_y = ۰$)

$$M_y = -D \left(\frac{\partial^2 w}{\partial y^2} + \nu \frac{\partial^2 w}{\partial x^2} \right) = 0 \quad (۳-۱۸)$$

A-۲- Membrane Boundary Conditions: -

At $y = ۰$ and $y = b$

Shear stress is equals to zero ($\tau_{xy} = 0$)

$$\tau_{xy} = \frac{\partial^2 \Phi}{\partial x \partial y} = 0 \quad (۳-۱۹)$$

Stress in y -direction is equals to zero ($\sigma_y = 0$)

$$\sigma_y = \frac{\partial^2 \Phi}{\partial x^2} = 0 \quad (۳-۲۰)$$

B-Loaded Edges

B-1- Flexural Boundary Conditions: -

At $x = 0$ and $x = a$

The deflection at edges is equal to zero ($w = 0$) and bending moment in x -direction is equal to zero ($M_x = 0$)

$$M_x = -D \left(\frac{\partial^2 w}{\partial x^2} + \nu \frac{\partial^2 w}{\partial y^2} \right) \quad (3-21)$$

B-2- Membrane Boundary Conditions: -

At $x = 0$ and $x = a$

Shear stress is equal to zero ($\tau_{xy} = 0$)

$$\tau_{xy} = \frac{\partial^2 \Phi}{\partial x \partial y} = 0 \quad (3-22)$$

Stress in x -direction is equal to ($N_x = \int \sigma_x dy$)

$$\int \sigma_x dy = \int \frac{\partial^2 \Phi}{\partial y^2} dy \quad (3-23)$$

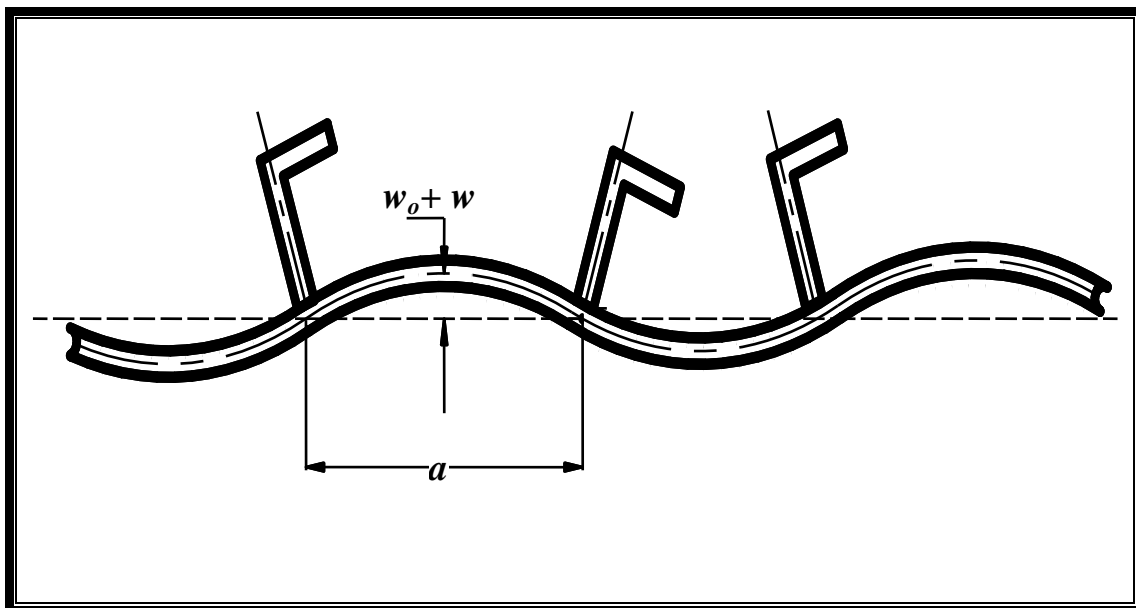


Figure (3.4) Buckled plate⁽⁷⁾

3.7 Membrane Stresses Distribution Inside The Plate

Figure (3.5) shows a typical example of the axial membrane stress distribution inside a plate element under predominantly longitudinal compressive loading, before and after buckling⁽¹⁾. It is noted that the membrane stress distribution in the loading x - direction can become non-uniform as the plate element deflects (or buckles). The membrane stress distribution in the y -direction also becomes non-uniform if the unloaded plate edges remain straight, while no membrane stresses will develop in the y -direction if the unloaded plate edges move freely in-plane. The maximum compressive membrane stresses are developed at the plate edges that remain straight, while the minimum tensile membrane stresses occur in the middle of the plate element where a membrane tension field is formed by the plate displacement since the plate edges remain straight.

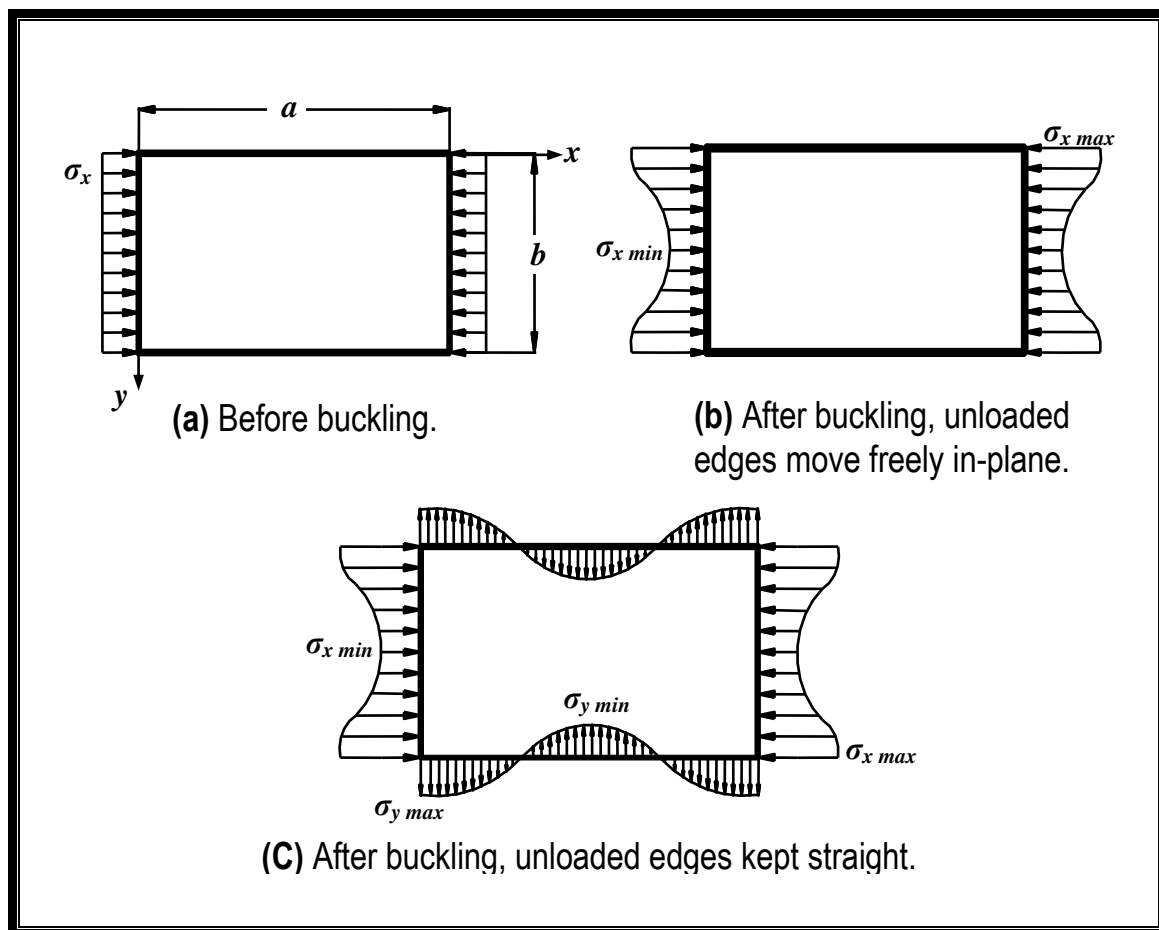


Figure (3.5) Membrane stress distribution inside plate element under longitudinal compressive loads⁽¹⁾.

ELASTO-PLASTIC ANALYSIS OF RECTANGULAR THIN PLATE WITH INITIAL IMPERFECTION

4.1 General

Because of the wide use of thin-walled structures such as bridges, cranes and hoists, steel-building structures, ship structures, and airplane structures, it is very important in the designing process of these structures not only to determine the load-carrying capacity (the ultimate load), but also to analyze the structure's behavior up to collapse. It is very important to know in what way the structure fails, that means either failure happens rapidly without earlier signs of catastrophe (brittle structure) or it proceeds slowly with warning against catastrophe (ductile structure). It is obvious that the second character of failure is more desirable.

The determination of the failure stress of thin-walled structures under compressive loads is a topic, which has attracted considerable attention over the past hundred years. **Box** [1883] appears to have been the first to propose a formula for the failure stress (σ_f) of a simply supported mild steel panel with uniform in-plane stress in one direction only. That is: -

$$\sigma_f = 1236(b/t)^{-0.5} \text{ MPa} \quad (4-1)$$

Over the last 60 years there has been a proliferation of formula which enables designers to estimate stresses but nearly all of these formulas to a lesser or greater extent include empirical rules. While it is



obviously desirable for designers is to have at their disposal simple rules such as equation (4-1), the rules should be based upon sound theoretical concepts with a back up of careful experiments. Failure of a mild steel panel is a complicated elasto-plastic process, which depends upon the geometry of the panel, its initial imperfections, the yield stress, and the boundary conditions (both in-plane and out-of-plane). It is self-evident that a simple formula such as equation (4-1) can not account for all these factors. An “exact” elasto-plastic analysis of a thin-walled structure up to and beyond (σ_f) is complicated even with the aid of present day computing techniques. There have so far been few attempts to follow the history of even a simple imperfect plate into the elasto-plastic range. Such analysis is expensive in computer time and it is unlikely that designers can use these techniques directly as design tools. Nor it is likely that design tables could be produced to cover the whole range of problems likely to confront designers⁽⁴⁻⁶⁾.

However “exact” theories, although limited in scope, are important because they provide a yardstick for judging other theories. There are many methods of analysis, which are usually easier to use than “exact” methods and they cover a wider range of problems.

This chapter will deal with an easier elasto-plastic analysis of thin steel plates with initial imperfection for constant and variable thickness by means of the finite difference method.

4.2 Material Non-linearity

This is introduced when material properties vary with the loading condition, i.e. the constitutive laws are a function of the current load so that the stress-strain relationship is non-linear. Plate structures are fabricated from ductile material whose behavior may be divided into elastic and plastic phases. It may also be assumed that the plastic strain does not grossly exceed the yield strain of the material⁽¹⁷⁾.

Material non-linearity does not require a formulation of the basic (governing) differential equation. The required elasto-plastic relationships between stresses and total strains may be derived from the simple two-dimensional relationship with the flow theory of plasticity being used to evaluate the plastic components of strains. To determine whether any given combination of stresses is sufficient to cause yield, it is necessary to define a yield criterion and elasto-plastic stress-strain relationships.

4.2.1 Yield Criterion

A yield criterion must be able to define the onset of the plasticity under combination of stress. The criterion established by **Tresca** [1864] and **Von-Mises** [1913] are well known. For plate structures, an account would be obtained by the Von-Mises criterion⁽¹⁷⁾.

This criterion is shown in 2-dimensional stresses as following: -

$$f = \frac{1}{\sigma_o^2} (\sigma_x^2 + \sigma_y^2 - \sigma_x \sigma_y + 3\tau_{xy}^2) \leq 1.0 \quad (4-1)$$

where

σ_o : is the uniaxial tensile yield stress, σ_x and σ_y are the direct (or normal) stress components in the x and y directions, and
 τ_{xy} : is the shear (xy)stress. The stresses which include the bending and membrane components are defined as: -



$$\begin{aligned}\sigma_x &= \pm\sigma_{bx} + \sigma_{mx} \\ \sigma_y &= \pm\sigma_{by} + \sigma_{my} \\ \tau &= \pm\tau_b + \tau_m\end{aligned}\quad (\xi-3)$$

In the present study, the cross section is divided into a number of layers, when the equivalent stress at a certain layer reaches the yield stress of the material in uniaxial tension, this layer is considered to yield.

4.2.2 Elasto-Plastic Stress-Strain Relationships

An ultimate strength analysis usually requires the non-linear behavior of the material to be taken into consideration. The macroscopic behavior of the material can be described by a mathematical model (plasticity theory). The two major plasticity theories are the deformation theory and the flow theory. The deformation theory assumes a unique relation between total stresses and the total strains⁽¹⁹⁾. Hencky proposed the following formula: -

$$\epsilon_{ij}^p = \frac{3}{2} \frac{G(\bar{\sigma})}{\bar{\sigma}} S_{ij} \quad (\xi-4)$$

where

S_{ij} : deviatoric stress tensor.

$\bar{\sigma}$: is the effective stress.

G : is the shear modulus.

However, experiments do not agree very well with Hencky's theory, especially for cyclic loading. The stress-strain relation for the real elastic-plastic material is not only a function of the present loading as equation ($\xi-4$) but the previous plastic deformations should also be incorporated.



In the flow theory the plastic deformations are “memorized” by integrating an equivalent plastic strain increment over the load history. It gives out an incremental relationship between stresses and strains. The mathematical model includes two major parts. The first assumption is that there exists a so-called loading function (f) in stress space. This function is such that the state of the material is given by the volume of (f) for structures composed of thin plates as in this study, the Von-Mises function may be used as the loading function. The other part of the flow theory is the flow rule, which gives the incremental stress-strain relation.

The flow theory is based on two major assumptions. The first is that elastic and plastic strains can be added. It is relevant here since the strains are small.

$$\varepsilon_{ij} = \varepsilon_{ij}^e + \varepsilon_{ij}^p \quad (\varepsilon-8)$$

The elastic and plastic strains can therefore be treated separately. The plastic deformation is assumed to be incompressible: -

$$\varepsilon_{ii}^p = 0 \quad (\varepsilon-9)$$

where the repeated index indicates summation ($i=1, 2, 3$).

The second assumption to be made is that the material is stable as defined by Drucker who considered an element initially in some state of stress to which by an external agency an additional set of stresses are slowly applied and slowly removed. In the cycle of application and removal of the added stresses, the work done by an external agency is non-negative. From the work of Prandtl-Reuss, the flow rule may be written as:

$$\Delta \varepsilon_{ij}^p = \Delta \lambda \sigma_{ij} \quad (\varepsilon-10)$$

where $\Delta \boldsymbol{\varepsilon}_{ij}^p$ is the plastic strain increment tensor, $\Delta \lambda$ is a factor of proportionality, $\boldsymbol{\sigma}_{ij}$ is the total stress.

The flow rule may be re-written as the associated flow rule:

$$\Delta \boldsymbol{\varepsilon}_{ij}^p = \Delta \lambda \frac{\partial f}{\partial \boldsymbol{\sigma}_{ij}} \quad (4-8)$$

For plastic flow to occur, a neutral loading condition must be maintained i.e.:

$$\frac{\partial f}{\partial \boldsymbol{\sigma}_{ij}} - d\boldsymbol{\sigma}_{ij} = 0 \quad (4-9)$$

4.3 Yield Criterion Formulation

The present theory involves a volume integral and based on Von-Mises yield criterion, which has been used in the computer program.

After yielding occurs, any change in the stress state which does not involve unloading must be such that the new stresses remain on the yield surface, i.e. the direction of the change in the stress must be tangential to the yield surface^(xy), or

$$\left(\frac{\partial f}{\partial \boldsymbol{\sigma}_j} \right) \Delta \boldsymbol{\sigma}_j = 0 \quad (4-10)$$

where $j = x, y, \tau$ and summation on a repeated subscript is implied, in this equation and in those that follow.

The incremental stress-strain equations can be expressed as: -

$$\Delta \boldsymbol{\sigma}_j = [E_{ij}] (\Delta \boldsymbol{\varepsilon}_i - \Delta \boldsymbol{\varepsilon}_i^p) \quad (4-11)$$

where $[E_{ij}]$ is the elastic modulus of rigidity and $\Delta \boldsymbol{\varepsilon}_i^p$ is the plastic part of the total strain $\Delta \boldsymbol{\varepsilon}_i$; the subscripts $i = x$ and y are used denote the x and y directions and τ denotes the shear (xy) direction.

Using the Prandtl-Reuss flow rule, the plastic strain components are normal to the yield surface, as equation (4-8).



Eliminating $\Delta \varepsilon_i^p$ from equations (4-18) and (4-19) gives:

$$\Delta \sigma_j = [E_{ij}] \left(\Delta \varepsilon_i - \Delta \lambda \frac{\partial f}{\partial \sigma_i} \right) \quad (4-19)$$

Substituting this expression for $\Delta \sigma_j$ into equation (4-19) yields:

$$\frac{\partial f}{\partial \sigma_j} [E_{ij}] \left(\Delta \varepsilon_i - \Delta \lambda \frac{\partial f}{\partial \sigma_i} \right) = 0 \quad (4-20)$$

This can be rearranged, using permissible changes of dummy subscripts, to give: -

$$\Delta \lambda = \frac{[E_{ij}] \left\{ \frac{\partial f}{\partial \sigma_j} \right\} \left\{ \frac{\partial f}{\partial \sigma_j} \right\}^T [E_{ij}]}{r} \quad (4-21)$$

where

$$r = \left\{ \frac{\partial f}{\partial \sigma_j} \right\}^T [E_{ij}] \left\{ \frac{\partial f}{\partial \sigma_j} \right\} \quad (4-22)$$

By substituting equation (4-21) back into equation (4-19) then: -

$$[\Delta \sigma] = [E]^* [\Delta \varepsilon] \quad (4-23)$$

where the elements of the symmetric matrix $[E]^*$ are given by^(r)

$$\begin{aligned} e_{11} &= \left(\frac{E}{(1-\nu^2)} \right) \left(1 - \alpha S_1^2 / S_4 \right) \\ e_{22} &= \left(\frac{E}{(1-\nu^2)} \right) \left(1 - \alpha S_2^2 / S_4 \right) \\ e_{33} &= \left(\frac{E}{(1-\nu^2)} \right) \left(\frac{1}{2} (1-\nu) - \alpha \left((1-\nu) \tau_{xy} \right)^2 / S_4 \right) \\ e_{12} &= \left(\frac{E}{(1-\nu^2)} \right) \left(\nu - \alpha S_1 S_2 / S_4 \right) \\ e_{13} &= \left(\frac{E}{(1-\nu^2)} \right) \left(-\alpha (1-\nu) S_1 \tau_{xy} / S_4 \right) \\ e_{23} &= \left(\frac{E}{(1-\nu^2)} \right) \left(-\alpha (1-\nu) S_2 \tau_{xy} / S_4 \right) \end{aligned} \quad (4-24)$$



where

$$\begin{aligned}
 S_1 &= S_x + \nu S_y \\
 S_2 &= S_y + \nu S_x \\
 S_3 &= S_1 \Delta \epsilon_x + S_2 \Delta \epsilon_y + (1 - \nu) \tau_{xy} \Delta \gamma_{xy} \\
 S_4 &= S_x^2 + 2\nu S_x S_y + S_y^2 + 2(1 - \nu) \tau_{xy}^2 \\
 S_x &= \frac{2\sigma_x - \sigma_y}{3}, S_y = \frac{2\sigma_y - \sigma_x}{3}
 \end{aligned} \tag{4-14}$$

Now $\alpha = 1$ when plastic flow occurs in the layer, i.e. when $\sigma_e^2 = \sigma_o^2$ and $S_r > 0$. However, $\alpha = 0$ when the strain increments are completely elastic, i.e. when $\sigma_e^2 < \sigma_o^2$ (no yielding) or when $\sigma_e^2 = \sigma_o^2$ and $S_3 \leq 0$ (elastic unloading from the yield surface).

Where

σ_e = is the effective stress.

Equations (4-16), (4-17) and (4-18) summarize the incremental stress-strain relationship, and are applicable whatever the elasto-plastic state of the material.

By using incremental strains, and the $[E]^*$ values used in the last incremental and the previous total stresses, the current total stresses in each layer are calculated

$$[\sigma]_{new} = [\sigma]_{old} + [E]^* [\Delta \epsilon] \tag{4-19}$$

These stresses are substituted into (4-2), if yield is occurring, and/or if it was occurring in the previous increment, the value of S_r is checked. If S_r is less than or equal to zero the rigidities for that layer at that node retain or are reset to their elastic values (the latter case arises, for instance, if unloading of the layer occurs). If S_r is greater than zero the stress components are used in the elasto-plastic rigidity formula to derive new values of $[E]^*$ for that layer.

4.4 Incremental Forms of the Governing Differential Equations

To study the elasto-plastic analysis of rectangular thin plates, the incremental method of solution is applied to this end, a set of incremental governing equations should be derived. First, the load is assumed to be applied incrementally, at the end of load step ($i-1$), the deflection and the stresses expressed by a stress function, which may be obtained and denoted by w_{i-1} , and Φ_{i-1} , respectively.

The governing differential equations (3-10) and (3-11) for this state may be written as follows: -

$$\begin{aligned} & \nabla^4 \Phi_{i-1} - F(\Phi_{i-1,xxx} + \Phi_{i-1,xyy}) + Z(\Phi_{i-1,xx} - \nu \Phi_{i-1,yy}) \\ & = Et_x \left[\begin{array}{l} w_{i-1,xy}^2 + 2w_{o,xy} w_{i-1,xy} - w_{i-1,xx} w_{i-1,yy} - \\ w_{o,xx} w_{i-1,yy} - w_{o,yy} w_{i-1,xx} \end{array} \right] \quad (4-20) \end{aligned}$$

$$\begin{aligned} & D\nabla^4 w_{i-1} + 2D_{(x),x}(w_{i-1,xxx} + w_{i-1,xyy}) \\ & + 2D_{(x),xx}(w_{i-1,xx} + \nu w_{i-1,yy}) = \\ & \left[\begin{array}{l} \Phi_{i-1,yy}(w_{i-1} + w_o)_{xx} + \Phi_{i-1,xx}(w_{i-1} + w_o)_{yy} - \\ 2\Phi_{i-1,xy}(w_{i-1} + w_o)_{xy} + q_{i-1} \end{array} \right] \quad (4-21) \end{aligned}$$

Applying the i th load increment, the deflection and the stress function increase by Δw and $\Delta \Phi$ and their total values may be written as follows: -

$$\begin{aligned} w_i &= w_{i-1} + \Delta w \\ \Phi_i &= \Phi_{i-1} + \Delta \Phi \end{aligned} \quad (4-22)$$

Substituting equations (4-22) into equations (4-20) and (4-21), the governing equations at the end of the i th load increment may be expressed as: -

$$\begin{aligned} & \nabla^4(\Phi_{i-1} + \Delta\Phi) - F\left((\Phi_{i-1} + \Delta\Phi)_{xxx} + (\Phi_{i-1} + \Delta\Phi)_{xyy}\right) + \\ & Z\left((\Phi_{i-1} + \Delta\Phi)_{xx} - \nu(\Phi_{i-1} + \Delta\Phi)_{yy}\right) = \\ & Et_x \left[\begin{aligned} & (w_{i-1} + \Delta w)_{xy}^2 + 2w_{o,xy}(w_{i-1} + \Delta w)_{xy} - \\ & (w_{i-1} + \Delta w)_{xx}(w_{i-1} + \Delta w)_{yy} - \\ & w_{o,xx}(w_{i-1} + \Delta w)_{yy} - \\ & w_{o,yy}(w_{i-1} + \Delta w)_{xx} \end{aligned} \right] \end{aligned} \quad (\xi-23)$$

$$\begin{aligned} & D\nabla^4(w_{i-1} + \Delta w) + 2D_{(x),x}\left((w_{i-1} + \Delta w)_{xxx} + (w_{i-1} + \Delta w)_{xyy}\right) \\ & + 2D_{(x),xx}\left((w_{i-1} + \Delta w)_{xx} + \nu(w_{i-1} + \Delta w)_{yy}\right) = \\ & \left[\begin{aligned} & (\Phi_{i-1} + \Delta\Phi)_{yy}(w_{i-1} + w_o + \Delta w)_{xx} \\ & + (\Phi_{i-1} + \Delta\Phi)_{xx}(w_{i-1} + w_o + \Delta w)_{yy} \\ & - 2(\Phi_{i-1} + \Delta\Phi)_{xy}(w_{i-1} + w_o + \Delta w)_{xy} \\ & + (q_{i-1} + \Delta q) \end{aligned} \right] \end{aligned} \quad (\xi-24)$$

Subtracting equation ($\xi-20$) from equation ($\xi-23$) and equation ($\xi-21$) from equation ($\xi-24$), the following two equations may be obtained: -

$$\begin{aligned} & \nabla^4(\Delta\Phi) - F(\Delta\Phi_{xxx} + \Delta\Phi_{xyy}) + Z(\Delta\Phi_{xx} - \nu\Delta\Phi_{yy}) = \\ & Et_x \left[\begin{aligned} & (\Delta w)_{xy}^2 + 2w_{i-1,xy}^t \Delta w_{xy} \\ & - w_{i-1,xx}^t \Delta w_{yy} - w_{i-1,yy}^t \Delta w_{xx} \\ & - \Delta w_{xx} \Delta w_{yy} \end{aligned} \right] \end{aligned} \quad (\xi-25)$$

$$\begin{aligned} & D\nabla^4(\Delta w) + 2D_{(x),x}(\Delta w_{xxx} + \Delta w_{xyy}) + 2D_{(x),xx}(\Delta w_{xx} + \nu\Delta w_{yy}) \\ & = \left[\begin{aligned} & \Phi_{i-1,yy} \Delta w_{xx} + \Delta\Phi_{i-1,yy} w_{i-1,xx}^t + \Delta\Phi_{yy} \Delta w_{xx} + \\ & \Phi_{i-1,xx} \Delta w_{yy} + \Delta\Phi_{i-1,xx} w_{i-1,yy}^t + \Delta\Phi_{xx} \Delta w_{yy} - \\ & 2(\Phi_{i-1,xy} \Delta w_{xy} + \Delta\Phi_{i-1,xy} w_{i-1,xy}^t + \Delta\Phi_{xy} \Delta w_{xy}) \\ & + (\Delta q) \end{aligned} \right] \end{aligned} \quad (\xi-26)$$

When these equations ($\xi-25$) and ($\xi-26$) are used for material non-linearity they become as: -



$$\nabla^4(\Delta\Phi) - F(\Delta\Phi_{xxx} + \Delta\Phi_{xyy}) + Z(\Delta\Phi_{xx} - \nu \Delta\Phi_{yy}) = E_{eq} t_x \begin{bmatrix} (\Delta w)_{xy}^2 + 2w_{i-1,xy}^t \Delta w_{xy} \\ -w_{i-1,xx}^t \Delta w_{yy} - w_{i-1,yy}^t \Delta w_{xx} \\ -\Delta w_{xx} \Delta w_{yy} \end{bmatrix} \quad (\xi-27)$$

$$D\nabla^4(\Delta w) + 2D_{(x),x}(\Delta w_{xxx} + \Delta w_{xyy}) + 2D_{(x),xx}(\Delta w_{xx} + \nu \Delta w_{yy}) = \begin{bmatrix} \Phi_{i-1,yy} \Delta w_{xx} + \Delta\Phi_{i-1,yy} w_{i-1,xx}^t + \Delta\Phi_{yy} \Delta w_{xx} + \\ \Phi_{i-1,xx} \Delta w_{yy} + \Delta\Phi_{i-1,xx} w_{i-1,yy}^t + \Delta\Phi_{xx} \Delta w_{yy} - \\ 2(\Phi_{i-1,xy} \Delta w_{xy} + \Delta\Phi_{i-1,xy} w_{i-1,xy}^t + \Delta\Phi_{xy} \Delta w_{xy}) \\ + (\Delta q) \end{bmatrix} \quad (\xi-28)$$

where

$$E_{eq} = (E_1 I_1 + E_2 I_2 + \dots + E_n I_n) / I_{tot} \quad (\xi-29)$$

$$I_{tot} = t^3 / 12 \quad (\xi-30)$$

$$w_{i-1}^t = w_{i-1} + w_o \quad (\xi-31)$$

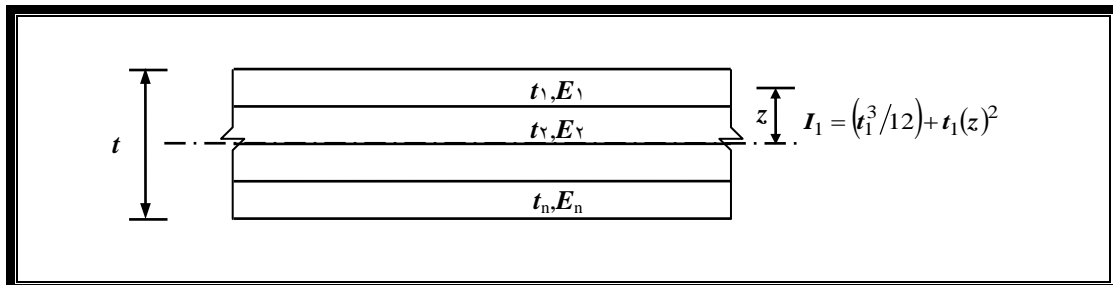


Figure (ξ.1): Section discretization into a number of layers.

Equations (ξ-27) and (ξ-28) are the incremental governing differential equations for the large deflection behavior of plates with initial imperfection.

Ueda, *et al.* derived these incremental equations but they neglected small quantities of higher order of (Δw and $\Delta\Phi$). Galerkin method used to solve these equations where at the end of load incremental i , the deflection contains an error (w_r) due to neglecting high order terms. In the present study, the small quantities of high order of (Δw and $\Delta\Phi$) are considered.



4.5 Ultimate Strength of Plate Panel under the Action of Complex Stress Distribution

The method of analysis of a plate panel subjected to both in-plane normal and shearing stresses is identical to that used in the analysis of the general case of a plate girder subjected to a system of complex stress distribution. The collapse mechanism of such condition is shown in Figure (4.2). Any other condition is a special case of the mechanism illustrated herein. It is known that the line mn and rh are parallel when the plate panel is subjected to shearing stresses only. This is because of the antisymmetry in the panel. But when also normal stresses exist then these lines will not be parallel^(4.5).

In the analysis of the mechanism as shown in Figure (4.2), it is considered that there are three stages as the loading stages up to collapse.

4.5.1 Unbuckled Behavior (Stage 1)

The plate remains flat until it reaches its critical stress. If the plate panel is subjected to pure shearing stresses then the critical shearing stress (τ_{cr}) is^(4.5): -

$$\tau_{cr} = k_{sh} \left[\frac{\pi^2 E}{12(1-\nu^2)} \right] \left(\frac{t}{b} \right)^2 \quad (4.32)$$

where

$$k_{sh} = 5.35 + 4 \left(\frac{b}{a} \right)^2 \quad \text{for } \frac{a}{b} > 1.0 \quad (4.33a)$$

$$k_{sh} = 5.35 \left(\frac{b}{a} \right)^2 + 4 \quad \text{for } \frac{a}{b} < 1.0 \quad (4.33b)$$

If the plate is subjected to bending normal stresses only, the critical bending stress (σ_{cr}) is:

$$\sigma_{cr} = 23.9 \left[\frac{\pi^2 E}{12(1-\nu^2)} \right] \left(\frac{t}{b} \right)^2 \quad (\text{4-29})$$

When shearing stresses and bending normal stresses act simultaneously, it is possible to determine their critical values by using either the finite element method or the finite difference method. However, accurate values are obtained by using the following equation:

$$\left(\frac{\sigma_{mb}}{\sigma_{cr}} \right)^2 + \left(\frac{\tau_m}{\tau_{cr}} \right)^2 = 1 \quad (\text{4-30})$$

where

σ_{cr} : is the critical value of the bending normal stress at the edge midway between the panel ends.

τ_{cr} : is the critical value of the of shearing stress when both shearing stresses and normal stresses act.

σ_{mb} = is the membrane bending stress.

τ_m = is the membrane shear stress.

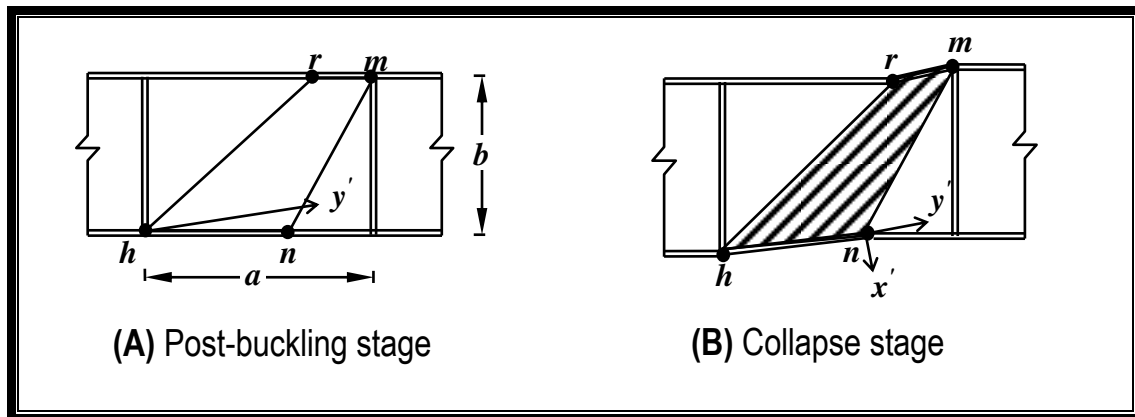


Figure (4.2): Analysis of plate panel subjected to in-plane normal and shearing stresses.

4.2.2 Post-buckling Behavior (Stage 2)

Once the critical stress is reached, the flat plate starts to buckle (for a plate with initial imperfection, the plate enters immediately the post-

buckling range) and the plate can not carry any increase in compressive stress. Any additional load has to be supported by the tension field action (Figure (ε.۲)). It is assumed that the shearing and bending stresses remain at their critical values (τ_m and σ_{mb}) and that there are additional membrane stress σ_t , this stress is inclined at an angle θ_s to the horizontal and it will carry any increase in the applied load.

ε.۳ Ultimate Load Behavior (Stage ۳)

When the material in the region (*mnrh*) reaches yield, the panel becomes a plastic mechanism and it can not sustain any further increase in load. In this ultimate state the additional membrane stress σ_t reaches its maximum value (σ_t^y). In order to evaluate the maximum load carrying capacity of the panels, the analysis for the mechanism is needed.

By transforming stresses using Mohr's circle, the state of stress at a point in the tensile region at a plane, which is inclined by an angle θ_s , could be found.

$$\begin{aligned}\sigma_{x'} &= -\sigma_{mb} \sin^2 \theta_s - \tau_m \sin 2\theta_s \\ \sigma_{y'} &= -\sigma_{mb} \sin^2 \theta_s + \tau_m \sin 2\theta_s \\ \tau_{x'y'} &= \frac{-\sigma_{mb}}{2} \sin 2\theta_s - \tau_m \cos 2\theta_s\end{aligned}\quad (\varepsilon-۳۶)$$

The failure condition is reached by adding (σ_t^y) to ($\sigma_{y'}$) and by introducing a yield criterion. Hence, by using Von Mises-Hencky criterion, the yield stress at the plate panel is ($\bar{\sigma}_y$) where:

$$\bar{\sigma}_y = \sqrt{(\sigma_{y'} + \sigma_t^y)^2 + \sigma_{x'}^2 - \sigma_{x'}(\sigma_{y'} + \sigma_t^y) + 3\tau_{x'y'}^2}\quad (\varepsilon-۳۷)$$



4.6 Solution of Non-Linear Equations by Numerical Methods

The numerical analysis of initially deformed plates of rectangular shape had been carried out by several authors (e.g. **Basu** and **Chapman**⁽⁴⁾ [1966], **Aalami** and **Chapman**⁽¹⁾ [1969], and **Fok**⁽¹⁴⁾ [1980]) using the finite difference method. Because of the non-linear nature of the Marguerre's equation, their equivalent finite difference equations are also non-linear and their solution is found by using iterative methods.

In the present study, the finite difference method employed to solve the basic (or governing) differential equations for buckling and post-buckling analysis. By applying the finite difference molecules, Figure (4.3), at the interior nodes of the subdivided plate, the equations are converted into matrix a expression. The set of equations can be written as: -

$$[A]\{\Phi\} + [B]\{w\} = 0 \quad (4-38)$$

$$[C]\{w\} + [D(w)]\{\Phi\} = q \quad (4-39)$$

where

$[A]$: is a square matrix of stress stiffness.

$[C]$: is a square matrix of displacements stiffness.

w, Φ : are displacement and stress function, respectively.

q : is the given loading.

At each of these node equations ((3-10) and (3-11) or (4-27) and (4-28)) give the finite difference equations with w and Φ as unknowns. The terms due to initial deflection (w_0), however, appear as numbers.

The solution is obtained by a method of successive approximation which is fairly convergent and which can be carried to any desired degree of accuracy. It may be noted that when numerical values are

assigned to (Φ) , equation $(\epsilon-39)$ becomes linear and similarly equation $(\epsilon-38)$ becomes linear when (w) is assigned by numerical values.

To facilitate the discussion of the sequence of the numerical computations, the following notation has been employed as: -

- 1- Define the desired load level.
- 2- As the out-of-plane displacement vector $\{w\}$ is not known; an initial displacement vector $\{w\}^1$ will be assumed likely (\dots) .
- 3- Put the assumed vector $\{w\}^1$ in equation $(\epsilon-38)$ to evaluate new stress vector $\{\Phi\}^1$.
- 4- Put stress vector $\{\Phi\}^1$ from step (3) and displacement vector $\{w\}^1$ in the second term of equation $(\epsilon-39)$ to evaluate the new displacement vector $\{w\}^2$.
- 5- Compare displacement vector $\{w\}^2$ with the corresponding deflection $\{w\}^1$. If the difference is greater than a specified percentage of errors $(\epsilon_r=0.1\%)$, calculate $\{w\}_{mean}^2 = 0.5\{w\}^1 + 0.5\{w\}^2$ and repeat the steps (3-5) until the desired convergence criterion is achieved. The whole procedure is repeated for the new increment load value.

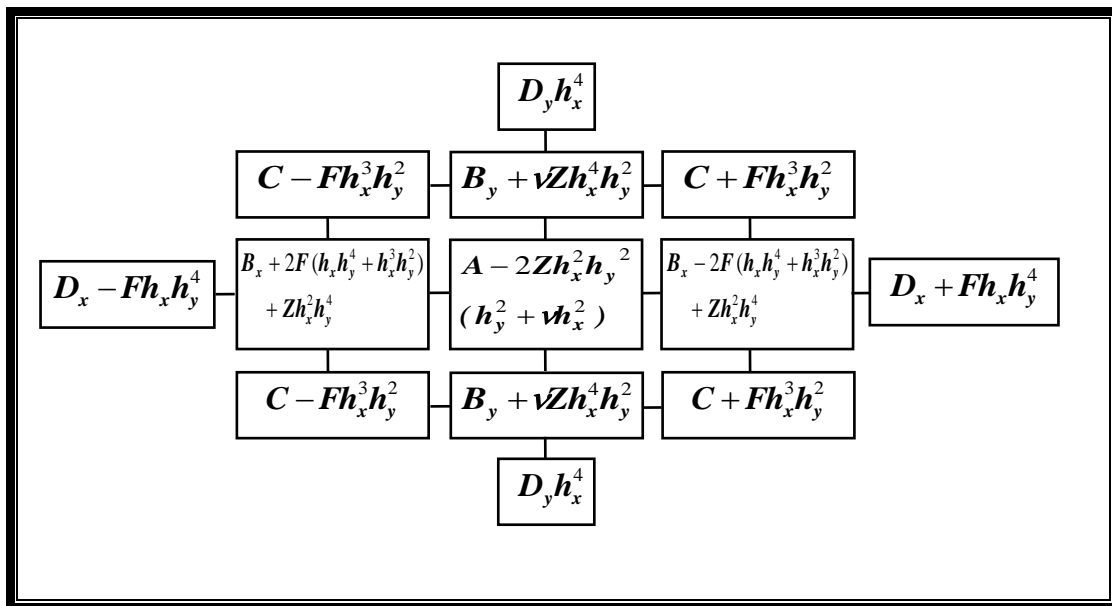


Figure $(\epsilon.3)$: Plate equation in finite difference molecule form (ϵ) .

where

$$A : 6h_x^4 + 6h_y^4 + 8h_x^2h_y^2$$

$$B_x : -4h_y^2(h_x^2 + h_y^2)$$

$$B_y : -4h_x^2(h_x^2 + h_y^2)$$

$$C : 2h_x^2h_y^2$$

$$D_x : h_y^4$$

$$D_y : h_x^4$$

h_x, h_y : Mesh size in x and y -direction, respectively.

APPLICATIONS AND DISCUSSIONS OF RESULTS

5.1 General

To study the effect of different parameters such as: slenderness ratio, aspect ratio, initial imperfection, boundary condition, and tapering ratio on the post-buckling and elasto-plastic behavior of rectangular thin plates, several plates are analyzed by using the finite difference method.

The analysis is made into two stages: -

- Studying the post-buckling behavior of the plates under in-plane compressive load and with various boundary conditions, various aspect ratios, and different values of tapering ratios.

Non-dimensional relationships of load-deflection and contour line diagram of the out-of-plane displacements are given to show the post-buckling behavior of these plates.

- Studying the elasto-plastic behavior of the plates under in-plane compressive load for simply supported plates with different values of slenderness ratio (b/t), and for constant and variable thickness, the relationships of non-dimensional average stress-average strain are introduced.

The results obtained are compared with the available experimental works and theoretical techniques.

5.2 Computer Program

A computer program is prepared, as a part of this study, for non-linear analysis of rectangular thin plates with various boundary conditions, various aspect ratios, different values of initial imperfection, and different values of tapering ratio.

The computer program not only solves the two sets of linear equations but also forms the necessary matrices and carries out automatically all the intermediate calculations and checks. Also the program can solve the characteristics equations.

The input data consists of the overall geometry of the plate, the material properties, type of boundary condition, type of loading, , value of initial imperfection, loading edges, and size of mesh.

The output of the computer program includes non-dimensional maximum deflection (w/t), non-dimensional load ($P_x b^2 / \pi^2 E t^3$), average strain, and average stress.

The computer program is written in FORTRAN 90 language executed by PC PENTIUM II at 533 MHz Intel processor compatible computer with 128 MB RAM. The structure chart of this program is given in Figure (5.1) to outline the main steps in the program.

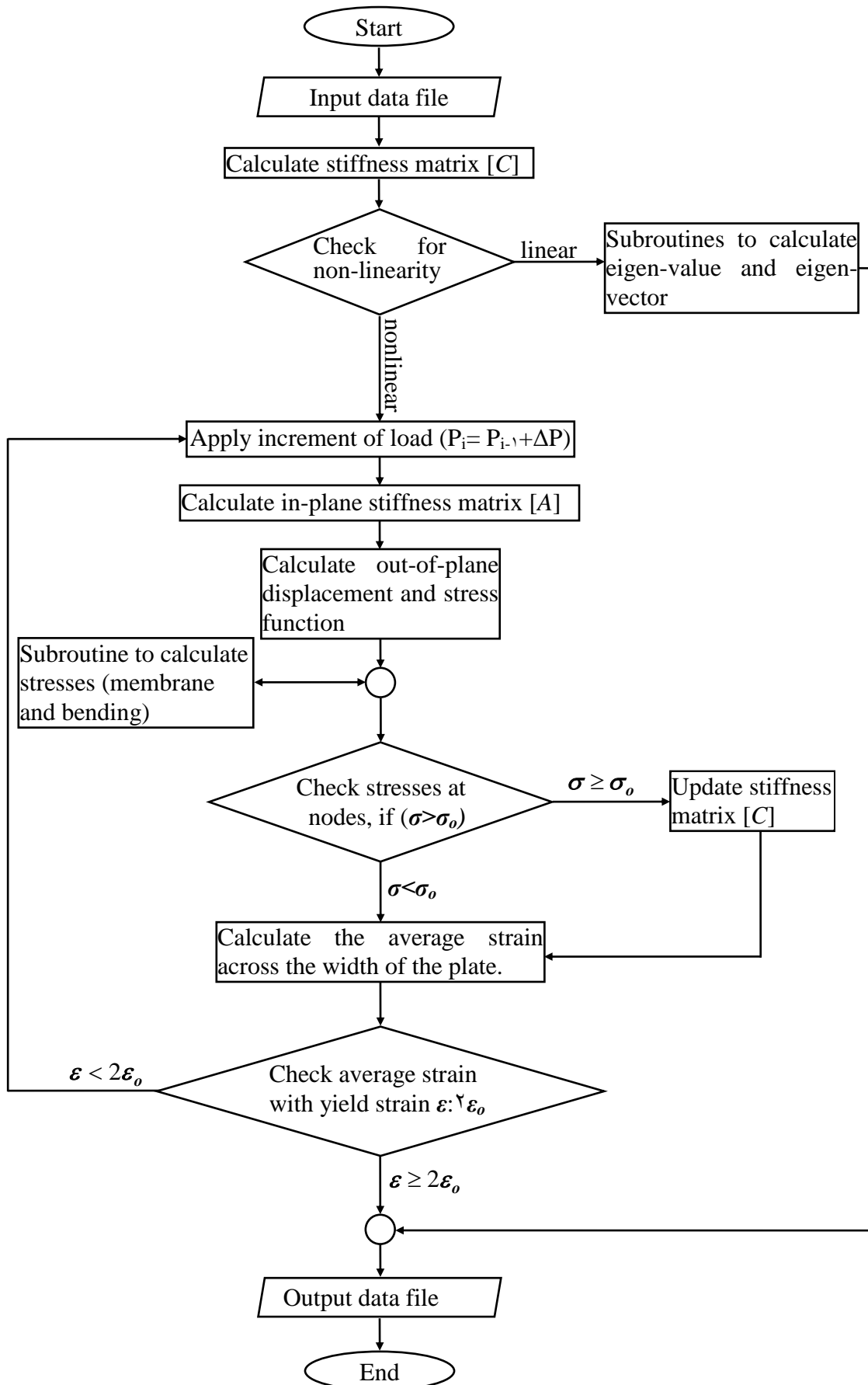


Figure (5.1): Structure chart of computer program.

5.3 Post-buckling Analysis

In order to study the effect of initial imperfections, boundary condition, and the variation of thickness on the geometric non-linearity of a plate under compressive load, several plates are analyzed.

5.3.1 Mesh Effect

The finite difference equations are solved, for a given value of load and amplitude of initial imperfection, using the successive iteration method. The rate of convergence of which depends on the mesh size and on the order of the finite difference approximation. The mesh effect has been investigated for a square plate. Table (5.1) gives a measure of convergence as a function of mesh size. It can be seen that (12×12) mesh for this problem which is shown in Figure (5.2) gives results to within 1% of the eventual asymptotes.

Table (5.1): Finite difference solution for a simply supported square plate subjected to uniaxial compressive load, ($P_x/P_{cr} = 1.25$, $w/t = 0$).

Mesh Intervals	Maximum Deflection (w/t)
8×8	0.881
10×10	0.871
12×12	0.866
14×14	0.863
16×16	0.860
18×18	0.859

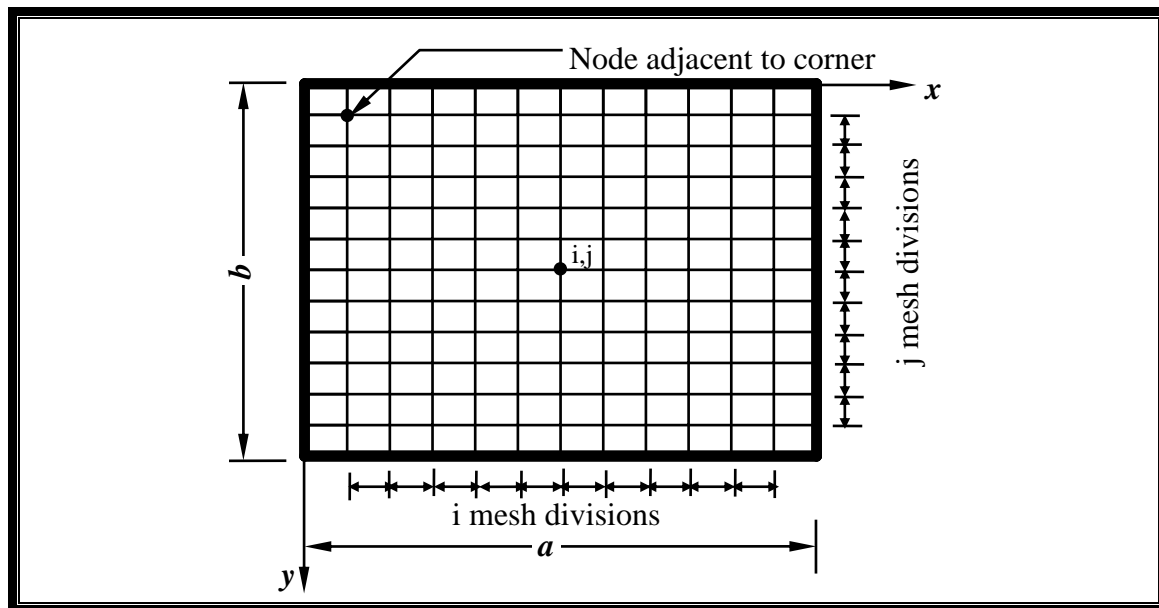


Figure (5.2): Plate geometry showing finite difference mesh^(5.2).

5.3.2 Comparison with Experimental Investigation

The accuracy of the results of the present study in the analysis of real panels is compared with the experimental and numerical results obtained by Mirambell, *et al*^(5.3) [1994] on simply supported panels. The properties of a specimen are shown in Figure (5.3). The numerical analysis of Mirambell, *et al* is based on the displacement formulation of the finite element method for the non-linear analysis of general steel shell structures.

In the present study, this plate is analyzed based on the prescribed procedure and it is divided into (24×12) divisions.

Figure (5.4) shows a comparison with the experimental and the numerical results for the out-of-plane displacements. The results obtained from the present study are closed to the test and theoretical results obtained by Mirambell, *et al* [1994]. The present study solves the differential equations directly but the finite element does not solve these equations. The load-deflection results are listed in Table (5.2).

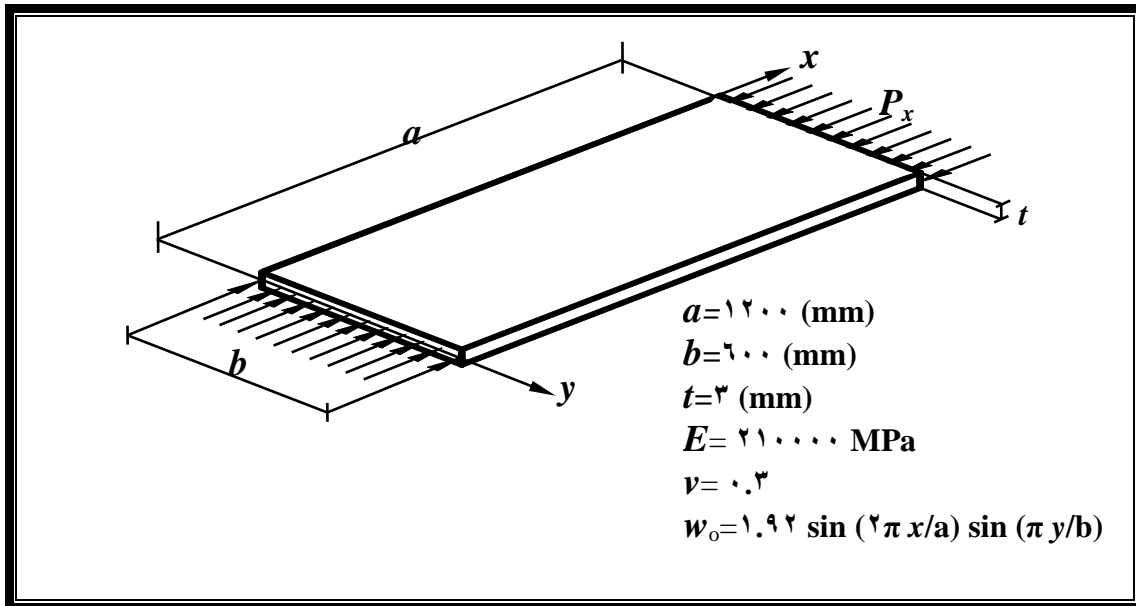
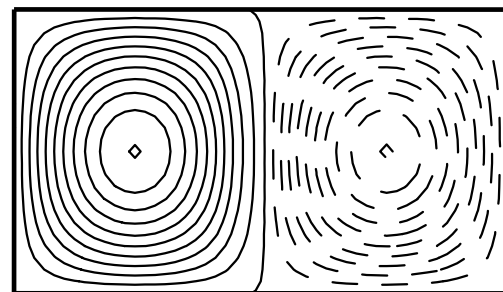
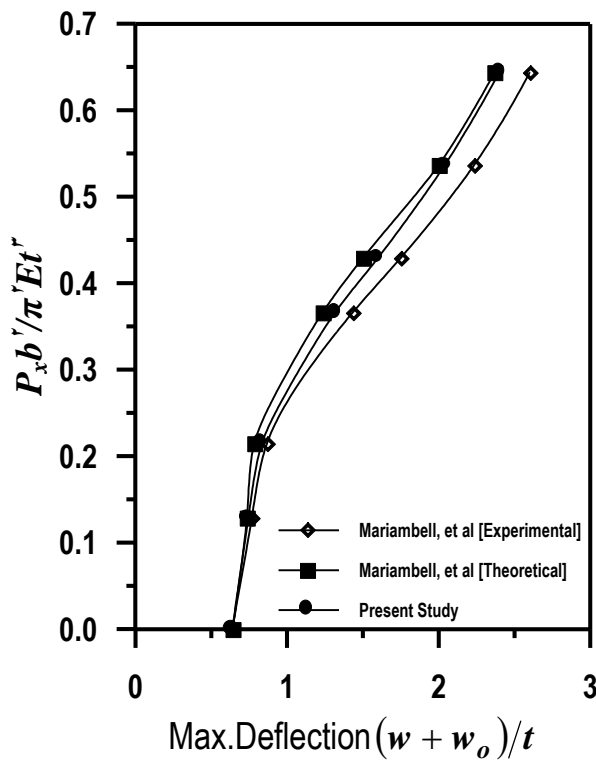


Figure (5.3): Details of a rectangular simply supported thin plate and material properties.



(b) Contour line diagram for out-of-plane displacements.

(a) Load-deflection curve

Figure (5.4): Post-buckling and contour line behavior of a rectangular simply supported thin plate under uniaxial compressive load.

Table (٥.٢): Comparison of results with experimental and theoretical studies.

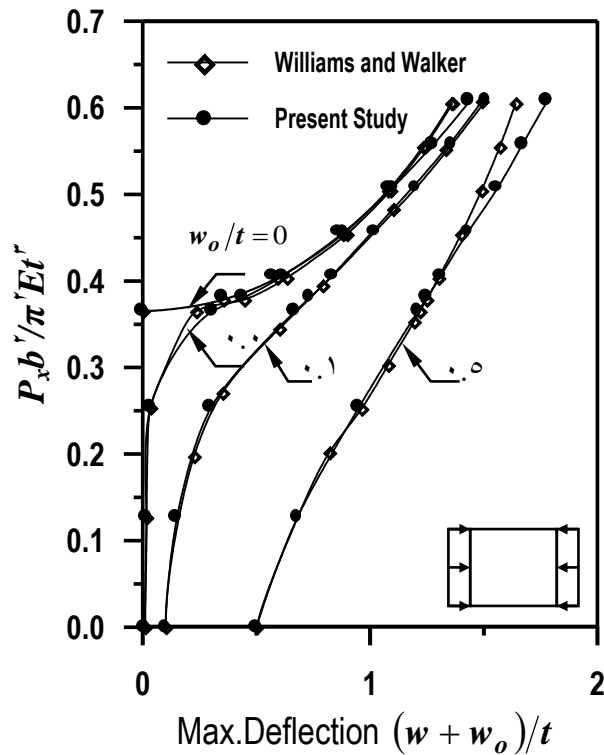
Load ($P_x b^2 / \pi^2 E t^3$)	Max. Deflection ($(w+w_0)/t$)		
	Experimental results ^(٤٠)	Theoretical results ^(٤١)	Present study
٠	٠.٦٤٠	٠.٦٤٠	٠.٦٤٠
٠.١٢٨	٠.٧٦٦	٠.٧٣٣	٠.٧٤٣
٠.٢١٤	٠.٨٦٦	٠.٧٨٣	٠.٨٣٣
٠.٣٦٦	١.٤٣٣	١.٢٣٣	١.٣١٦
٠.٤٢٩	١.٧٥٠	١.٥٠٠	١.٦٠٠
٠.٥٣٦	٢.٢٣٣	٢.٠٠٠	٢.٠٤٠
٠.٦٤٤	٢.٦٠٠	٢.٣٦٦	٢.٤٠٠

٥.٣.٣ Comparison with Available Theoretical Investigation

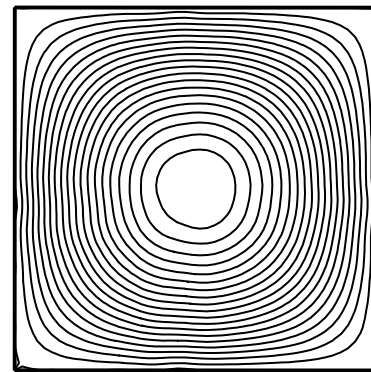
The following comparisons concern a plate model of thickness $t=٠.٠١$ (m), $E=٢ \times ١٠^٦$ kN/m^٢, and $\nu=٠.٣$. The plates have initial imperfection (w_0/t) of (٠, ٠.٠١, ٠.١, and ٠.٥). The shape of initial imperfection is considered to be sinusoidal where w_0 is the amplitude of the initial imperfection at the center of the plate. The influence of the type of loading on post-buckling behavior is studied.

A- Simply Supported Square Plate under Uniaxial Compressive Load

Figure (٥.٥) shows the load-deflection curve and the contour line diagram for the out-of-plane displacements of a simply supported thin square plate under uniform compressive load. The results of the present study are compared with the results of Williams and Walker study^(٧٥). Good agreement with these theoretical results is achieved. This comparison is listed in Table (٥.٣).



(a) Load-deflection curve



(b) Contour line diagram for out-of-plane displacements.

Figure (5.5): Post-buckling and contour line behavior of a square simply supported thin plate under uniaxial compressive load.

Table (5.3): Comparison of results of a simply supported thin square plate under uniaxial compressive load with initial imperfection ($w_o/t=0.5$).

Load $P_x b^3 / \pi^3 E t^3$	Max. deflection $((w+w_o)/t)$	
	Williams and Walker ^(5.5) study	Present study
0	0.000	0.000
0.126	0.670	0.680
0.203	0.960	0.949
0.374	1.214	1.210
0.380	1.247	1.200
0.400	1.300	1.310
0.406	1.399	1.430
0.507	1.490	1.560
0.507	1.570	1.670
0.608	1.640	1.780

B- Simply Supported Square Plate under Biaxial Compressive Load

Figure (5.6) shows the load-deflection curve and the contour line diagram for the out-of-plane displacements of a simply supported thin square plate under uniform compressive load in two directions. The results of the present study are compared with the results of Williams and Walker⁽⁵⁶⁾ study. Good agreement with these theoretical results is achieved.

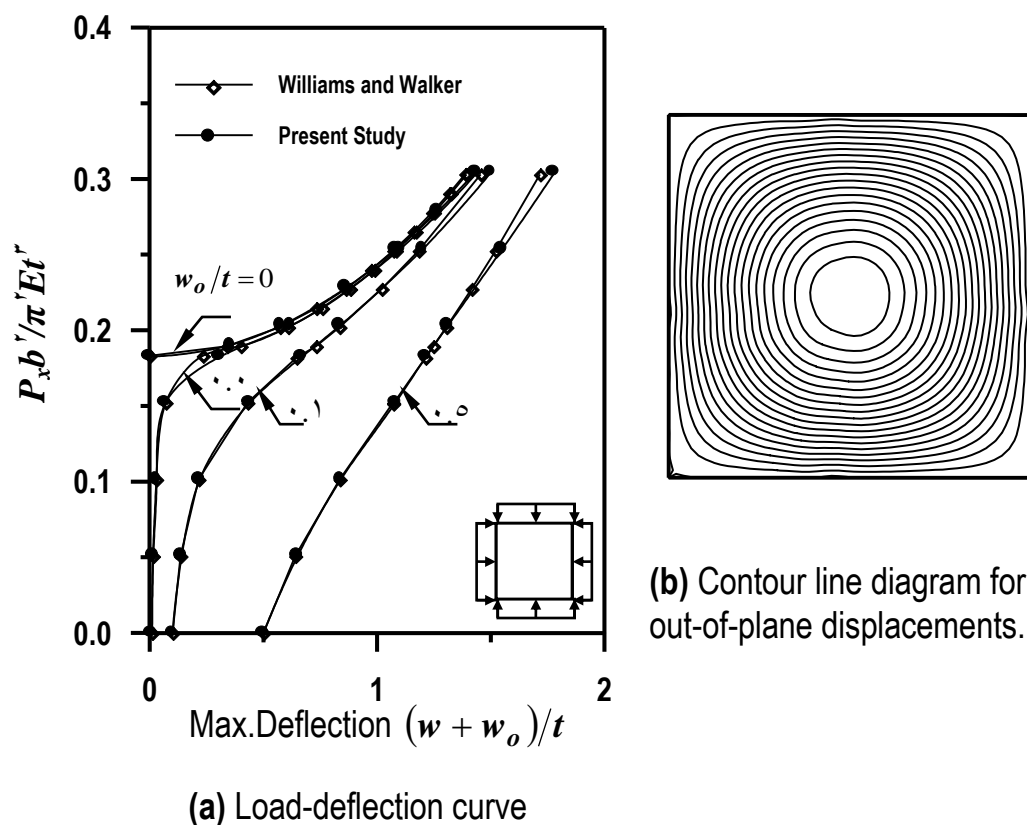


Figure (5.6): Post-buckling and contour line behavior of a simply supported thin square plate under biaxial compressive load.

C- Simply Supported Square Plate under Triangular Compressive Load

Figure (5.7) shows the load-deflection curve and the contour line diagram for the out-of-plane displacements of a simply supported thin square plate under varying in-plane compressive load. This type is similar to a plate girder. This figure shows a comparison of the present study with

available results of Williams and Aalami^(v1). This comparison shows good agreement with their numerical results.

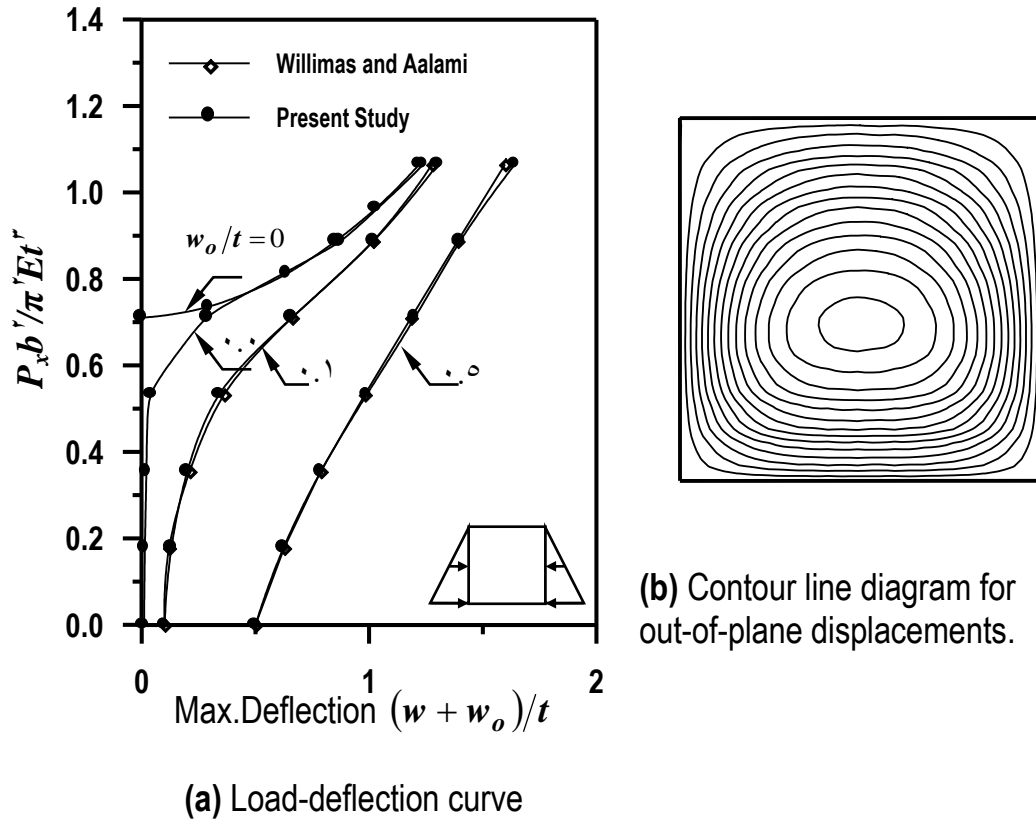


Figure (v1): Post-buckling and contour line behavior for a simply supported thin square plate under uniaxial varying compressive load.

D- Simply Supported Rectangular Plate under Compressive Load

Figure (v2) shows the load-deflection curve and the contour line diagram for the out-of-plane displacements of a simply supported thin rectangular plate with aspect ratio $(a/b=0.75)$ and under compressive load in longitudinal direction. This figure shows a comparison of the present study with those of Williams and Walker^(v2) study. Good agreement with their theoretical results is noticed.

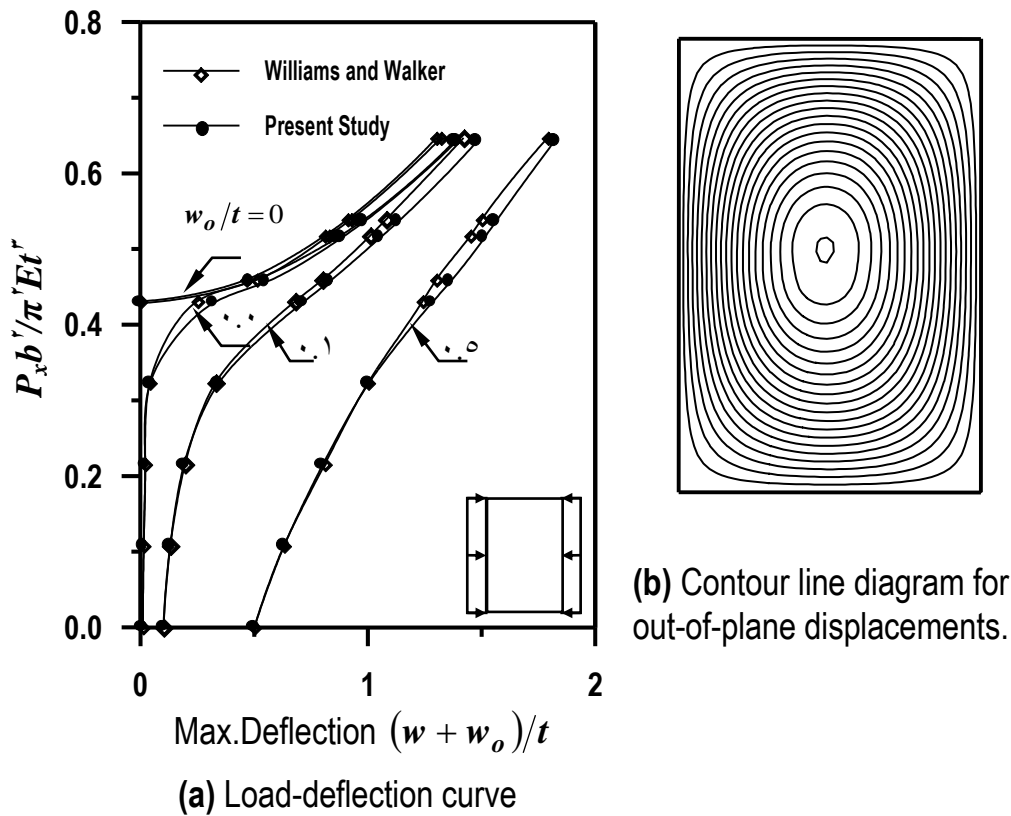


Figure (5.8): Post-buckling and contour line behavior for a simply supported thin rectangular plate under uniaxial compressive load in longitudinal direction.

From these figures, it can be noticed that: -

١. The behavior of thin plates is very sensitive to initial imperfections. The out-of-plane displacements are increased with increasing the magnitude of the initial imperfection.
٢. The plate under biaxial compressive load will buckle under the load less than the buckling load for a plate under uniaxial compressive load.
٣. The plate under varying compressive load will buckle under the total load more than the buckling load for a plate under uniform compressive load.
٤. Rectangular thin plates under compressive load in longitudinal direction will buckle under the load more than the buckling load for the square plate under compressive load but the post-buckling

stiffness of this type of plate is less than the post-buckling stiffness of a square simply supported plate.

5.3.4 Parametric Study

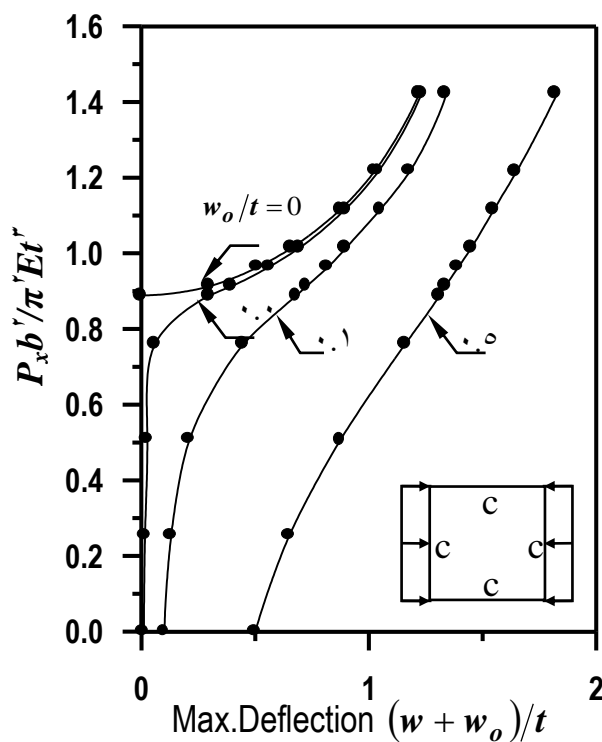
The effects of two parameters (boundary conditions and tapering ratio) are studied and discussed in the following sections.

5.3.4.1 Effect of Boundary Conditions

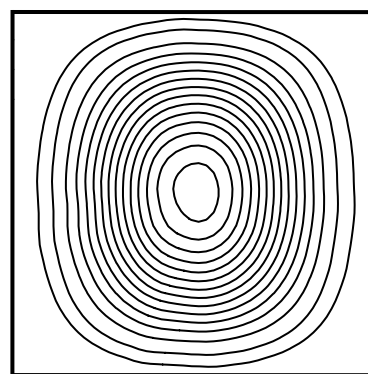
The effect of boundary conditions on the post-buckling behavior is studied for a plate with constant thickness. The initial imperfection (w_o/t) is taken to be in the range (0, 0.01, 0.1, and 0.5).

A- All Edges Clamped

Figure (5.9) presents the load-deflection curve and the contour line diagram for the out-of-plane displacements of a square thin plate with all edges clamped. The initial imperfection was considered to be a sinusoidal curve.



(a) Load-deflection curve



(b) Contour line diagram for out-of-plane displacements.

Figure (5.9): Post-buckling and contour line behavior for a rectangular thin plate under uniaxial compressive load.

B- Loaded Edges Simply Supported and the Other Edges Clamped

Figure (5.10) presents the load-deflection curve and the contour line diagram for the out-of-plane displacement of a square thin plate with loaded edges being simply supported and the other edges clamped. The initial imperfection was considered to be a sinusoidal curve. This figure shows that the plate buckles in two waves in the x -direction.

C- Loaded Edges Clamped and the Other Edges Simply Supported

Figure (5.11) presents the load-deflection curve and the contour line diagram for the out-of-plane displacements of a square thin plate with loaded edges clamped and the other edges simply supported.

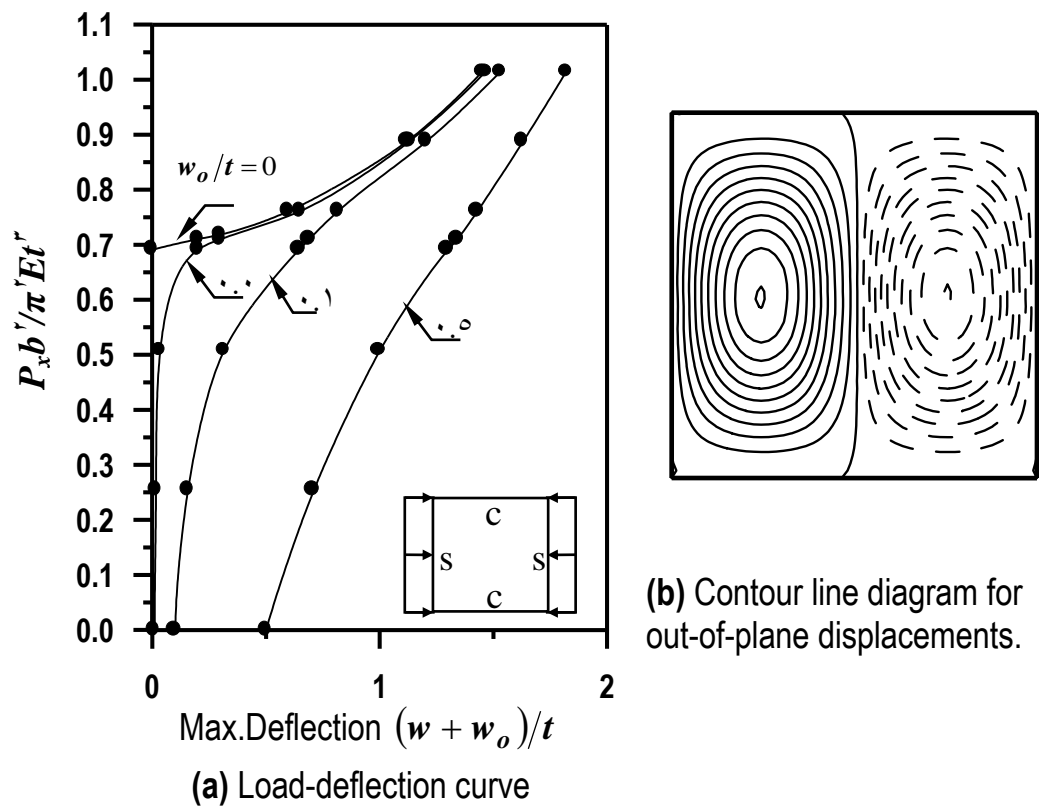


Figure (5.10): Post-buckling and contour line behavior for a square thin plate under uniaxial compressive load.

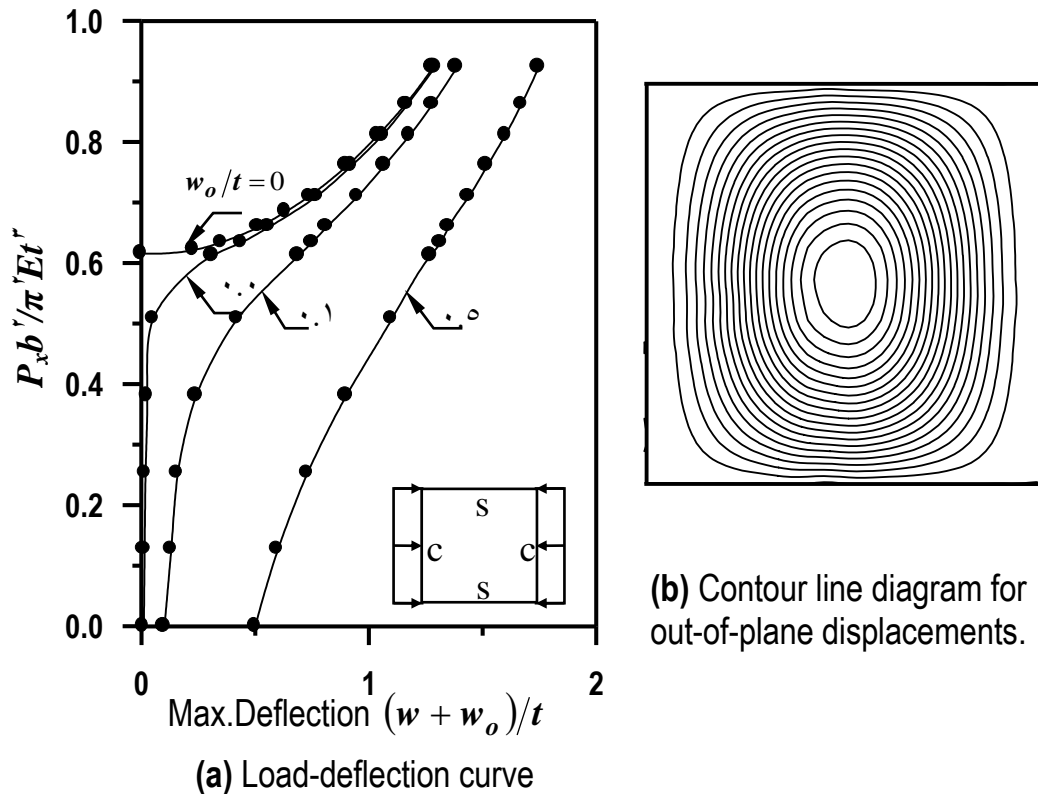


Figure (9.11): Post-buckling and contour line behavior for a rectangular thin plate under uniaxial compressive load.

Form these figures, it can be noticed that: -

١. The buckling load for a plate with all edges clamped is greater than the buckling load for the plates having simply supported edges.
٢. The buckling load for a plate with loaded edges simply supported and the unloaded edges clamped is more than the buckling load for the plate with loaded edges being clamped and the unloaded edges simply supported, because of the restraint in the unloaded edges.

Effect of Tapering Ratio

The effect of tapering ratio on the post-buckling behavior is considered in the present study. The values of tapering ratio (t_a/t_o) is taken to be (1.0, 1.25, 1.5, 1.75, and 2.0). The initial imperfection (w_o/t) is taken to be in the range (0 and 0.1) and the effect of load direction is also taken into account.

Figure (5.12) presents the load-deflection curve for a simply supported thin square plate under uniaxial load in x - direction (the direction parallel to thickness variation). This figure shows a comparison between a plate with constant thickness and variable thickness and for perfect and imperfect condition. The load-deflection results of the imperfect plate are listed in Table (5.8).

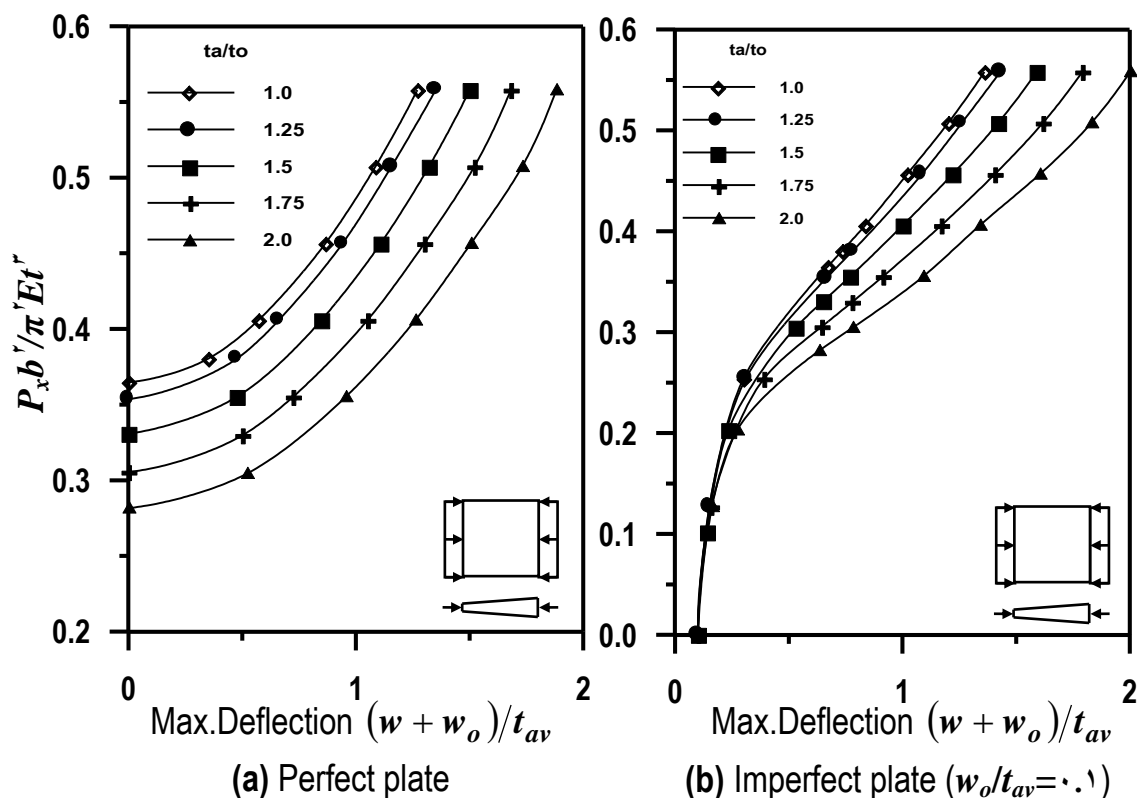
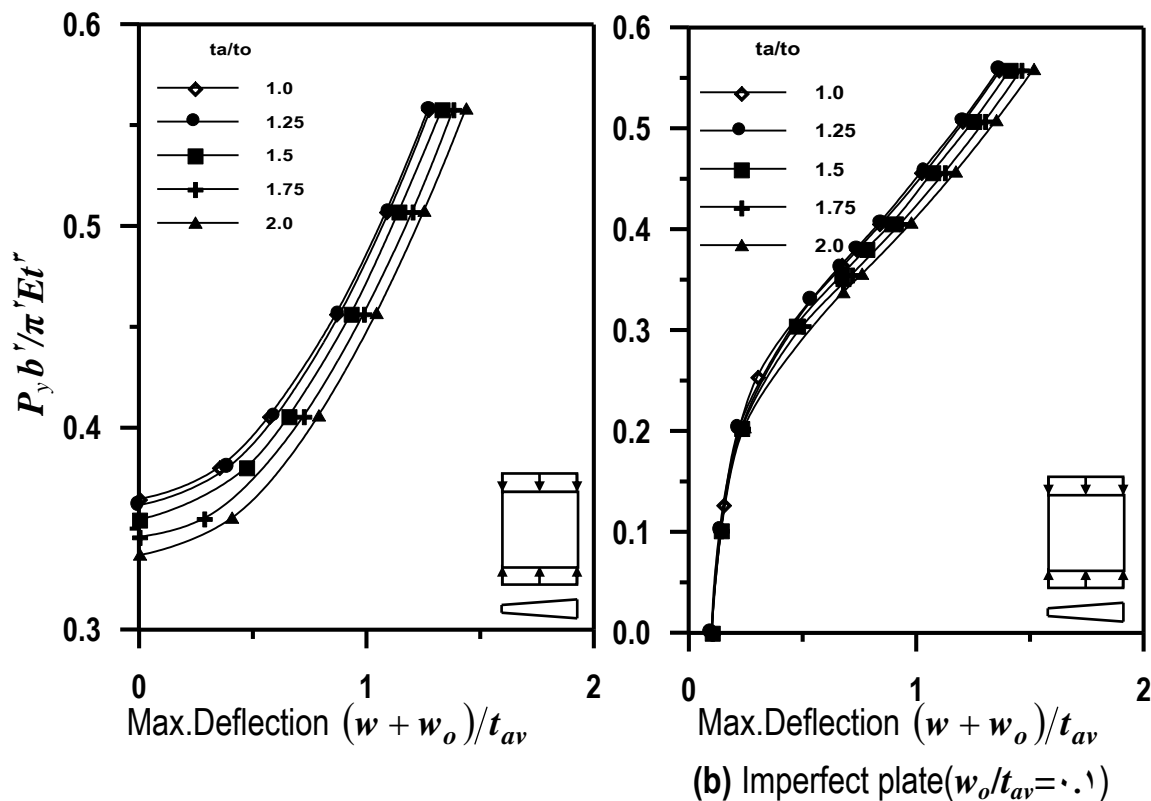


Figure (5.12): Post-buckling behavior of a simply supported thin square plate with variable thickness under uniaxial compressive load in x -direction.

Table (5.4): Load-deflection results of imperfect plate ($w_o/t_{av}=0.1$).

Load $P_x b^2 / \pi^2 E t^3$	Max. deflection $((w+w_o)/t_{av})$				
	t_d/t_o				
	1.0	1.25	1.5	1.75	2.0
0	0.100	0.100	0.100	0.100	0.100
0.126	0.100	0.100	0.100	0.108	0.162
0.203	0.300	0.310	0.328	0.390	0.566
0.364	0.670	0.710	0.810	0.909	1.144
0.400	0.830	0.883	1.000	1.170	1.340
0.406	1.020	1.084	1.220	1.400	1.603
0.507	1.200	1.260	1.420	1.617	1.830
0.507	1.360	1.430	1.590	1.790	2.000

Figure (5.13) presents the load-deflection curve for a simply supported thin square plate under uniaxial compressive load in y-direction (the direction normal to thickness variation). This figure shows a comparison between a plate with constant thickness and variable thickness for perfect and imperfect condition.



(a) Perfect plate

Figure (5.13): Post-buckling behavior of a simply supported thin square plate with variable thickness under uniaxial compressive load in y -direction.

Figure (5.14) presents the load-deflection curve of a simply supported thin square plate under biaxial ($P_x=P_y$) compressive load. This figure shows a comparison between plate with constant thickness and variable thickness and for perfect and imperfect condition.

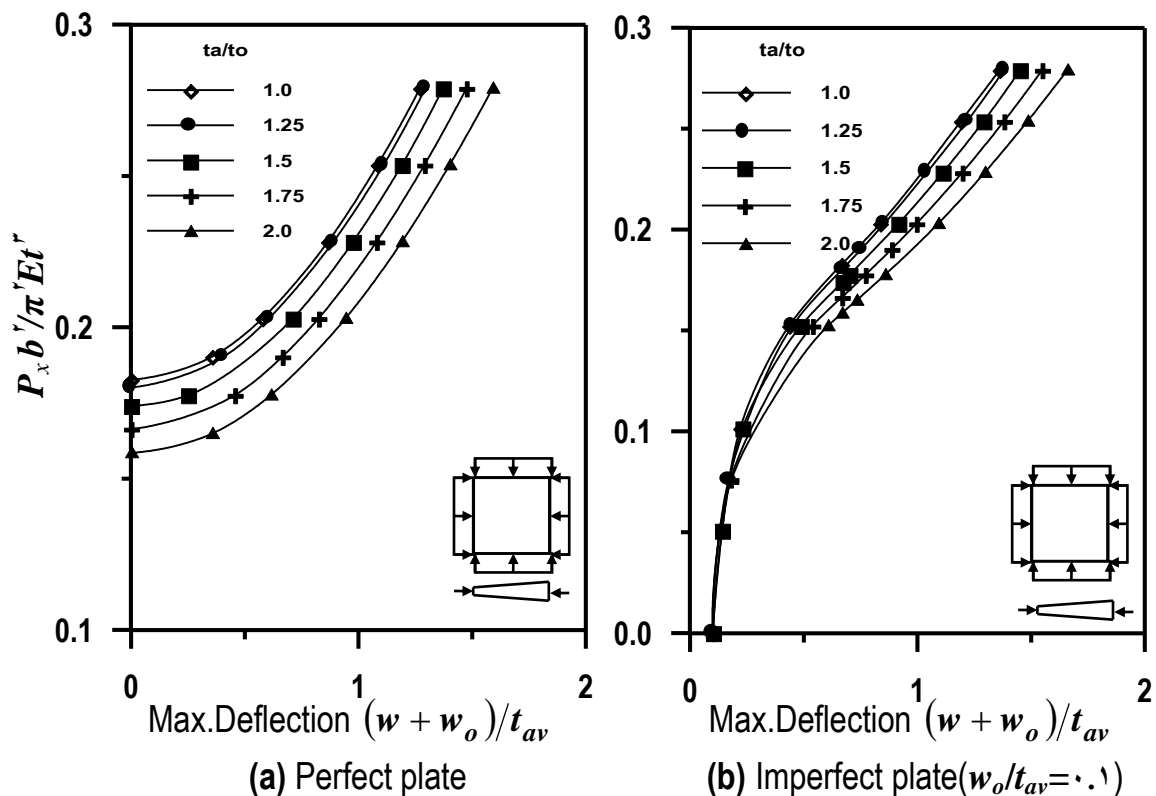


Figure (5.14): Post-buckling behavior of a simply supported thin square plate with variable thickness under biaxial compressive load.

From these figures, it can be noticed that: -

1. Buckling loads decreases with the increase of thickness variation.
2. Post-buckling stiffness decreases with increase of thickness variation.
3. The direction of the load (parallel or normal to the variation of thickness) affects the buckling and post-buckling behavior.
4. The rate of reduction in post-buckling stiffness when the load is in x -direction (the direction parallel to thickness variation) is more than

the reduction when the load is in y -direction (the direction normal to thickness variation).

5.4 Elasto-plastic Analysis

5.4.1 Plate Dimensions and Properties

To study the effect of material non-linearity in addition to geometric non-linearity for a plate in compression, several plates with various width/thickness (b/t) were analyzed.

In the analysis, the plate dimensions (a) and (b) were taken as [$a=0.870$ (m), and $b=1$ (m)] to give an aspect ratio (a/b) equal to 0.870 . The effect of aspect ratio will be discussed in the next section. Different plate thicknesses were selected to give width/thickness (b/t) ratios of $(30, 40, 50, 80)$ so that a range from the stocky plate to slender plate was considered. The initial imperfection was assumed to be a sinusoidal curve. The plate was loaded by the imposition of an in-plane compressive load. The material properties of a steel plate were assumed to be as follows: -

Modulus of elasticity (E)= 2.07×10^5 MPa.

Material yield stress (σ_o)= 250 MPa.

Poisson ratio (ν) = 0.3 .

5.4.2 Effect of Plate Aspect Ratio (a/b)

In the analysis, a single imperfect plate element with a prescribed aspect ratio (a/b) is considered. The plate is assumed simply supported along all four edges. This implies, in the structures, a distribution of out-of-flatness uniformly and symmetrically rippled to the desired amplitude in

both x and y directions forming a grid of rectangles $a \times b$. The fact that such a distribution will never occur in practice should not be allowed to be obscure. The important influence of (a/b) was studied by Little⁽³⁸⁾ [1977]. There are several cases where the plate behavior is influenced more strongly by (a/b) than by (w_o/t) . For each case, if a random distribution of out-of-flatness exists in the structure, there will be a strong tendency for failure to occur where conditions are most favorable for buckles of the preferred half-wave length. There will be some modification of behavior because the edges of each plate element are not perfectly simply supported, owing not only to the random (w_o) distribution but also to the rotational restraint provided by stiffeners. However, the assumption of simply supported condition is necessary for the results to be on the safe side, especially at relatively low values of w_o/t (38).

Moxham⁽⁴⁴⁾ suggested that $(a/b=0.875)$ is a suitable figure for general application, basing this conclusion on a limited number of calculations for very small (w_o) values. Little⁽³⁸⁾ and Crisfield⁽¹¹⁾ supported this conclusion. Consequently, the theoretical results produced by Moxham, Little, and Crisfield for the elasto-plastic analysis of plates in compression were represented for plates with an aspect ratio $(a/b=0.875)$.

However, the results produced by Harding⁽²⁷⁾ and Frieze⁽¹⁰⁾ were for plates with an aspect ratio $(a/b=1.0)$.

In the present study, the aspect ratio was considered to be (0.875) in the specific examples. Of course, the computer program is completely general and can be applied to any required aspect ratio.



5.4.3 Comparison with Other Investigations

The results obtained from the present study are compared with other studies by Moxham⁽⁴⁴⁾, Little⁽³⁸⁾, Harding⁽³⁷⁾, Crisfield⁽¹⁷⁾, and Mathlum⁽³⁹⁾.

Moxham and Little used the energy methods in their analysis. Harding used the finite difference method. Crisfield and Mathlum used the finite element method. Here it is sufficient to note that the results obtained from the various solutions differ in detail from one to other, but that, in general, the agreement between the solutions is good when account is taken from the different approaches of approximations required in the analyses. In the figures the average applied compressive stress (σ) is plotted on the vertical axis as a ratio of the uniaxial yield stress (σ_o). Similarly, the axial strain (ϵ) is plotted on the horizontal axis as a ratio of the uniaxial yield strain (ϵ_o); the value of ϵ_o is calculated as (σ_o/E).

Figures (5.15) and (5.16) present the load-deflection curves of two slender plates under compressive load and with the edges of the plate simply supported. These cases were first analyzed by Moxham⁽⁴⁴⁾; the other results shown are those due to Crisfield⁽¹⁷⁾, and Mathlum⁽³⁹⁾.

Figures (5.17) to (5.20) present the average stress-strain curve of a simply supported plate under compressive load and with slenderness ratios (b/t) (30, 40, 50, and 60). These results are presented for two values of initial imperfection [$w_o = 0.001b$ and $0.002b$].



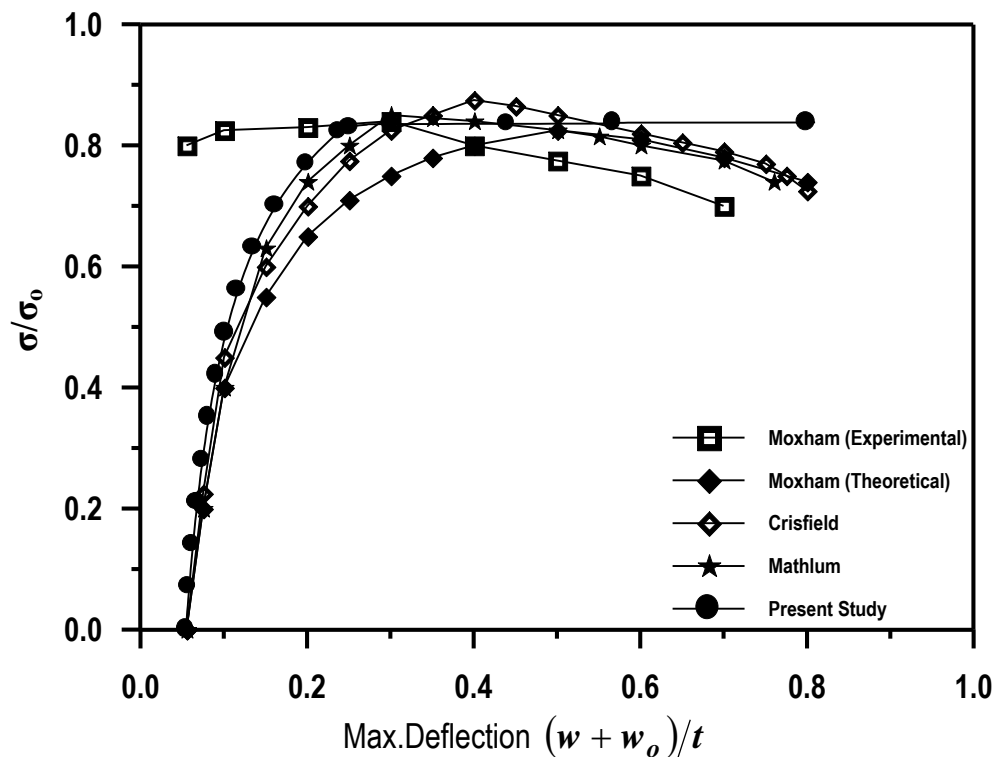


Figure (5.15): Load – deflection curve of a simply supported thin rectangular plate under compressive load, ($b/t=0.0, a/b=0.170, w_0/t=0.000$).

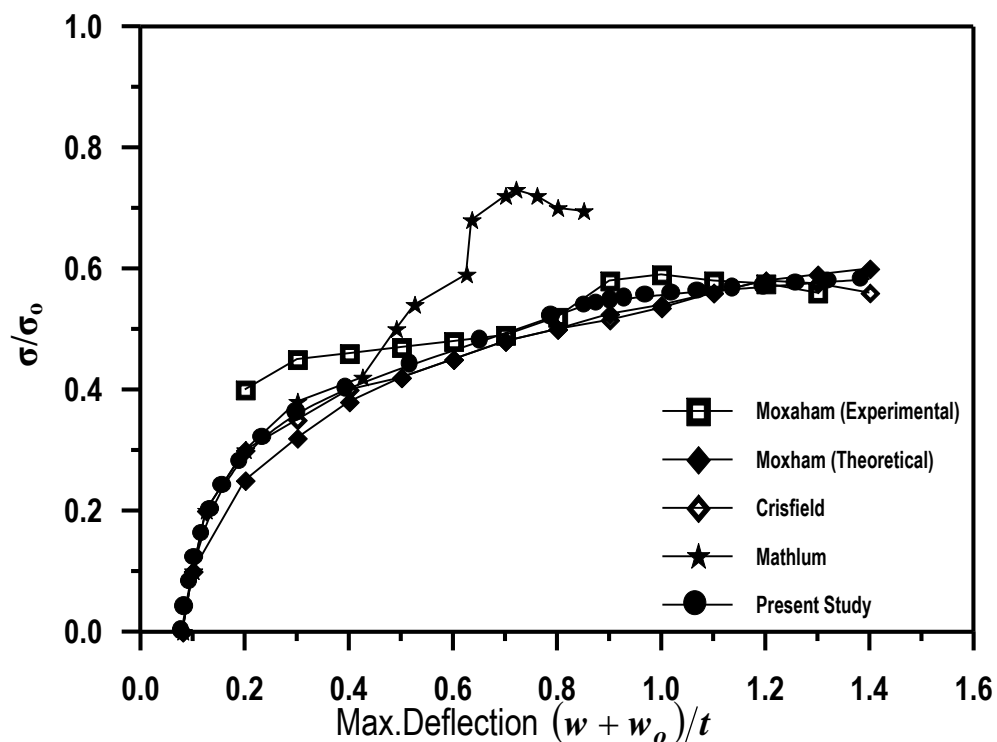
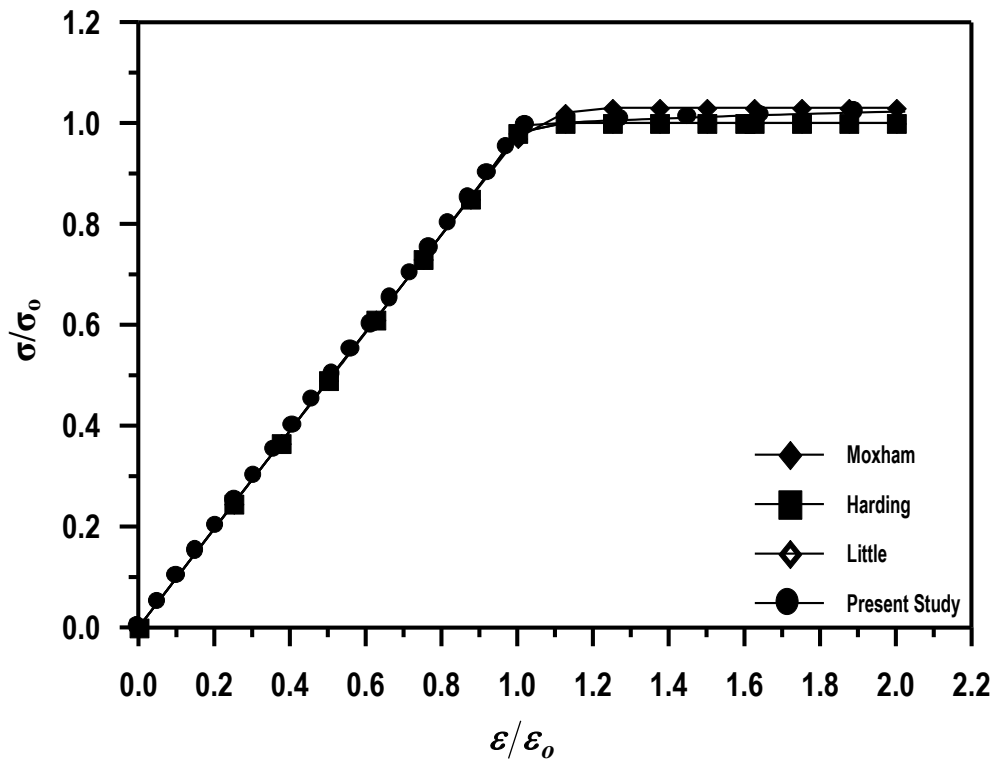
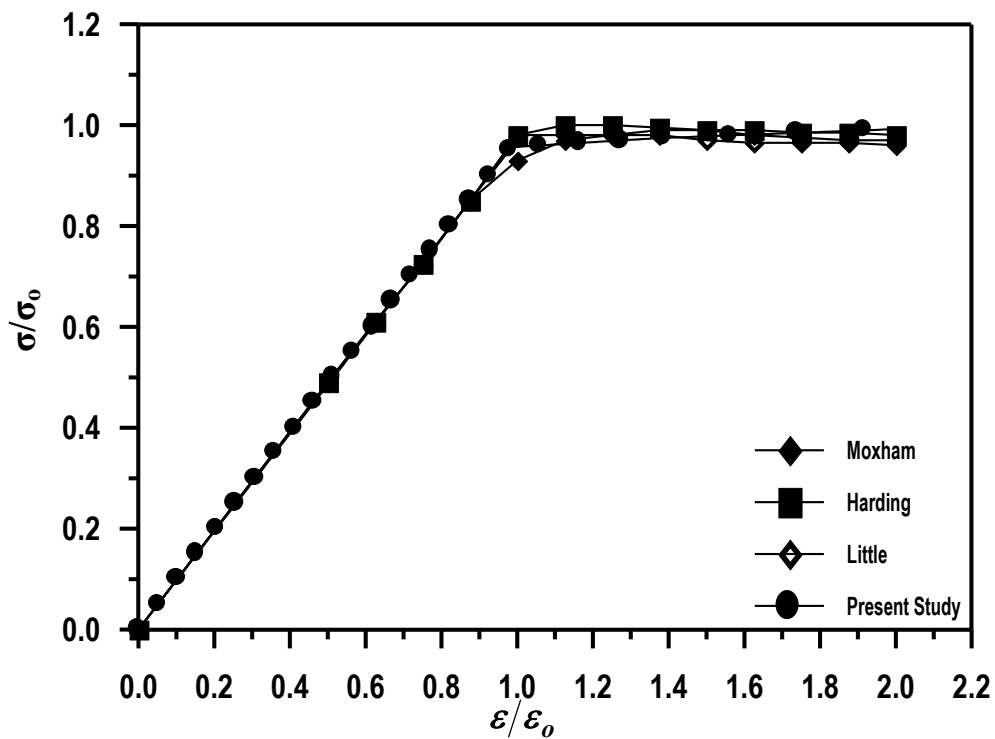


Figure (5.16): Load-deflection curve of a simply supported thin rectangular plate under compressive load, ($b/t=1.0, a/b=0.170, w_0/t=0.000$).



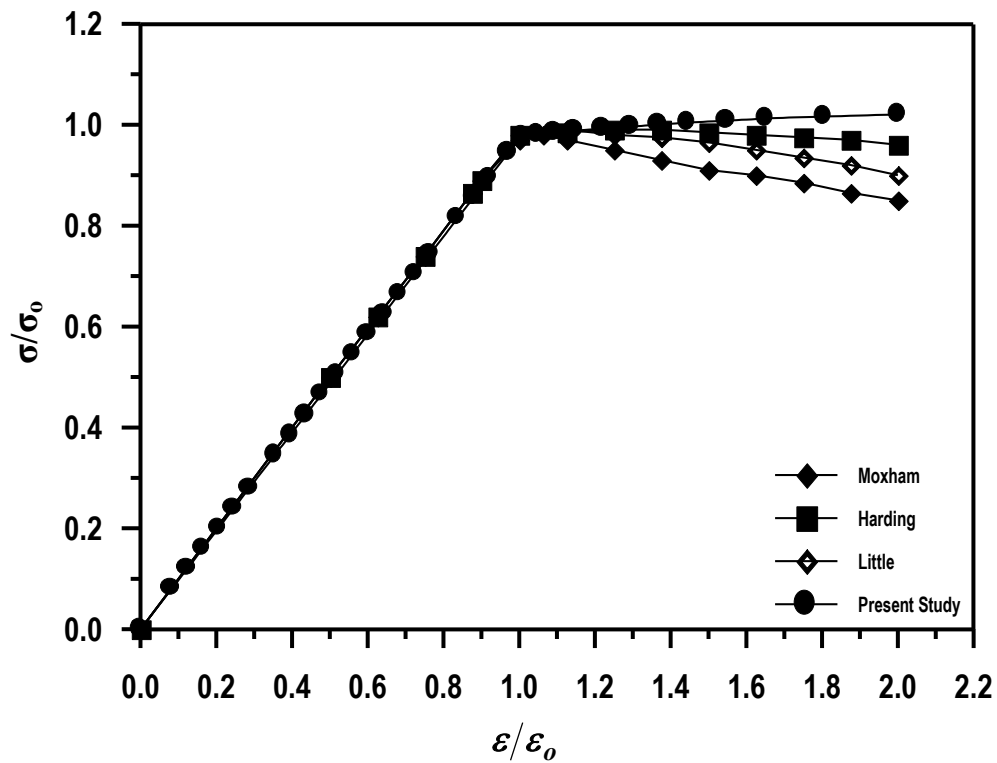


(a) A plate with initial imperfection ($w_0 = 0.001b$)

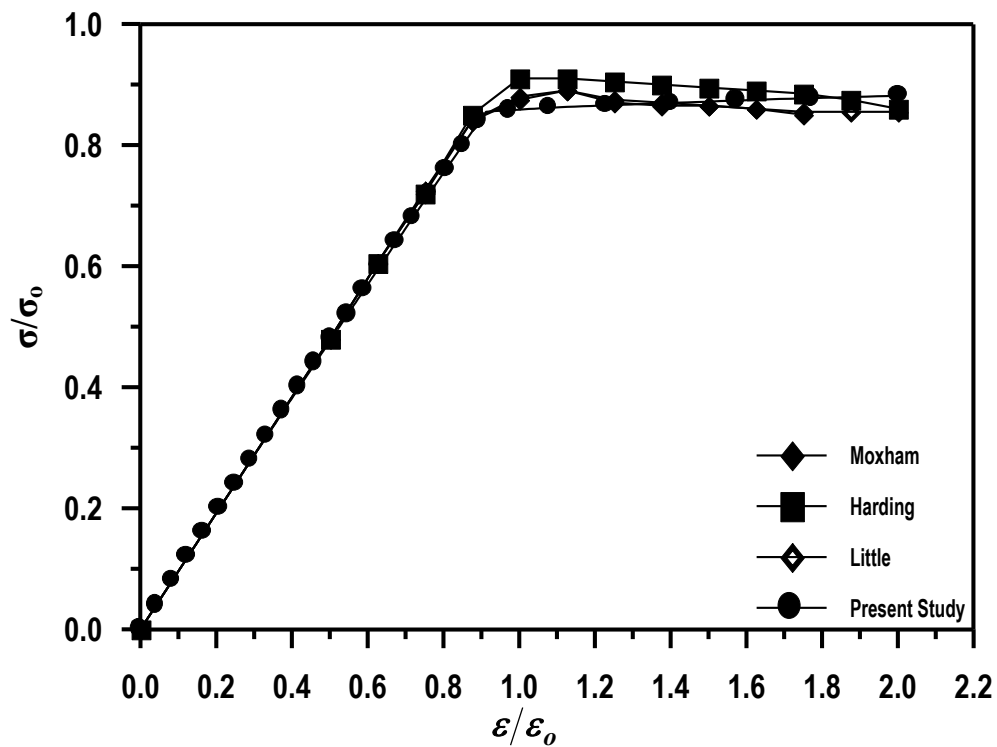


(b) A plate with initial imperfection ($w_0 = 0.002b$)

Figure (5.17): Average stress-strain curve of a simply supported thin rectangular plate under compressive load, ($b/t = 30, a/b = 0.875$).



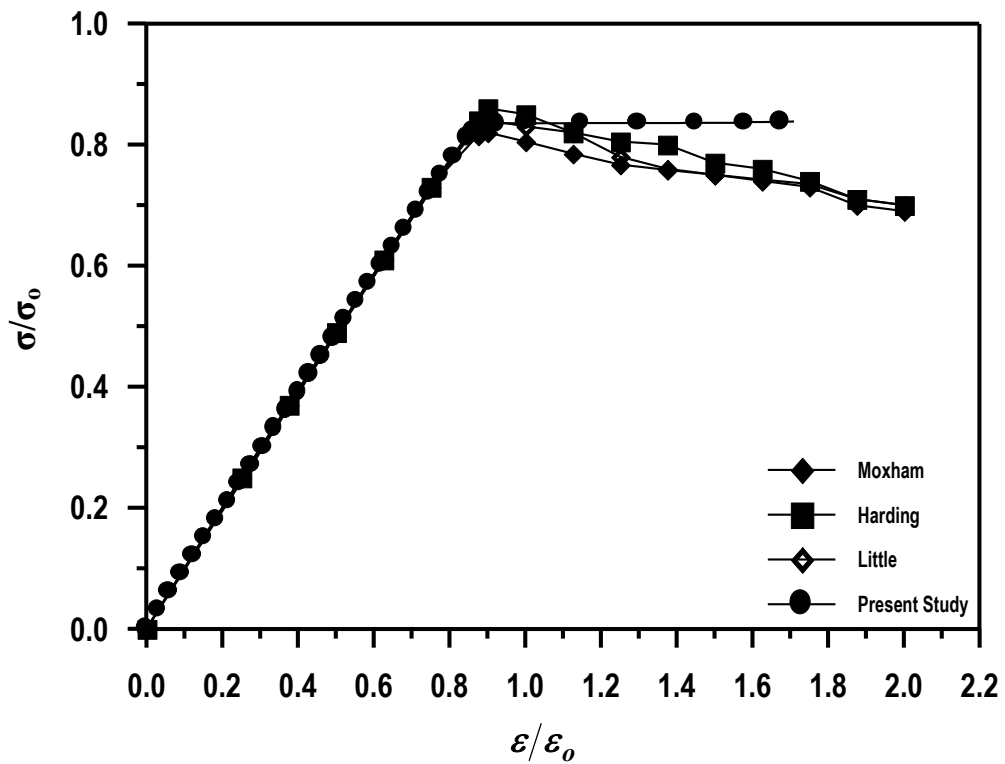
(a) A plate with initial imperfection ($w_0 = 0.1b$)



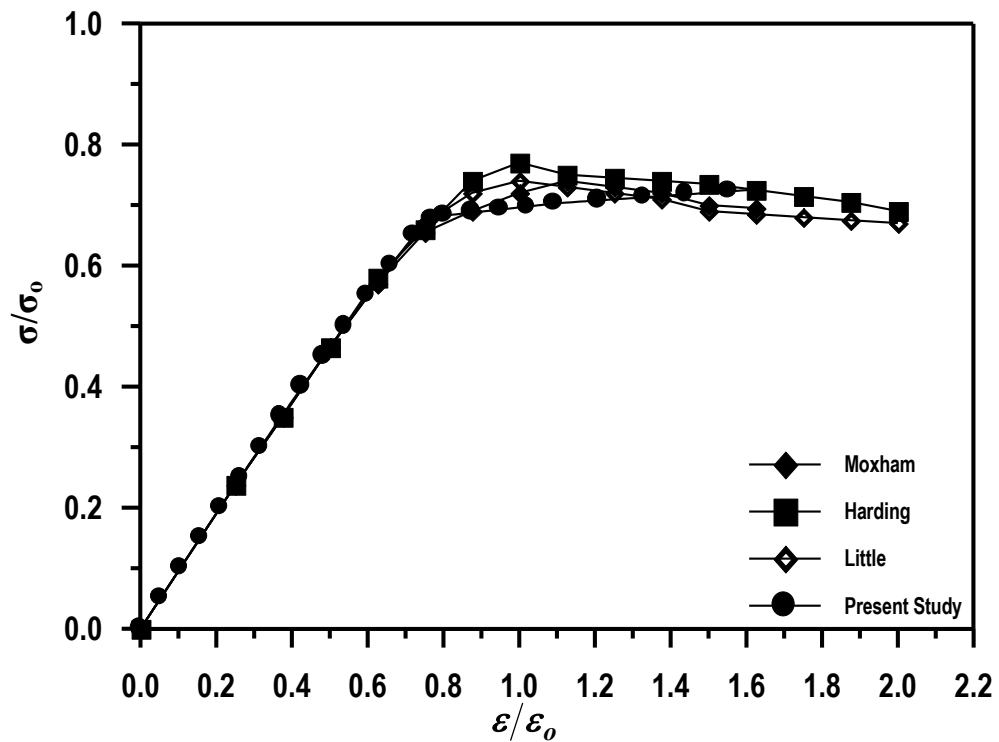
(b) A plate with initial imperfection ($w_0 = 0.05b$)

Figure (5.11): Average stress-strain curve of a simply supported thin rectangular plate under compressive load, ($b/t = 20$, $a/b = 1.5$).





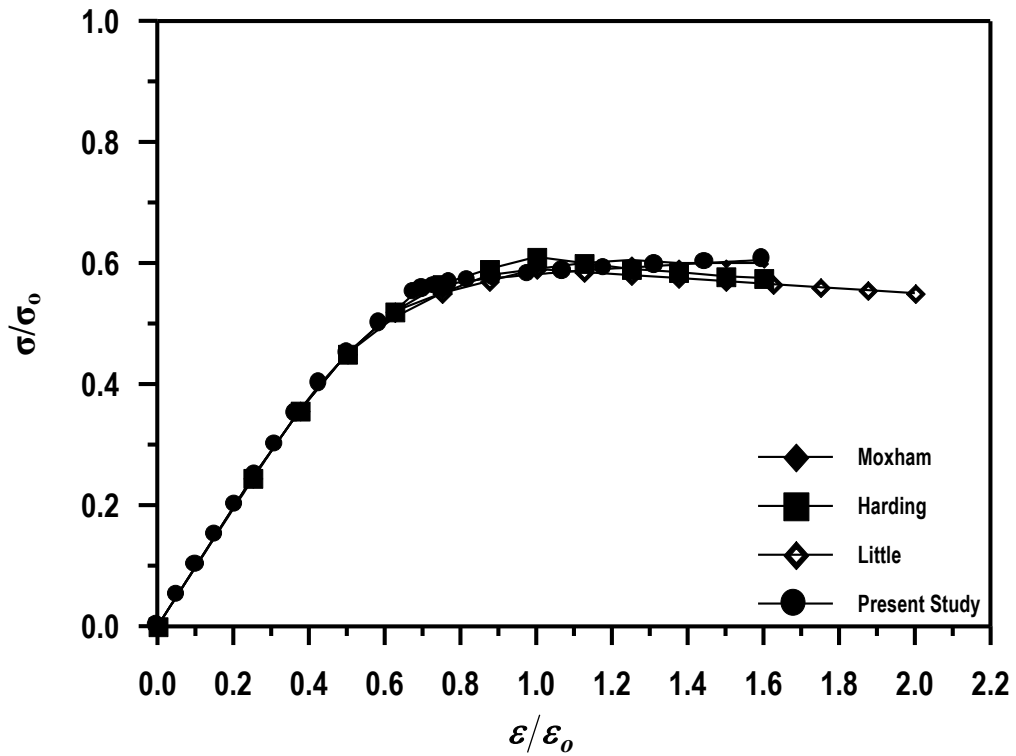
(a) A plate with initial imperfection ($w_0 = 0.1b$)



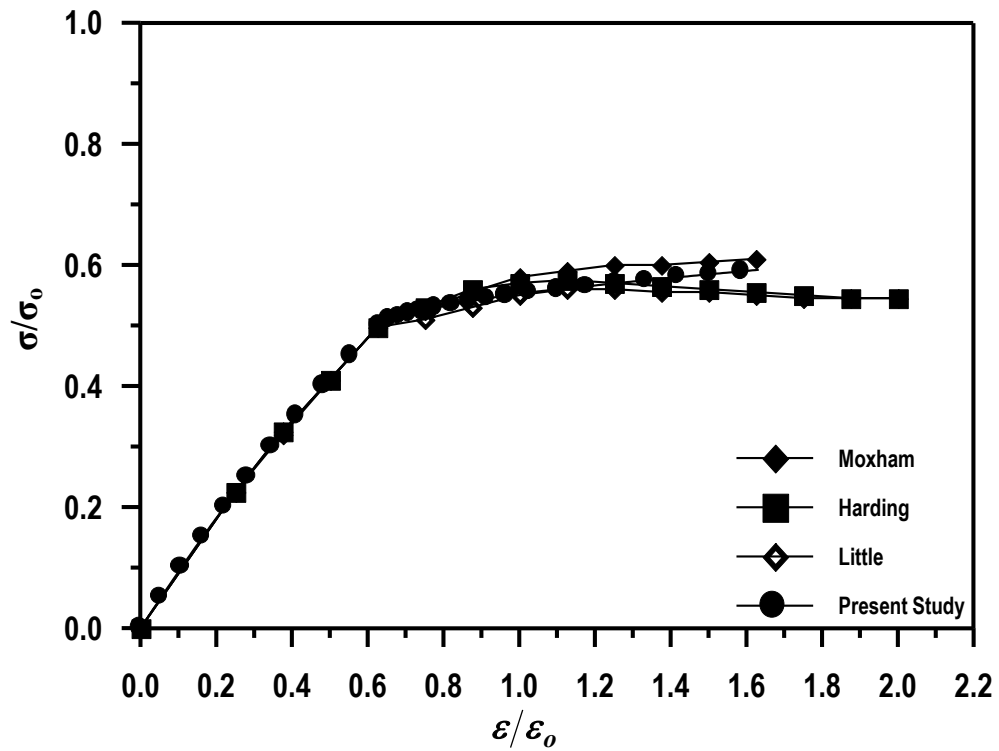
(b) A plate with initial imperfection ($w_0 = 0.05b$)

Figure (5.19): Average stress-strain curve of a simply supported thin rectangular plate under compressive load, ($b/t = 100, a/b = 1.875$).





(a) A plate with initial imperfection ($w_0 = \dots b$)



(b) A plate with initial imperfection ($w_0 = \dots b$)

Figure (5.2): Average stress-strain curve of a simply supported thin rectangular plate under compressive load, ($b/t = 10$, $a/b = 1.75$).

From these figures, it can be noticed that: -

١. For $b/t=٣$, all the solutions give comparable results for the peak load levels. The level of imperfection has a marked effect on the peak loads.
٢. For $b/t=٤$, all the solutions give comparable results for the peak load levels with some differences in the unloading paths.
٣. For $b/t=٥$ all the solutions give comparable results for the peak load levels with some differences in the unloading paths because the present study used load control while other solutions used the displacement control.
٤. For $b/t=٨$, all the solutions give comparable results for the peak load level.
٥. These figures indicate that with the increasing of the initial imperfection, the in-plane stiffness of the plate decreases and a large amount of the ultimate strength is reduced.



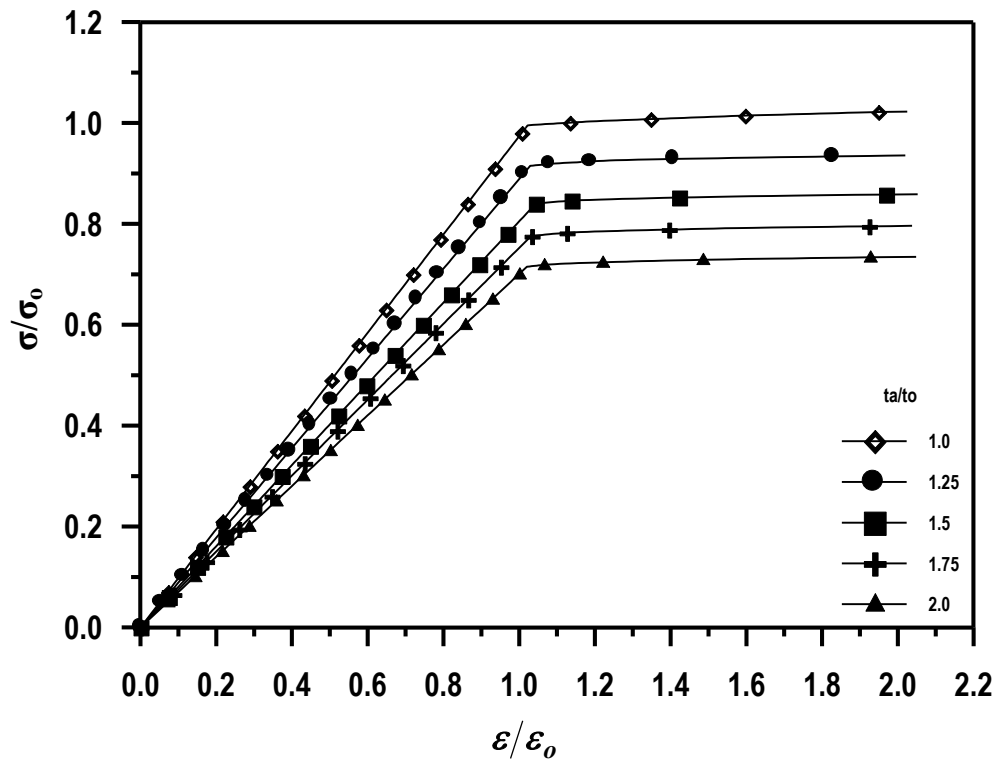
5.4.4 Parametric Study

The effect of tapering ratio on the elasto-plastic behavior is considered. Two plates are selected to study the effect of tapering ratio having slenderness ratio ($b/t=3, 8$). The first plate is represented a stocky plate and the second plate is represented as a slender plate. The magnitude of initial imperfections are set as ($w_0=0.001m$ and $0.0005m$). The effect of load direction is considered in the present study.

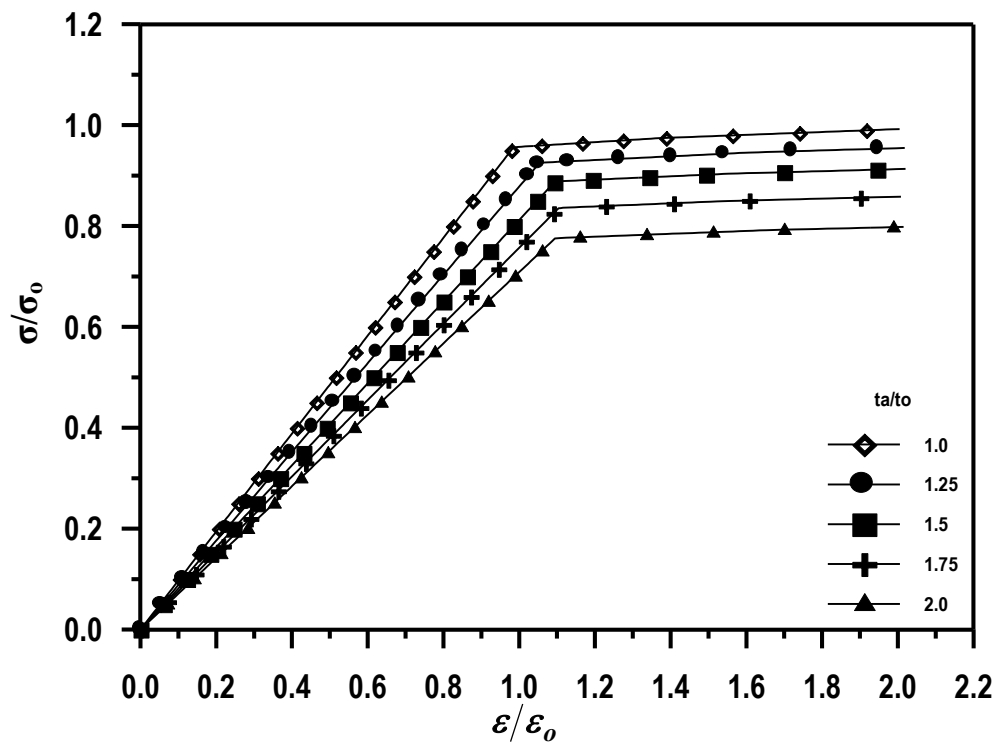
Figures (5.21) and (5.22) present the average stress-strain curve of a simply supported plate with slenderness ratios (b/t) (3, and 8) respectively, and in-plane displacements of the unloaded edges are unrestrained so that little membrane stresses in the transverse direction may occur. These figures are presented for two values of initial imperfection, $w_0=0.001b$ and $w_0=0.0005b$. The compressive load is in x -direction (the direction parallel to thickness variation). These figures show the influence of the thickness variation on the ultimate strength of the plate in comparison with the ultimate strength for a plate with constant thickness.

Figure (5.23) and (5.24) present the average stress-strain curve of a simply supported plate ($b/t=3$, and 8), respectively. These figures are presented for two values of initial imperfection, $w_0=0.001a$ and $w_0=0.0005a$. The compressive load is in y -direction (the direction normal to thickness variation).



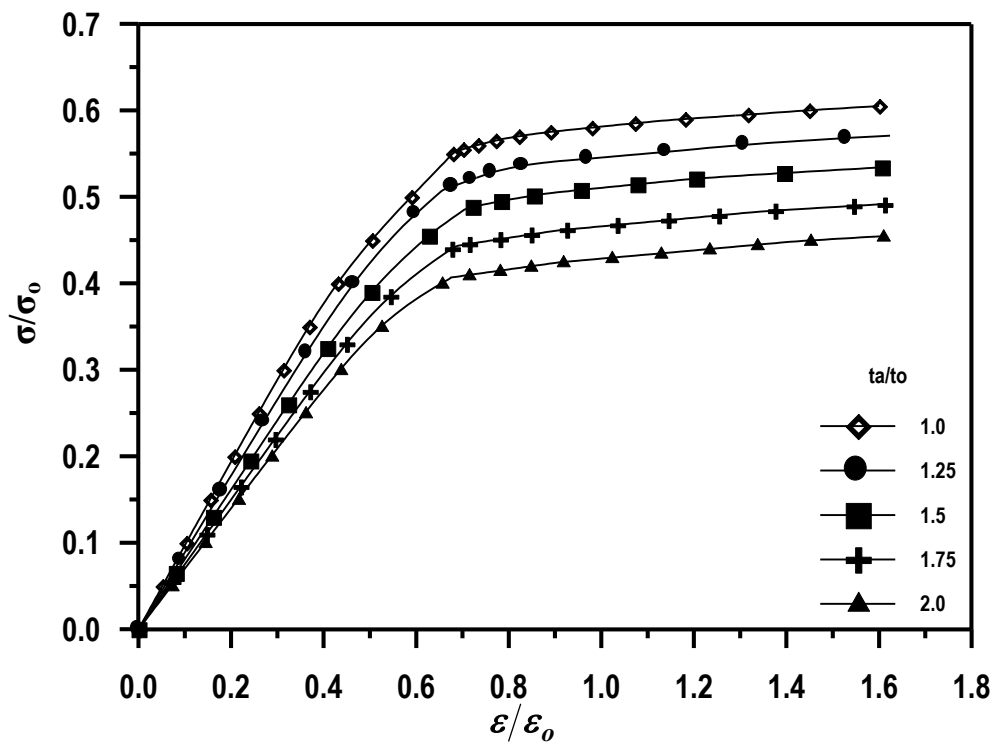


(a) A plate with initial imperfection ($w_0 = \dots \cdot b$)

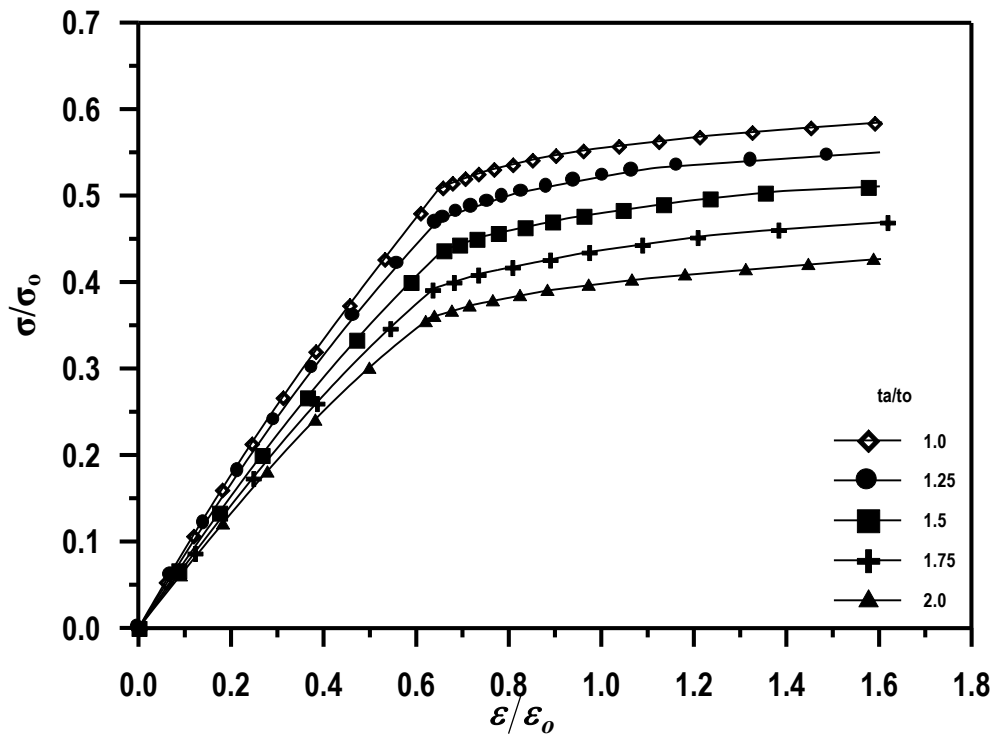


(b) A plate with initial imperfection ($w_0 = \dots \cdot b$)

Figure (5.11): Average stress-strain curve of a simply supported thin rectangular plate under compressive load, ($b/t_{av} = 3, a/b = 1.75$).

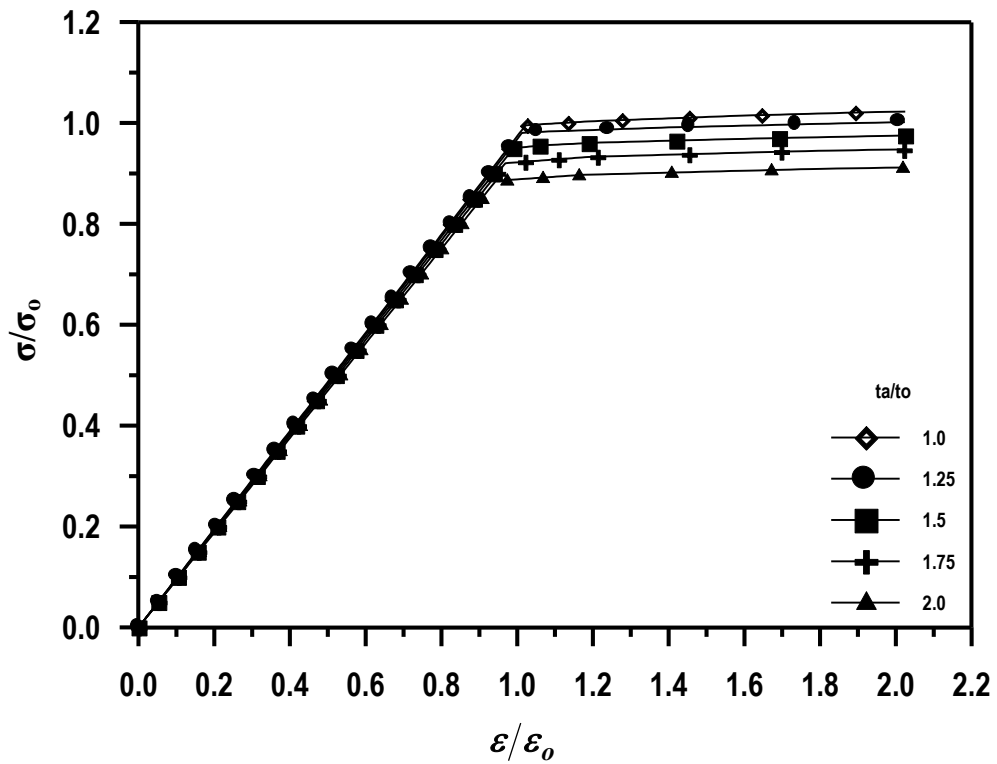


(a) A plate with initial imperfection ($w_0 = \dots b$)

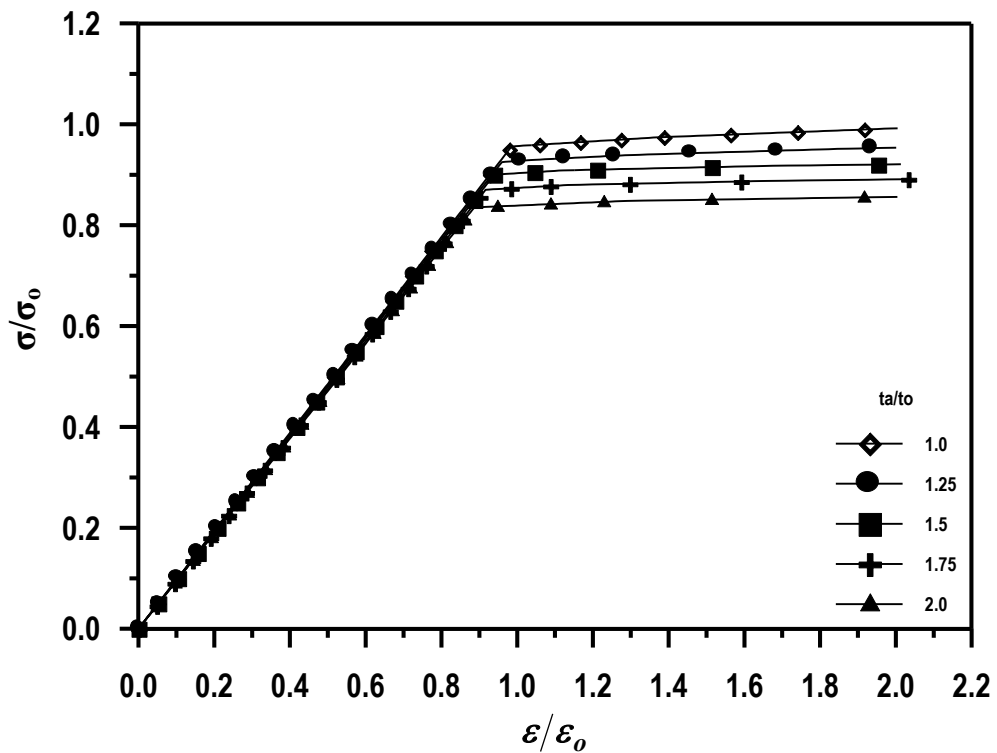


(b) A plate with initial imperfection ($w_0 = \dots b$)

Figure (9.22): Average stress-strain curve of a simply supported thin rectangular plate under compressive load, ($b/t_{av} = 1.0, a/b = 0.175$).

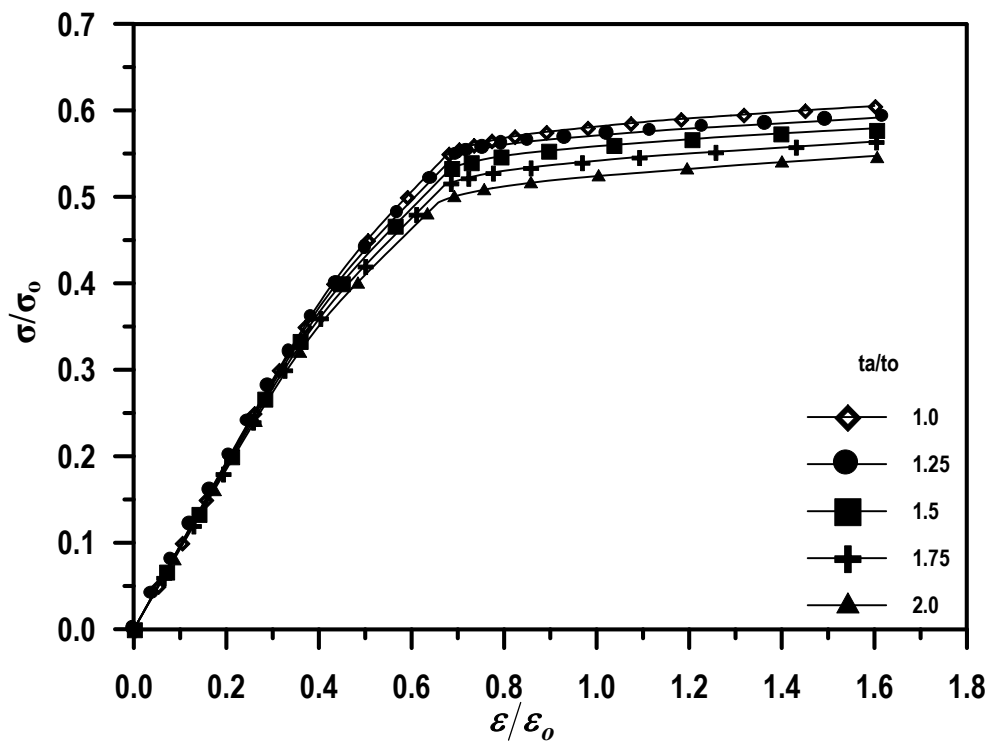


(a) A plate with initial imperfection ($w_0 = 0.1a$)

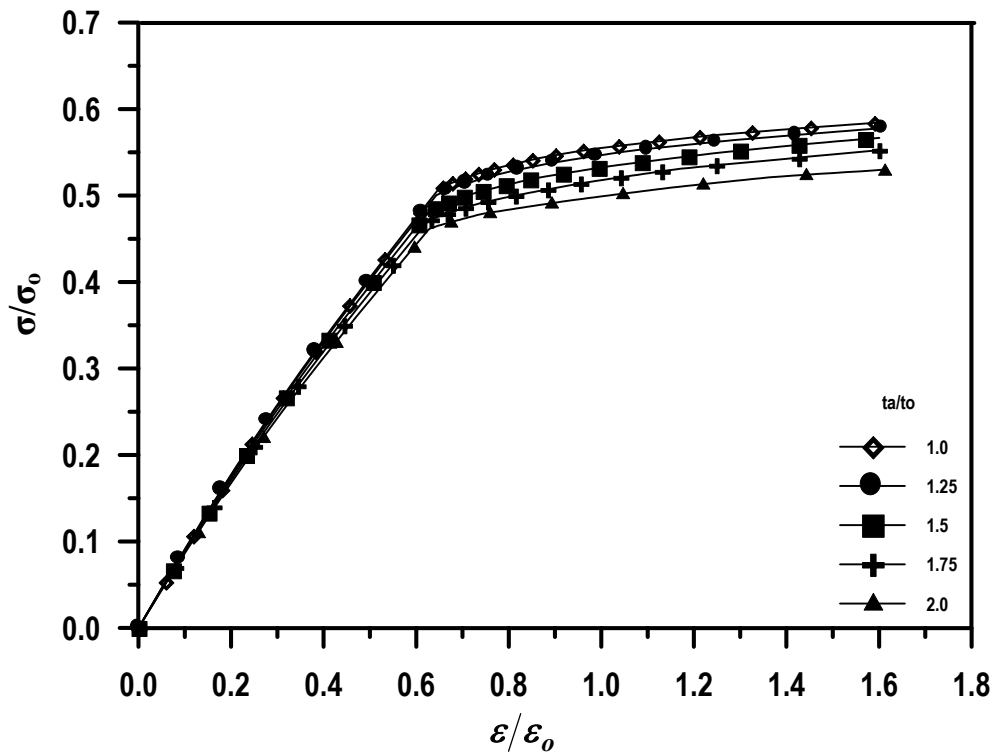


(b) A plate with initial imperfection ($w_0 = 0.2a$)

Figure (5.23): Average stress-strain curve of a simply supported thin rectangular plate under compressive load, ($b/t_{av} = 3, b/a = 0.875$).



(a) A plate with initial imperfection ($w_0 = 0.001a$)



(b) A plate with initial imperfection ($w_0 = 0.0001a$)

Figure (5.24): Average stress-strain curve of a simply supported thin rectangular plate under compressive load, ($b/t_{av} = 10, b/a = 0.875$).

From these figures, it can be noticed that: -

١. The increase of the tapering ratio, in-plane stiffness of the plate decreases and a large amount of the ultimate strength is reduced.
٢. When the load is in x -direction (the direction parallel to thickness variation), the decrease in ultimate strength is more than the decreasing in ultimate strength when the load is in y -direction (the direction normal to thickness variation).
٣. The decrease in the in-plane stiffness of the plate starts from the low level of loading, when the load is in x -direction (the direction parallel to thickness variation).

CONCLUSIONS AND RECOMMENDATIONS

٦.١ General

From the theoretical analysis and the comparison with available studies which is described in the previous chapters. The following conclusions can be drawn with regard to the results obtained for plates under compressive load.

The recommendations for the future work are also presented herein.

٦.٢ Conclusions

١. The finite difference method is very suitable for programming and sufficiently accurate for post-buckling and ultimate strength analysis of thin rectangular plate with constant or tapering thickness, as it tends to a convergent solution when the nodes' density is increased.
٢. The load limit in the post-buckling range for which the plate is still in a stable equilibrium depends on the type of boundary conditions.
٣. The behavior of a thin plate is very sensitive to the amount of initial imperfections.
٤. The behavior of a thin plate with variable thickness is very sensitive to the tapering ratio (for plate with the same volume) such that the increase of the tapering ratio will induce higher increase in the out-of-plane displacements.
٥. When the load is in x -direction (the direction parallel to thickness variation), the out-of-plane displacements will be more

than the out-of-plane displacement when the load is in y -direction (the direction normal to thickness variation).

٦. The imposition of an in-plane load makes the solution unstable at the higher loads, so that an increase in the load would then produce an infinite deflection.
٧. For the plates under uniaxial compressive load, the stocky plate simply yields without buckling while the very slender plate buckles elastically. Approximately the plate with about $(b/t=100)$ represents a “critical buckling plate”, where buckling and yielding occurs almost simultaneously.
٨. The increase of the initial imperfection causes a decrease in the ultimate strength.
٩. The increase of the tapering ratio causes a decrease in the ultimate strength.
١٠. For plates with variable thickness, when the load is in x -direction (the direction parallel to thickness variation), the in-plane stiffness of the plate decreases at the low level of loading.
١١. The decrease in the ultimate strength when the load is in x -direction (the direction parallel to thickness variation) is more than the decrease in the ultimate strength when the load is in y -direction (the direction normal to thickness variation).

٦.٣ Recommendations

From the present study the following recommendations are suggested for further studies.

١. An extensive study of the influence of initial imperfection shape on the behavior of thin plate.

- ϲ. The buckling, post-buckling, and elasto-plastic behavior of thin plates with variable thickness and under pure shear load.
- ϳ. The buckling, post-buckling, and elasto-plastic behavior of thin plates under uniaxial patch loading.
- ϴ. Using the displacement control technique to march for the ultimate stage in the post-yielding range.
- ϵ. Making a parametric study for an imperfect plate subjected to complex membrane forces (combined compressive and shear loading).
- ϶. Making an ultimate investigation for an imperfect stiffened plate.
- Ϸ. Making an investigation for post-buckling and ultimate strength behavior for an imperfect plate with internal holes.

REFERENCES

١. Aalami, B., and Chapman, J.C., "Large Deflection Behavior of Orthotropic Plates under Transverse and In-plane Loads", Proc. ICE, London, England, Vol. ٤٢, Mar., ١٩٦٩, pp. ٣٤٧-٣٨٢.
٢. Abbas, F. K., and Mathlum, M. K., "Large Deflection Elasto-Plastic Analysis of Plates by Finite Element Methods", Eng. And Technology, Baghdad, Vol. ١٩, No. ٤, ٢٠٠٠, pp. ٨٨-١٠٨.
٣. Abdel-Sayed, G., "Effective Width of Thin Plates in Compression", ASCE, J. Struct. Eng., Vol. ٩٥, No. ST١٠, Oct., ١٩٦٩, pp. ٢١٨٣-٢٢٠٣.
٤. Basu, A.C., and Chapman J.C., "Large Deflection Behavior of Transversely Loaded Rectangular Orthotropic Plates", Proc., ICE, London, England, Vol. ٣٥, Sept., ١٩٦٦, pp. ٧٩-١١٠.
٥. Bhaumik, A. K., and Hanley, J. T., "Elasto-Plastic Plate Analysis by Finite Differences", ASCE, J. Struc.Div., Vol. ٩٣, No. ST٥, Oct., ١٩٦٧, pp. ٢٧٩-٢٩٤.
٦. Bjelajac, N., "Evaluation of Post-buckling Equilibrium Branches for Perfect and Imperfect Plates by Finite Difference Method", Numerical Methods in Continuum Mechanics, Liptovský Jačn, Slovak Republic, ٢٠٠٠, pp. ١-١٨.
٧. Bradfield, C.D., "An Evaluation of The Elastic-Plastic Analysis of Plates Loaded by Uniaxial In-Plane Compression", Int. J. Mech. Sci., Vol. ٢٤, No. ٣, ١٩٨٢, pp. ١٢٧-١٤٦.
٨. Bradfield, C.D., and Stonor, R.W.P., "Simple Collapse Analysis of Plates in Compression", ASCE, J. Struc. Eng., Vol. ١١٠, No. ١٢, Dec., ١٩٨٤, pp. ٢٩٧٩-٢٩٩٣.
٩. Bryan, G. H., "On The Stability of a Plate under Thrusts in its Own Plane with Application to The Buckling of The Sides of Ships" Proc. London Math. Soc., Vol. ٢٢, ١٨٩١, pp. ٥٤-٦٧, cited in [٤٥].

10. Chajes, A., "Principles of Structural Stability Theory", Prentice-Hall, Inc., Englewood Cliffs, New Jersey, 1974.
11. Chehil, D.S., and Dua, S.S., "Buckling of Rectangular Plates With General Variation in Thickness ", ASME, J. Appl. Mech., Vol. 40, 1973, pp. 740-751.
12. Chia, C.Y., "Nonlinear Analysis of Plates", McGraw- Hill International Book Company, 1980.
13. Chin, C. K., AL-Bermani, F. G. A., and Kitipornchai, S., "Finite Element Method for Buckling Analysis of Plates Structure", ASCE, J. Struct. Eng, Vol. 119, No. 4, Apr., 1993, pp. 1050-1068.
14. Coan, J.M., "Large Deflection Theory for Plates with Small Initial Curvature Loaded in Edge Compression", ASME, J. Appl. Mech., Vol. 18, June, 1951, pp. 143-151.
15. Colville, J., Becker, E.B., and Furlong, R.W., "Large Deflection Analysis of Thin Plates", ASCE, J. Struc. Div., Vol. 99, No. ST3, Mar., 1973, pp. 349-364.
16. Colville, J., and Kuen-Yaw Shye, "Post-buckling Finite Element Analysis of Flat Plates", ASCE, J. Struc. Div., Vol. 100, No. ST2, Feb., 1974, pp. 297-311.
17. Crisfield, M.A., "Full-range Analysis of Steel Plates Stiffened Plating under Uniaxial Compression", Proc., ICE, Vol. 69, Part 2, Dec., 1970, pp. 693-724.
18. Fok, C. D. "Effects of Initial Imperfections on the Elastic Post-buckling Behavior of Flat Plates." Ph. D. Thesis, Monash University, cited in [40].
19. Fok, W.C., "Evaluation of Experimental Data of Plate Buckling", ASCE, J. Eng. Mech., Vol. 110, No. 4, 1984, pp. 577-588.

٢٠. Frieze, P.A., Hobbs, R.E., and Dowling, P.J., "Application of Dynamic Relaxation to The Large Deflection Elasto-Plastic Analysis of Plates", *Comp. & Struc.*, Vol.٨, ١٩٧٨, pp.٣٠١-٣١٠.
٢١. Gallagher, R.H., "Finite Element Analysis Fundamentals", Prentice-Hall, Inc., Englewood Cliffs, New Jersey, ١٩٧٣.
٢٢. Gaylord, E.H., and Gaylord, C.N., "Design of Steel Structures", McGraw- Hill Kogakuasha, LTD., ١٩٧٢.
٢٣. Harding, J.E., Hobbs, R.E., and Neal, B.G., "The Elasto-Plastic Analysis of Imperfect Square Plates under In-plane Loading", *Proc. ICE*, Part ٢, Vol.٦٣, Mar., ١٩٧٧, pp.١٣٧-١٥٨.
٢٤. Hodge, P. G., "Plastic Analysis of Structures" McGraw-Hill, New York, ١٩٥٩.
٢٥. Husain, H.M., Al-Daami, H., and Amash, H.K., "Buckling Behavior of Rectangular Plate with Variable Thickness." *Eng. And Technology*, Baghdad, Vol.٢١, No.١٠, ٢٠٠٢, pp.٧٣٦-٧٤٥.
٢٦. Jaeger, L.G., "Elementary Theory of Elastic Plates", Pergamon Press LTD. Headington Hill Hall, Oxford, ١٩٦٤.
٢٧. Jayachandran, S.A., Gopalakrishnan, S., and Narayana, R., "Explicit Incremental Matrices for the Post-buckling Analysis of Thin Plates with Small Initial Curvature", *Struct. Eng. and Mech.*, Vol.١٢, No.٣٠, ٢٠٠١, pp.٢٨٣-٢٩٥.
٢٨. Jia-Rang, F., "Plates of Varying Thickness with Four Simply Supported Edges", *ASCE, J. Eng. Mech. Div.*, Vol.١٠٨, No. EM١, Feb., ١٩٨٢, pp.١٦٧-١٧٩.
٢٩. Johnson, W., and Mellor, P.B., "Engineering Plasticity" Van Nastrand Reinhold Company, LTD., ١٩٧٣.
٣٠. Koopman, D.C., and Lance, R.H., "On Linear Programming and Plastic Limit Analysis" *J.Mech. and Phy. Solids*, London, Vol.١٣, ١٩٦٥, pp.٧٧-٨٧, cited in [٥]

٣١. Kopayashi, H., and Sonoda, K., "Buckling of Rectangular Plates with Tapered Thickness", ASCE, J. Struct. Eng., Vol. ١١٦, No. ٥, May, ١٩٩٠, pp. ١٢٧٨-١٢٨٩.
٣٢. Lam, S.S., "Post-buckling Analysis of Strut with General Initial Imperfection", Int. J. Num. Meth. Eng., Vol. ٤٣, ١٩٩٨, pp. ١٠١٧-١٠٢٨.
٣٣. Lee, S.C., and Yoo, C.H., "Strength of Plate Girder Web Panels under Pure Shear", ASCE, J. Struct. Eng., Vol. ١٢٤, No. ٢, Feb., ١٩٩٨, pp. ١٨٤-١٩٤.
٣٤. Lee, S.C., and Yoo, C.H., "Experimental Study on Ultimate Shear Strength of Web Panels", ASCE, J. Struct. Eng., Vol. ١٢٨, No. ٨, Aug., ١٩٩٩, pp. ٨٣٨-٨٤٦.
٣٥. Lee, S.C., and Yoo, C.H., and Yoon, D.Y., "Behavior of Intermediate Transverse Stiffness Attached on Web Panels", ASCE, J. Struct. Eng., Vol. ١٢٨, No. ٣, March, ٢٠٠٢, pp. ٣٣٧-٣٤٥.
٣٦. Lin, T.H., and Ho, E.Y., "Elasto-Plastic Bending of Rectangular Plates", ASCE, J. Eng. Mech. Div., Vol. ٩٤, No. EM١, Feb., ١٩٦٨, pp. ١٩٩-٢١٠.
٣٧. Lin, T.H., Lin, S.R., and Mazelsky, B., "Elasto-Plastic Bending of Rectangular Plates with Large Deflection", Trans. ASME, Vol. ٣٩, Dec., ١٩٧٢, pp. ٩٧٨-٩٨٢.
٣٨. Little, G.H., "Rapid Analysis of Plate Collapse by Live-Energy Minimization", Int. J. Mech. Sci., Vol. ١٩, ١٩٧٧, pp. ٧٢٨-٧٤٤.
٣٩. Mathlum, M.K., "Large Deflection Elasto-Plastic Analysis of Plates by Finite Element Method", M.Sc. Thesis, Department of Building and Costruction, Universty of Technology, Iraq, ١٩٩٧.
٤٠. Mirambell, E., Costa, J., and Arnedo, A., "Analytical and Experimental Study on the Behavior of Steel Panels under Plane Compression", Proc. Int. Conf. On Steel Struc., CI-Premier Pte. Ltd, Jakarta, Indonesia, ١٩٩٤, pp. ٢٠٥-٢١٢



٤١. Mirambell, E., Zarate, A.V., “Web Buckling of Tapered Plate Girders”, Proc. Inst. Civ. Eng. Structs & Bldgs, Vol. ١٤٠, Feb., ٢٠٠٠, pp. ٥١-٦٠.
٤٢. Mohammed, A.M., “Effect of Initially Imperfect and Boundary Condition on The Buckling and Post-buckling Behavior of Steel Plates”, M.Sc. Thesis, Department of Building and Construction, University of Technology, Iraq, ٢٠٠١.
٤٣. Moy, S. S., “Plastic Methods for Steel and Concrete Structures”, Macmillan Publishers, LTD, ١٩٨٥.
٤٤. Moxham, K.E. “Theoretical Prediction of The Strength of Welded Steel Plates in Compression” Cambridge University Report No. CUED/C-Struct. TR٢, ١٩٧١, cited in [٧].
٤٥. Murray, N.W., “Introduction to Theory of Thin Walled Structures”, Oxford Univ. Press, New York, ١٩٨٦.
٤٦. Ohga, M., Shigematsu, T., and Kawagouchi, K., “Buckling Analysis of Thin-Walled Members with Variable Thickness”, ASCE, J. Struct. Eng., Vol. ١٢١, No. ٦, June, ١٩٩٥, pp. ٩١٩-٩٢٤.
٤٧. Paik, J.K., and Kim, Y., “A Simplified Finite Element Method for The Ultimate Strength Analysis of Plates with Initial Imperfection”, Journal of The Society of Navel Architects of Korea, Vol. ٢٦, No. ١, Mar., ١٩٨٩, pp. ٢٤-٣٨.
٤٨. Paik, J.K., “A New Concept of the Effective Shear Modulus for a Plate Buckled in Shear”, J. Ship Research, Vol. ٣٩, No. ١, Mar., ١٩٩٥, pp. ٧٠-٧٥.
٤٩. Paik, J.K., Ham, J.H., and Ko, J.H., “A New Plate Buckling Design Formula”, Journal of The Society of Navel Architects of Japan, Vol. ١٧٢, ٢nd report, Dec., ١٩٩٢, pp. ٤١٧-٤٢٨.
٥٠. Paik, J.K., Thayamballi, A.K., Wang, G., and Kim, B.J., “On Advanced Buckling and Ultimate Strength Design of Ship Plating”, The Society of Navel Architects and Marine Engineers, ٢٠٠٠.

٥١. Rerkshanandana, N., Usami, T., and Karasudhi, P., "Ultimate Strength of Eccentrically Loaded Steel Plates and Box Sections", *Comp. & Struct.*, Vol. ١٣, ١٩٨١, pp. ٤٦٧-٤٨١.
٥٢. Rushton, K.R., "Post-buckling of Tapered Plates", *Int. J. Mech. Sci.*, Vol. ١١, ١٩٦٩, pp. ٤٦١-٤٨٠.
٥٣. Rushton, K.R., "Large Deflection of Plates with Initial Curvature", *Int. J. Mech. Sci.*, Vol. ١٢, ١٩٧٠, pp. ١٠٣٧-١٠٥١.
٥٤. Salvadori, M.G., "Numerical Computation of Buckling Loads by Finite Differences", *ASCE, Trans.*, Dec., ١٩٤٩, pp. ٥٩٠-٦٣٦.
٥٥. Save, M.A., and Massonnet, C. E., "Plastic Analysis and Design of Plates, Shells and Disks", North-Holland Publishing Company- Amsterdam, ١٩٧٢.
٥٦. Saxena, H.C., "The Calculus of Finite Differences", S. Chand & Company, LTD, ١٩٨٠.
٥٧. Shanley, F.R., "Mechanics of Materials", McGraw-Hill Kogakuasha, ١٩٦٧.
٥٨. Sherbourne, A.N., and Korol, R.M., "Post-buckling of Axially Compressed Plates", *ASCE, J. Struc. Div.*, Vol. ٩٨, No.ST١٠, Oct., ١٩٧٢, pp. ٢٢٢٣-٢٢٣٤.
٥٩. Shnan, W.F., "A Proposed Plastic Collapse Mechanism for The Prediction of Ultimate Load Capacity of Plated Structures", M. Sc. Thesis, Dep. of Building and Construction Eng., Univ. of Tech., Baghdad, ٢٠٠١.
٦٠. Sridharan, S., and Graves-Smith, T.R., "Post-buckling Analysis with Finite Strips", *ASCE, J. Eng. Mech. Div.*, Vol. ١٠٧, No.EM٥, Oct., ١٩٨١, pp. ٨٦٩-٨٨٨.
٦١. Stein, M., "Behavior of Buckling Rectangular Plates", *ASCE, J. Eng. Mech. Div.*, Vol. ٨٦, No.EM٢, Apr., ١٩٦٠, pp. ٥٩-٧٦.

٦٢. Sun, G., and Williams, F.W., “An Initial Post-buckling Analysis for Prismatic Plate Assemblies under Axial Compression”, Int. J. Solids Structures, Vol. ٣٤, No. ٢٨, ١٩٩٧, pp. ٣٧٠٥-٣٧٢٥.
٦٣. Sun, G., Kennedy, D., Williams, F.W., “A Post-buckling Analysis for Isotropic Prismatic Plate Assemblies under Axial Compression”, Int. J. Mech. Sci. , Vol. ٤٢, ٢٠٠٠, pp. ١٧٨٣-١٨٠٣.
٦٤. Szilard, R., “Theory and Analysis of Plates: Classical and Numerical Methods”, Prentice- Hall, Inc., Englewood Cliffs, New York, ١٩٧٤.
٦٥. Timoshenko, S.P., and Woinowsky, S., “Theory of Plates and Shells”, ٢nd Ed, McGraw-Hill Book Co., Inc., New York, ١٩٥٩.
٦٦. Timoshenko, S.P., and Gere, J.M., “Theory of Elastic Stability”, ٢nd Ed, Mc Graw-Hill Book Co., Inc., New York, ١٩٦١.
٦٧. Turvey, G.J., and Salehi, M., “Elasto-Plastic Response of Uniformly Loaded Sector Plates : Full-section Yield Model Predictions and Spread of Plasticity”, Comp. & Struc., Vol. ٧٩, ٢٠٠١, pp. ٢٣٣٥-٢٣٤٨.
٦٨. Ueda, Y., and Yao, T., “The Plastic Node Method: A New Method of Plastic Analysis”, Computer Methods in Applied Mechanics and Engineering, Vol. ٣٤, ١٩٨٢, pp. ١٠٨٩-١١٠٤.
٦٩. Ueda, Y., Rashed, S.M.H., and Paik, J.K., “An Incremental Galerkin Method for Plates and Stiffened Plates”, Comp. & Struct., Vol. ٢٧, No. ١, ١٩٨٧, pp. ١٤٧-١٥٦.
٧٠. Ugral, A.C., “Stresses in Plates and Shells”, McGraw-Hill, Inc, ١٩٨١.
٧١. Usami, T., “Post-buckling of Plates in Compression and Bending”, ASCE, J. Struc. Eng., Vol. ١٠٨, No. ST٣, Mar., ١٩٨٢, pp. ٥٩١-٦٠٩.

٧٢. Usami, T., "Effective Width of Locally Buckled of Plates in Compression and Bending", ASCE, J. Struct. Eng., Vol. ١١٩, No. ٥, May, ١٩٩٣, pp. ١٣٥٨-١٣٧٣.
٧٣. Wah, T., "Large Deflection Theory of Elasto-Plastic Plates", ASCE, J. Eng. Mech. Div., Vol. ٨٤, No. EM٤, Oct., ١٩٥٨, pp. ١-٢٤.
٧٤. Wang, P.C., "Numerical Matrix Method in Structural Mechanics", John Wiley & Sons, Inc., New York, London, Sydney, ١٩٦٦.
٧٥. Williams, D.G. and Walker, A. C. "Explicit Solution for The Design of Initially Deformed Plates Subject to Compression" Proc., ICE, London, England, Vol. ٥٩, Part ٢, ١٩٧٥, pp. ٧٦٣-٧٨٧.
٧٦. Williams, D.G., and Aalami, B., "Thin Plate Design for In-Plane Loading", Halsted Press, A Division of John Wiley & Son, Inc., New York, ١٩٧٩.
٧٧. Yamaki, N., "Post-buckling Behavior of Rectangular Plates with Small Initial Curvature Loaded in Edge Compression", ASME Trans., J. Appl. Mech., Vol. ٢٦, ١٩٥٩, pp. ٤٠٧-٤١٤.
٧٨. Zou, G., and Gao, P., "Higher Order Finite Strip Method for Post-buckling Analysis of Imperfect Composite Plates" J. Eng. Mech., Vol. ١٢٨, No. ٩, Sep., ٢٠٠٢, pp. ١٠٠٨-١٠١٥.